Fall 2016

Enhanced phagocytic capacity endows chondrogenic progenitor cells with a novel scavenger function within injured cartilage

Cheng Zhou
University of Iowa

www.manaraa.com

ENHANCED PHAGOCYTIC CAPACITY ENDOWS CHONDROGENIC
PROGENITOR CELLS WITH A NOVEL SCAVENGER FUNCTION WITHIN
INJURED CARTILAGE

by

Cheng Zhou

A thesis submitted in partial fulfillment
of the requirements for the Doctor of Philosophy
degree in Biomedical Engineering in the
Graduate College of
The University of Iowa

December 2016

Thesis Supervisor: Associate Professor James A. Martin

Copyright by

Cheng Zhou

2016

All Rights Reserved

Graduate College
The University of Iowa
Iowa City, Iowa

CERTIFICATE OF APPROVAL

_____

PH.D. THESIS

_____

This is to certify that the Ph.D. thesis of

Cheng Zhou

has been approved by the Examining Committee for
the thesis requirement for the Doctor of Philosophy degree
in Biomedical Engineering at the December 2016 graduation.

Thesis Committee: _____
James A. Martin, Thesis Supervisor

_____
Michael J. Schnieders

_____
Edward A. Sander

_____
Nicole M. Grosland

_____
Michael A. Mackey

To my beloved wife and family

ACKNOWLEDGEMENTS

It has been a long journey of my Ph.D. study in Biomedical Engineering at University of Iowa. This journey is filled with a lot of challenges and obstacles. I am sure I would be appreciated that I chose this difficult path and this experience would be priceless treasure in my life. A very important lesson I learnt from last five years is to appreciate the tough time as much as the great time.

There are so many people who support and help me I would like to thank. First of all, I would express my deepest gratitude to Dr. James A. Martin who is my research supervisor and mentor. He provided me the valuable opportunity to perform researches in the Orthopaedic and Cell Biology lab. His scientific originalities and continuous mentoring always encourage and motivate me to devote myself to academic research. I would sincerely acknowledge Dr. Michael J. Schnieders, who is my academic advisor, providing me a variety of critical advices during my graduate study. So many thanks to other committee members, Dr. Edward A. Sander, Drs. Nicole M. Grosland, and Dr. Michael A. Mackey for their valuable perspectives.

My Ph.D. research cannot be accomplished without the support of my colleagues. I would like to thank Hongjun Zheng, Dongrim Seol, Marc J. Brouillette, Yin Yu, Babara J. Laughlin, Hyounghun Choe, Keewoong Jang, Abigail D. Smith, Gail L. Kurriger, John F. Bierman, Lei Ding and other lab members.

Last but not least, I would like to acknowledge sincerely to my wife, Laura Jiao, and my parents for their unconditional love and supports.

ABSTRACT

Articular cartilage underwent serious joint injuries seldom repair spontaneously and might progress to post-traumatic osteoarthritis. This is majorly because articular cartilage's unique properties that lack blood and nerve supply intrinsically. This peculiar structure, in addition, generates an unfavorable environment for certain phagocytes (macrophages, monocytes, neutrophils, etc) to infiltrate to cartilage to scavenge debris from cartilage matrix and cell caused from joint injuries. Therefore, physiological and functional regeneration of damaged cartilage is urgently needed and several clinical techniques have been developed, including microfracture, autograft transplantation, autologous chondrocytes implantation.

We previously identified highly migratory cells emerged and repopulated in cartilage damaged surface after ~10 days of artificial cartilage injury. These cells were later named chondrogenic progenitor cells (CPCs) due to their enhanced potential of chondrogenic differentiation. However, this important finding contrasts the conventional theory that cartilage harbors only one cell type, chondrocytes. Here we hypothesize that CPCs are a distinct cell type in cartilage, and more importantly, one of CPCs' crucial natures is to phagocytose debris more effectively than chondrocytes.

To test these, we first harvested CPCs from cartilage surfaces, chondrocytes, synovial cells (synoviocytes and synovial fluid cells) for microarray assay to evaluate the closeness among these joint cells on whole gene expression level. Quantitative PCR were then conducted to verify gene expression of certain functional interests. Moreover, debris from cell and extracellular matrix were generated and incubated with CPCs and

iv

chondrocytes to compare their phagocytic capacity *via* multiple experimental assessments.

In confocal microscopy examination, the emergence of CPCs could be clearly observed after cartilage injury. Aside from their distinguishable morphology compared to chondrocyte, CPCs possess several vital properties including highly migratory, chemotactic, clonogenic. Microarray data revealed that CPCs, from gene expression profile, are distinctively isolated from chondrocytes and are more akin to synovial cells. Additionally, the series of phagocytosis related experiments showed that CPCs are dramatically superior to chondrocytes in engulfing debris, along with enhanced lysosomal activities indicating the following debris degradation.

Taken all these data together, CPCs, activated by cartilage injury, emerged and migrated to damaged sites. They are a distinct cell type residing in cartilage apart from chondrocytes. Their enhanced capacity to sustainably phagocytose and clear debris provides a novel insight for cartilage regeneration and prevention of osteoarthritis.

PUBLIC ABSTRACT

Osteoarthritis (OA) is one of most worldwide degenerative joint diseases dramatically affecting human health, over 27 million people in US are suffering from OA. Although aging is considered as the primary cause for OA, the pathogenesis of OA is still poorly understood. In addition, cartilage injures caused from continuous overuse and acute trauma often progress to OA. Due to the complicated and unique properties (lack of nerve and blood supply), cartilage has extremely limited capacity to repair spontaneously after injury.

A distinct cell type, chondrogenic progenitor cells (CPCs), have been identified on cartilage surface post injury, they function differently compared to chondrocytes, native cartilage cells. In this study, we focused on distinguishing CPCs from chondrocytes on global gene expression level. We also investigated how cartilage scavenges debris from injury. Since professional phagocytes (macrophage, monocytes, neutrophils, etc) are extremely unlikely to relocate to injured cartilage surface, we speculated that CPCs could act the scavenger role in injured cartilage.

From the heat map generated from microarray, the distinctive relation between CPCs and chondrocyte was revealed on global gene expression level. Additionally, CPCs are more akin to certain cells from joints (e.g. synoviocytes and synovial fluid cells). Based on a series of phagocytosis related experiments, we found that CPCs, compared to chondrocytes, could scavenge debris from cartilage injury more efficiently to the level of professional phagocytes.

Collectively these significant findings indicate that CPCs are a distinct cell type residing in cartilage performing a scavenger role in clearing cartilage debris from trauma injury.

TABLE OF CONTENTS

viii

LIST OF TABLES

LIST OF FIGURES

CHAPTER 1

INTRODUCTION

Articular cartilage is one of the most complicated soft tissue in human body, they are located at the end of articulating bones and play a crucial role in load distribution and lubrication within joint. Chondrocytes, as conventionally thought to be the only cell type in cartilage, are the terminally differentiated and specialized cartilage cells. They execute multiple metabolic activities to maintain the integrity of extracellular matrix (ECM). For example, collagen, proteoglycan, and other glycoproteins synthesized by chondrocytes are major structural molecules for cartilage ECM. Malfunction and death of chondrocytes, often resulted from trauma or aging, lead to progressive degeneration of cartilage and eventually osteoarthritis (OA). OA, featured with progressive loss of cartilage and restricted joint movement, is one of most worldwide diseases. More than 20 million people in US are suffering from OA. Trauma related joint injury often induces in massive acute death of chondrocytes, and this irreversible chondrocytes loss is considered as a major factor for pathogenesis of post-traumatic osteoarthritis (PTOA). Due to the limited repairing capacity (lack of vascular and lymphatic system), cartilage is seldom recovered after focal trauma injury. Functional restoration of injured cartilage has long been in demand and several clinical methods have been dramatically developed during last couple decades, including microfracture, autograft transplantation (mosaicplasty graft), and autologous chondrocyte/mesenchymal stem cell implantation. These techniques have shown promises in promoting healing of small cartilage defects in young patients. However, the cartilage regenerated from implanted chondrocytes or bone marrow stromal cells is relatively soft, fibrocartilaginous.

1

Although results from cell-based strategies were relatively varying and hindered the development of cartilage regeneration, the discovery of chondrogenic progenitor cells (CPCs) illuminates and clears the path. Multiple researches have been performed to identify the existence of the stem/progenitor cells in damaged cartilage during last decade. CPCs were first identified on the surface of articular cartilage, Dowthwaite and coworkers found these cells are enhanced in binding fibronectin along with high clonogenicity and over-expression of Notch 1 [1]. Although CPCs account low percentage in cartilage (<5%), they over-express multiple stem cell markers, such as CD105 and CD166 [2]. In addition, Hattori and coworkers also identified progenitor/stem cells in cartilage by side population assay, their capacity of producing superficial zone protein indicates these progenitor/stem cells can specifically differentiate to superficial zone chondrocytes. Like mesenchymal stem cells, CPCs are extensively superior to chondrocytes in term of migratory ability, clonogenicity, chemotaxis, and self-repairing capacity, these features substantially endows CPCs the capacity to migrate locally to focal damaged area and differentiate to regenerate cartilage tissue, but the understanding of the CPCs' function and mechanism in post-traumatic OA is still incomplete and highly needed for further evaluation.

Human knee is a closed synovial joint encapsulated by thin synovial membrane (synovium), synovium is a major source to synthesize and produce synovial fluid into knee joint. A number of molecules lubricating joint surface were found in synovial fluid, such as hyaluronic acid, phospholipids, and lubricin. Imbalance of the breakdown and production of these lubricating molecules results in synovial fluid becomes more watery and cartilage gradually wears away. Cells from synovium and synovial fluid

2

(synoviocytes and synovial fluid cells) play an important role in maintaining joint lubrication and homeostasis. Clinical observations have well documented the relevance between synovial fluid and osteoarthritis. Mild degree of synovial inflammation, and calcium pyrophosphate or apatite crystals are commonly existing in OA patients [3-5].

Phagocytosis is a defending process by which phagocytes or immune cells (macrophages, monocytes, neutrophils, dendritic cells, etc.) engulf foreign materials or debris from necrotic/apoptotic cells to destroy them, this process often and regularly occurs in vascularized tissue under the supply of consistent circulating blood, through which phagocytes can easily migrate and function to scavenge debris. The fact of very few reports of phagocytosis events in cartilage is due to the intrinsically avascular nature of cartilage. Although synoviocytes are one of the major professional phagocytes within joint, it is still unlikely for them to relocate to cartilage upon injury because of cartilage's peculiar anatomy structure. Regrettably, what continues to be poorly understood is the mechanism that scavenges debris from cartilage injury. How to unfold phagocytosis events in trauma injured or even osteoarthritic cartilage is an urgent need to better clarify the pathogenesis of osteoarthritis and to improve the clinical development of cartilage regeneration.

To fully evaluate the functions of CPCs is of great interest to facilitate towards cartilage regeneration and better understand the pathogenesis and treatments of OA. Our laboratory previously identified the emergence of CPCs post cartilage injury in bovine knee osteochondral explants. These CPCs actively migrated and repopulated to damaged cartilage surface around 10 days after initial cartilage injury. Since CPCs are morphologically distinct to native chondrocytes, we hypothesize CPCs form a distinct

3

cell type in cartilage and are more close to synovial cells. To test this, we isolated CPCs from injured bovine cartilage surfaces and compared to chondrocytes, and cells from synovial joints on gene expression level by microarray technique. Quantitative PCR will then be used to validate certain genes of interests. In addition to distinguish CPCs from chondrocytes, we also hypothesize CPCs possess enhanced phagocytic capacity to clear and engulf debris from cells and cartilage ECM. Multiple techniques, including confocal microscopy, flow cytometry, gene and protein expression, will be utilized to extensively evaluate the scavenger role of CPCs in injured cartilage.

4

CHAPTER 2

BACKGROUND

2.1 Articular cartilage

Articular cartilage is considered as specialized thin connective tissue covering the articulating surfaces of diarthrodial bones (Figure 2.1). The major functions of articular cartilage are to provide a considerable cushion allowing bones to glide over each other and to reduce friction while in movement, as well as distribute and weight loads evenly [6, 7]. Due to its hypo-cellularity and lack of vascular, neuro, or lymphatic supply, cartilage has extremely limited spontaneous regenerative capacity upon injury.

2.1.1 Anatomy of knee joint

Composed of articular cartilage, bottom of femur, top of tibia, menisci, ligaments, synovium, muscles and tendon (Figure 2.2), Knee is one of the largest and most complicated joints in human body. Among these tissues, articular cartilage is located in multiple bones, including femur, tibia and patella. Tendons connect the knee bones to the leg muscles that move the knee joint while ligaments join the knee bones and provide stability to the knee joint. Two C-shape menisci are located in between femur and tibia acting as shock absorbers.

2.1.2 Zonal structure of cartilage

Based on the cellularity of chondrocytes along the cartilage depth and functionalities of cartilage matrix, articular cartilage can be divided into four vertical zones – superficial, middle (or transitional), deep (or radial), and calcified zones with varying matrix composition, collagen orientation, and mechanical properties (Figure 2.3).

5

Each zone performs a variety of activities to maintain the normal functions of articular cartilage.

2.1.2.1 Superficial zone

Superficial zone serves as the articulating layer providing a smooth and lubricant gliding surface. 10 – 20% of the whole articular cartilage depth was counted in this zone, which is thinnest among four zones. It contains most abundant amount of collagen fibers and highest cellularity. Chondrocytes in this zone are relatively elongated and functioning to produce and secrete some specific lubricating proteins that smoothen and protect articular cartilage, including superficial zone protein (SZP, also known as lubricin) [8]. This protein is also widely used to distinguish superficial zone chondrocytes from chondrocytes from deeper zones [9]. The mechanical strength of superficial zone is relatively low, which might be easily disrupted under acute cartilage injury.

2.1.2.2 Middle zone

40 – 60% of the total cartilage thickness is taken for the middle zone, providing greater resistance to compressive load compared to superficial zone. Chondrocytes in this zone are morphologically spherical and randomly distributed. One major function of middle zone is transmitting force applied on cartilage surface to deep zones.

2.1.2.3 Deep zone

The deep zone of cartilage takes around 30% of the total cartilage volume, containing highest deposition of proteoglycan and lowest chondrocytes cellularity. The collagen fibrils in this zone are largest in term of diameter, which are oriented in radial

6

direction. These paralleling collagen fibrils, perpendicular to the surface, provides the strongest resistance to compressive forces and strengthens the connection between cartilage and underlying bone [10]. Moreover, chondrocytes in deep zone are far more active in the context of synthesize ECM matrix than chondrocytes in superficial zone [8].

2.1.2.4 Calcified zone

The calcified zone is considered as a transitional zone in between of cartilage to subchondral bone. Cellularity and metabolic activity of chondrocytes in this zone are extremely low [10]. Chondrocytes are tended to produce type X collagen that strengthen structural integrity and absorb shock [10, 11].

2.1.2.5 Tidemark

The tidemark is a visible basophilic line that separates deep zone from calcified cartilage. The major function of this layer is to transmit mechanical forces from cartilage to the underlying subchondral bone [12].

2.1.3 Chondrocytes

Articular cartilage, which until recently, is conventionally thought to harbor only one cell type, the chondrocytes (Figure 2.4). They account for less than 5 – 10% of the total cartilage volume [13].Chondrocytes are terminally differentiated cells with remarkable properties and capabilities, which sets them apart from other types of mesenchymal cells. With the varying size, morphology, orientation, cellularity and the distribution of chondrocytes in different zone, the primary functions of chondrocytes are to synthesize and maintain the matrix of the cartilage (collagens, proteoglycans, and noncollagenous proteins) [6, 14-16]. Chondrocytes are generally of rounded shape,

7

located in the cavities along the cartilage matrix (cartilage lacunae) (Figure 2.5). Chondrocytes are well differentiated to accommodate the low oxygen environment in cartilage (as low as 1%) [17]. In addition to maintaining functionalities of articular cartilage, chondrocytes are also performing nutrition/waste exchange via simple diffusion from synovium tissue and synovial fluid.

2.1.4 Cartilage matrix

Besides chondrocytes, the major components of cartilage matrix are fluid phase (interstitial water and electrolytes), solid ECM (collagens and proteoglycans), and noncollagenous proteins. The fibrillar network, formed by type II collagen, entraps aggrecan which is a main proteoglycan of articular cartilage [18] (Figure 2.6). Aggrecan is majorly connected with sulfated glycosaminoglycans, long unbranched polysaccharides capped by charged water-binding sulfate groups. Due largely to this water-binding property of aggrecan, cartilage matrix exhibits a remarkable resistance to compression, which is a pivot physiologic function of cartilage [19].

2.2 Synovium and synoviocytes

The synovium tissue, also named as synovial membrane, is the soft tissue between the joint cavity and articular capsule (Figure 2.7). This thin connective tissue is functioning to maintain normal activities and homeostasis of knee joint by synthesizing and secreting hyaluronan and lubricin [20]. Additionally, synovium tissue is vascularized and porous, in which way could exchange and provide nutrients to joint fluid through circulating blood.

The major cell types in synovium tissue are macrophage-like type A cells and fibroblast-like type B cells (also known as synoviocytes). Originally derived from bone-marrow myeloid precursors, type A cells produce synovial fluid and phagocytose antigens. These cells are nourished mainly from the vascular network in the sub-lining layer [21]. The hyaluronan synthesized by synoviocytes contributes to the viscosity and lubrication of synovial fluid [22]. Dramatic elevated expression of type I collage, VCAM-1, and CD44 (a receptor for hyaluronan) were found in synoviocytes compared to cells isolated from other connective tissues. Synovium tissue was found with elevated hypertrophy, vascularity and infiltration of the underlying tissue, which are characteristics of inflammatory changes, in osteoarthritic patients [23].

2.3 Synovial fluid and synovial fluid cells (SFCs)

Characterized by viscosity and non-Newtonian, synovial fluid exist in the cavities of multiple synovial joints, including knee, elbow. Synovial fluid is majorly synthesized and produced into the joint cavity by type A cells in synovium tissue. A healthy human knee joint normally contains around 2 ml synovial fluid, consisting of a mixture of lubricin, hyaluronan, proteinase, collagenases and prostaglandins [24]. The vital functions of synovial fluid are lubricating articular cartilage, absorbing shocks and providing nourishment to cartilage via simple diffusion.

Lubrication of cartilage surface is an effective prevention of cartilage from damage and maintains normal functionalities of cartilage [25]. Two most crucial lubricating molecules in synovial fluid, hyaluronan (HA) and proteoglycan 4 (PRG4)

9

[26], adhere to the cartilage surface. PRG4 is one of the mucinous glycoproteins and produced by synoviocytes and superficial zone chondrocytes to enhance the lubricating and protecting ability of the joint from tissue injury. In addition to PRG4, HA also makes contributions to hydrodynamic and boundary lubrication in the knee joint.

Furthermore, a variety of biomarkers existing in synovial fluid are able to be detected for pathogenesis of relevant diseases, such as osteoarthritis, rheumatoid arthritis, pyogenic bacterial infection and tumors. This unique property provides synovial fluid an important usage in clinic diagnoses [27].

2.4 Articular cartilage injury and osteoarthritis (OA)

Articular cartilage injuries is featured by tear of extracellular matrix, leading to massive chondrocytes death in cartilage, functional and physiologic properties loss of joint, eventually to the friction of subchondral bones. Post-trauma osteoarthritis (PTOA), such as falling, sports related injuries, might be accelerated by alarmins release, including tumor necrosis factor–α (TNF-α), interleukin (IL) and matrix metalloproteinase (MMP) families [28-31].

Osteoarthritis (OA), characterized by the structural or functional failure of the joints, is the most common cause of chronic joint pain and disability, which involves progressive cartilage degradation and subchondral bone hardening [32] (Figure 2.8). The major causes of OA include endocrine imbalance, overweight, aging, joint trauma and inflammation [32-34]. However, the pathogenesis of OA still remains unclear even though aging and excessive usage of joints are seen as most common factors [6, 33, 35] [36]. OA not only has huge impact on human health, also cause tremendous economic

burden to the whole society. 10% of people in the world and over 27 million people in the US are currently suffering from OA are estimated by the World Health Organization (WHO), as well as 128 billion dollars are spent for the medical cost of OA [37-39].

Massive chondrocytes death caused by acute cartilage injury is considered as a vital role in the pathogenesis of post-traumatic osteoarthritis [6, 40, 41]. Chondrocytes from OA patients are inclined to over-produce a variety of inflammatory cytokines that are associated with cartilage degradation, including TNF-α, interleukin-1β (IL-1β), IL-6, and IL-8 [3, 29, 30, 42]. Our previous work has demonstrated that continuous chondrocytes death post cartilage injury is majorly due to the dramatically elevated production of reactive oxygen species (ROS) in mitochondria. Thus, suppression of the ROS production immediately after cartilage injury could potentially prevent progressive chondrocytes death [41, 43].

2.5 Cartilage repair and regeneration

Articular cartilage has extremely limited capacity to repair and regenerate spontaneously after injury due to the lack of circulating blood supply and nervous system. Great demands of effective cartilage repairing strategies are highly needed for clinical exploration, including microfracture, auto- or allo- graft transplantation (mosaicplasty), autologous chondrocytes implantation (ACI), and total knee arthroplasty (TKA).

2.5.1 Microfracture

Microfracture is a surgery technique performed by arthroscopy. Tiny fractures in the subchondral bone plate will be drilled after the cartilage is cleaned. Blood and bone marrow will seep out through those fractures to form blood clots, which contain

11

considerable amount of bone marrow derived mesenchymal stem cells (MSCs) [44]. The MSCs then start to differentiate and build new cartilage (Figure 2.9.A). Microfracture technique is most effective and beneficial to patients who have relatively small lesion of cartilage [45, 46]. However, reports have been made that microfracture is dependent of patients' MSC population [47], as well as that chondral defects may not be fully filled which could lead to mechanically inferior fibrocartilage to rather than hyaline cartilage.

2.5.2 Autograft transplantation (mosaicplasty graft)

Autograft transplantation (mosaicplasty graft) is performed by transferring one or more cylindric osteochondral autografts from low or non load-bearing area (i.e. femoral condyle) to knee cartilage defect area (Figure 2.9.B). After debridement, a few large diameter autografts are harvested from the trochlea and press-fit to defects with exactly same depth. The procedures are repeated until gap region are fully covered. This method has shown promise on young patients with osteochondral defects of less than 3 cm [48].

2.5.3 Autologous chondrocytes/mesenchymal stem cells implantation (ACI)

ACI is one of the cell-based cartilage repairing strategies. The patients' chondrocytes are harvested from non-load bearing area arthroscopically. Those chondrocytes will be culture to proliferate *in vitro* to reach sufficient amount. After around 6 weeks, the chondrocytes will be injected into cartilage defects with scaffold matrix. The implanted chondrocytes will then proliferate and integrate with surrounding tissue to synthesize hyaline cartilage [49-51] (Figure 2.9.C).

In addition to autologous chondrocytes, mesenchymal stem cells (MSCs) are also utilized by surgeons to cell implantation technique toward cartilage repair. Similar, MSCs are isolated from patients' bone marrow and culture *in vitro* for chondrogenic

12

differentiation and then cells are injected to defect area [52, 53]. However, some drawbacks might limit the application of autologous MSCs implantation: An invasive biopsy is required for isolating MSCs and *ex vivo* culture might result in deleterious changes in MSCs' phenotype [53, 54].

2.5.4 Total knee arthroplasty (TKA)

Total knee arthroplasty (TKA) is a surgical procedure to replace the load-bearing surface of the knee joint with artificial material. It is an effective and required treatment for those patients suffering from end-stage osteoarthritis, knee trauma related or other rare destructive diseases of joints. Patients need to be strictly evaluated both pre- and post- operations.

Though relatively few complications occur during or after TKA procedures, postoperative infection, blood clots, osteolysis (when plastic and metal fragments released from the knee implant into cause inflammation) might hinder the application of TKA. Another risk is often encountered in younger patients who are likely to be more active, thereby augmenting trauma to the replaced joint.

2.6 Stem/progenitor cells in articular cartilage

Stem cells are multipotent to differentiate to terminated cells in wide range of tissue, while progenitor cells are unipotent or oligopotent (able to differentiate one or two related cell types), which are in the midway between stem cells and fully terminated cells. Unlike stem cells' indefinite replicating property, progenitor cells have relatively limited replicative capacity. Progenitor cells are quiescent in the tissue where they reside under

13

normal condition, they appeared to migrate to damaged sites upon injury in order to repair and maintain local tissue [55, 56].

Progenitor cells were reported to be residing in bovine cartilage as a subpopulation of superficial zone cells, which are named chondrogenic progenitor cells (CPCs) [1, 57]. Moreover, CPCs are extremely abundant in cartilage of late-stage of osteoarthritic patients and they exhibit a variety of stem cells feature, including multipotency, clonogenicity, elevated migratory activity and over-expression of MSC markers (CD105 and CD166) [2, 58]. CPCs are also identified in the deeper zones in a relatively small amount [59]. Our previous work has revealed that CPCs respond to cartilage injury and massively migrate to injury sites [60] (Figure 2.10). In addition CPCs appeared to be more close to synoviocytes and synovial cells other than chondrocytes, even though they reside in cartilage [61]. Furthermore, CPCs over-expressed proteoglycan 4 (PRG4), also known as lubricin (a crucial protein marker for superficial zone chondrocytes), in both gene and protein level, which profoundly suggests that CPCs perform an important role in repairing lubricant coating of cartilage surface resulted from mechanical damage.

Even though the origin of CPCs still remains unclear, the discovery and initial studies of CPCs provide a promising therapeutic and clinical application in compensation to the limited self-repairing property of cartilage. Nevertheless, recent work from our lab also suggests that CPCs might be involved in inflammatory pathway associated with pathogenesis of osteoarthritis.

14

2.7 Phagocytosis and phagocytosis in cartilage

Internalization of particles by cells is a critical biological step, it includes pinocytosis, receptor-mediated endocytosis, and phagocytosis. Phagocytosis is the process by which phagocytes, such as macrophages, monocytes, neutrophils, etc. internalize and engulf solid particles and substances to eliminate debris and pathogens (Figure 2.11). As a major mechanism in immune system, phagocytosis plays a vital role in clearing pro-inflammatory cytokines and chemokines, as well as maintaining physiological homeostasis. Phagocytosis often occurs in vascularized tissue where circulating blood provides ongoing macrophages serving as sentinels against foreign pathogens. The cytoskeletal rearrangements and cell membrane trafficking are initiated when the pathogens are binding to the phagocytes via phagocytic receptors [62-64], forming phagosomes and endosomes. After the pathogens are engulfed, the phagosomes transition to phagolysosomes, where pathogens are eliminated by multiple mechanisms, including reactive oxygen, nitrogen intermediates and toxic peptides [65]. Phagocytosis by macrophages is crucial for the uptake and degradation of pathogens and apoptotic cells, it is also involved in development, tissue remodeling, immune response, and inflammation.

Reports regarding phagocytosis in injured cartilage can be rarely found is majorly because the peculiar anatomy of knee joint. Due to the lack of vascular system and remote from synovium tissue, macrophages, synoviocyte, and other resident phagocytes in circulating blood are unlikely migrate to injured cartilage. Chondrocytes isolated from osteoarthritic patients possess certain phagocytic capacity [66] but their intrinsic

15

nature, largely intertwined by entangling extracellular matrix, exhibit their migratory ability is extremely limited.
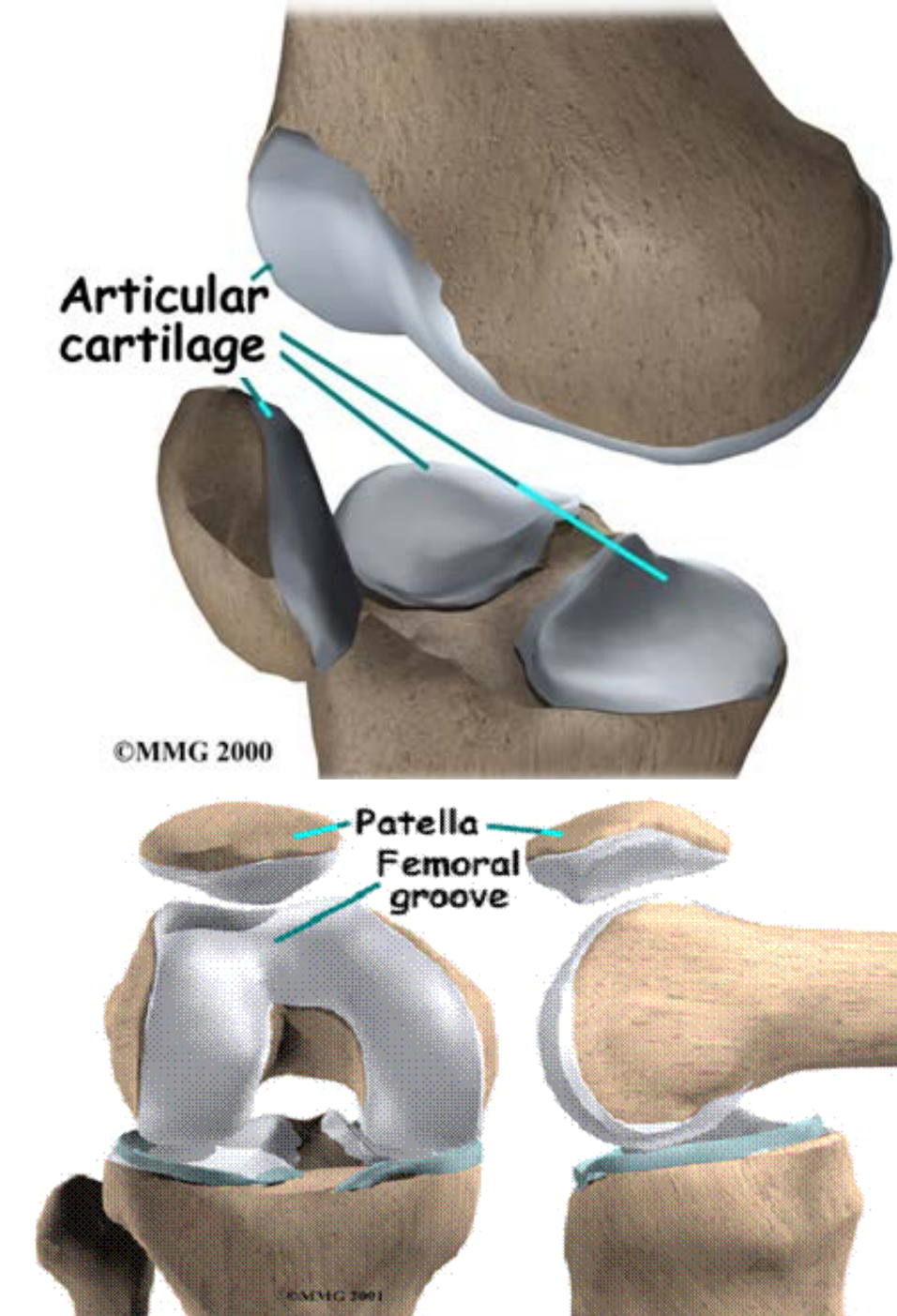
Figure 2.1 Articular cartilage in knee joints. Articular cartilage covers the ends of bones (patella, femur and tibia). Articular cartilage's smooth and slippery surfaces allow the bones of the knee joint to slide over each other with negligible friction.

17
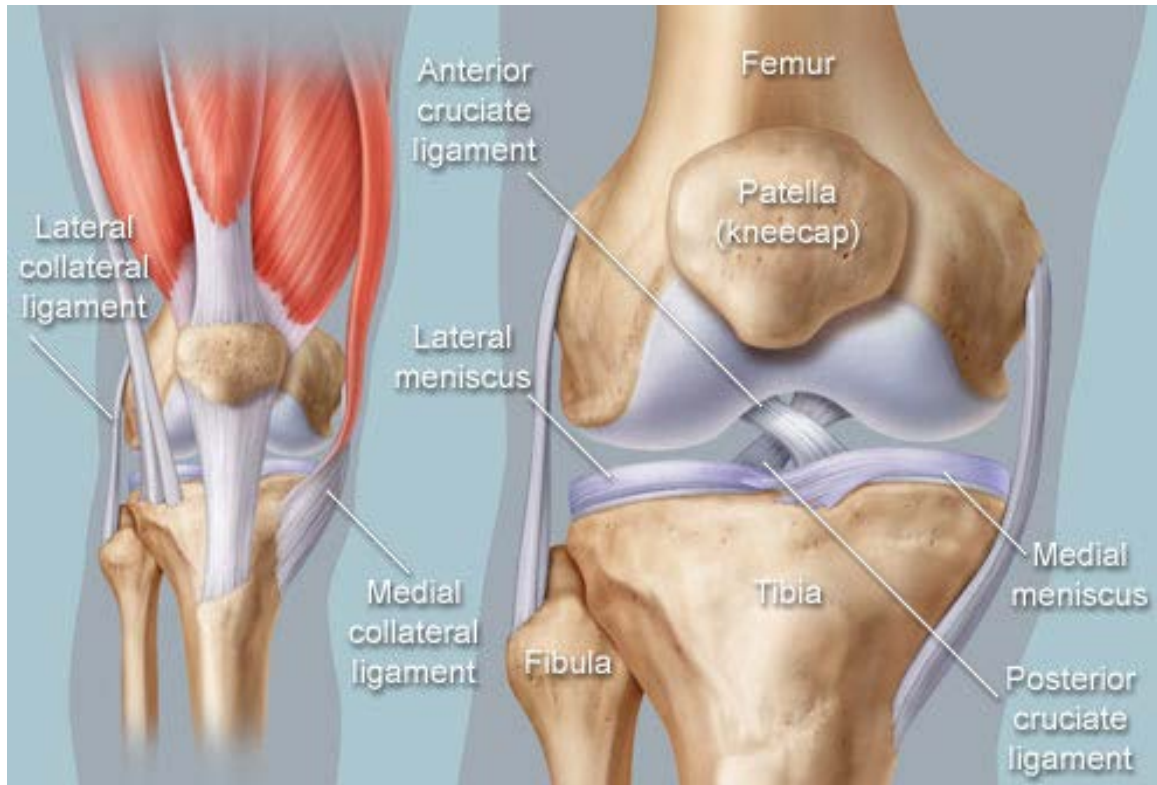
Figure 2.2 Anatomy of typical knee joints. The knee joins the thigh bone (femur) to the shin bone (tibia). The smaller bone that runs alongside the tibia (fibula) and the kneecap (patella) are the other bones that make the knee joint. Tendons connect the knee bones to the leg muscles that move the knee joint. Ligaments join the knee bones and provide stability to the knee. Two C-shaped pieces of cartilage called the medial and lateral menisci act as shock absorbers between the femur and tibia.

18
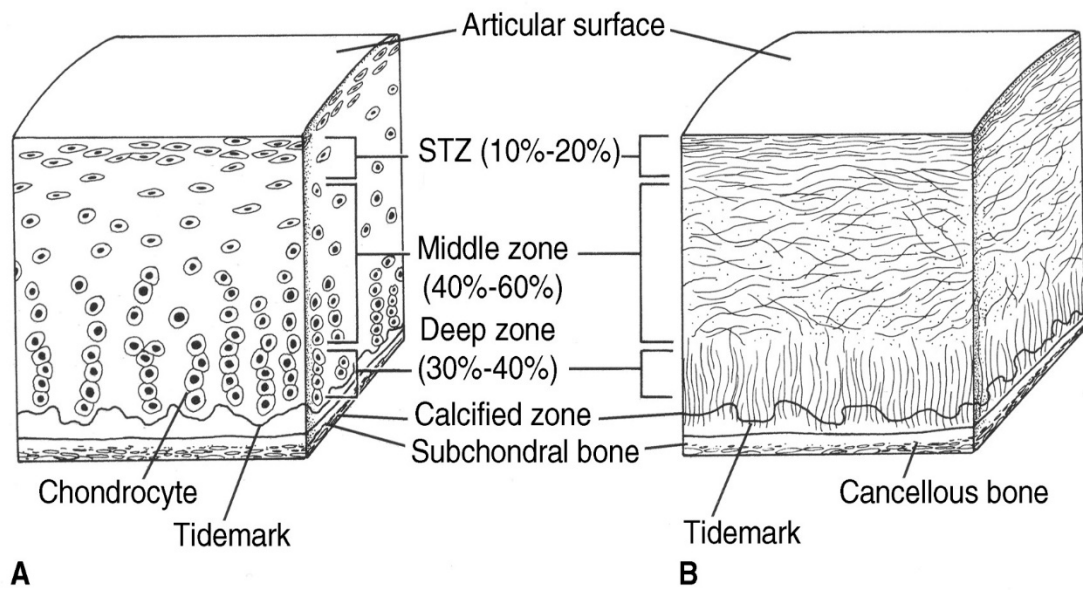
Figure 2.3 Zonal structure of articular cartilage. Articular cartilage can be divided into four different zones (superficial, middle, deep and calcified zones) based on the cellularity and alignment of collagen fibers.

19
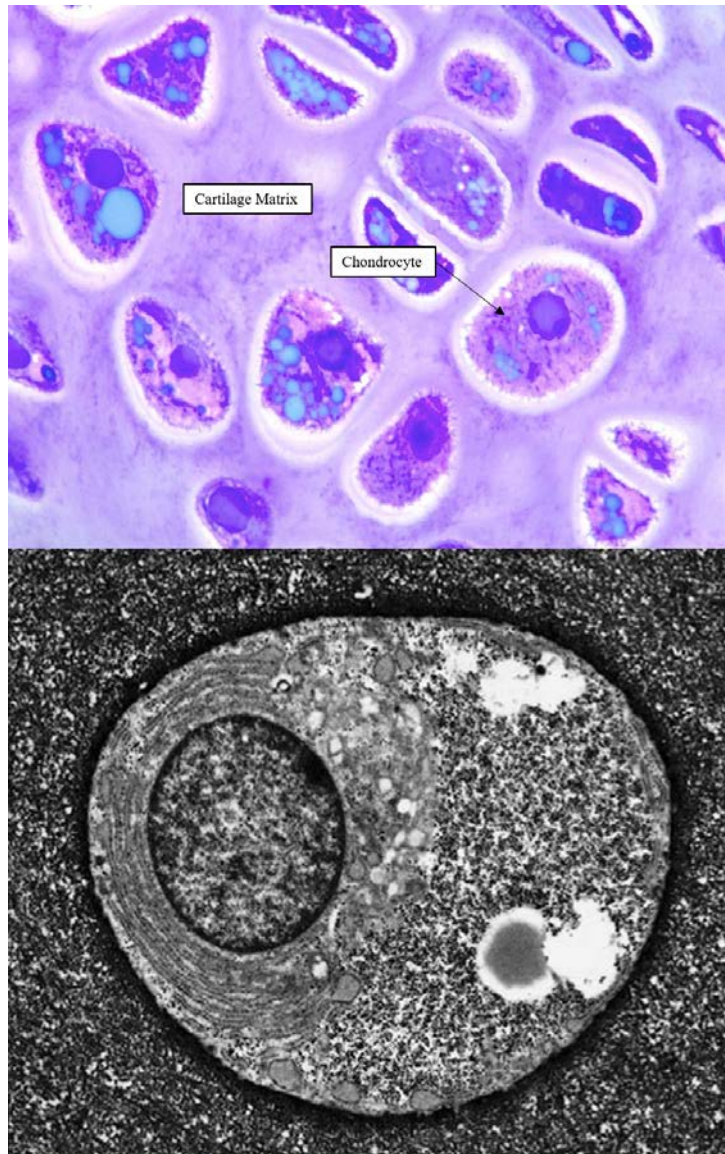
Figure 2.4 Histology (upper) and electron micrograph (lower) of typical chondrocytes. Chondrocytes produce the structural components of cartilage, including collagen, proteoglycans and glycosaminoglycans. Chondrocytes are present in cartilage as individuals or in isogenic groups.
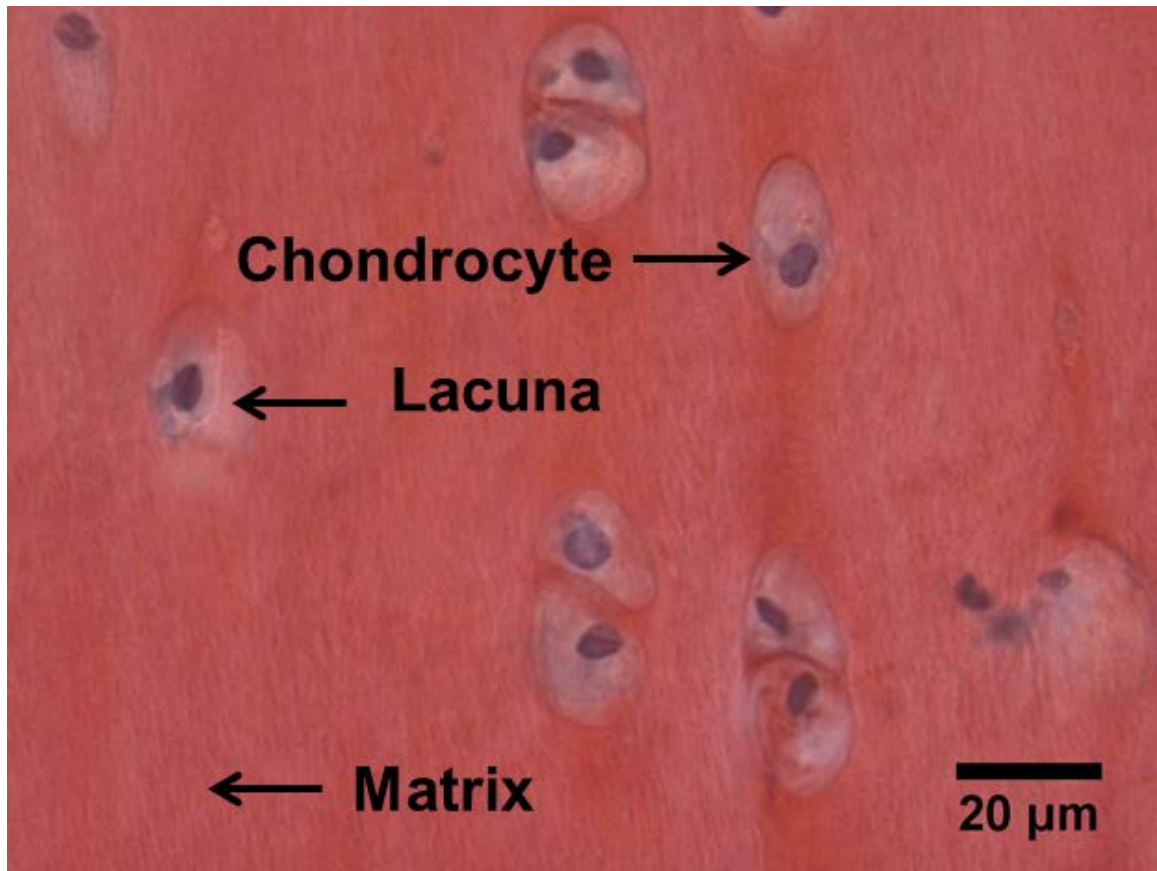
Figure 2.5 Location of chondrocytes. Chondrocytes reside in lacunae throughout the articular cartilage.
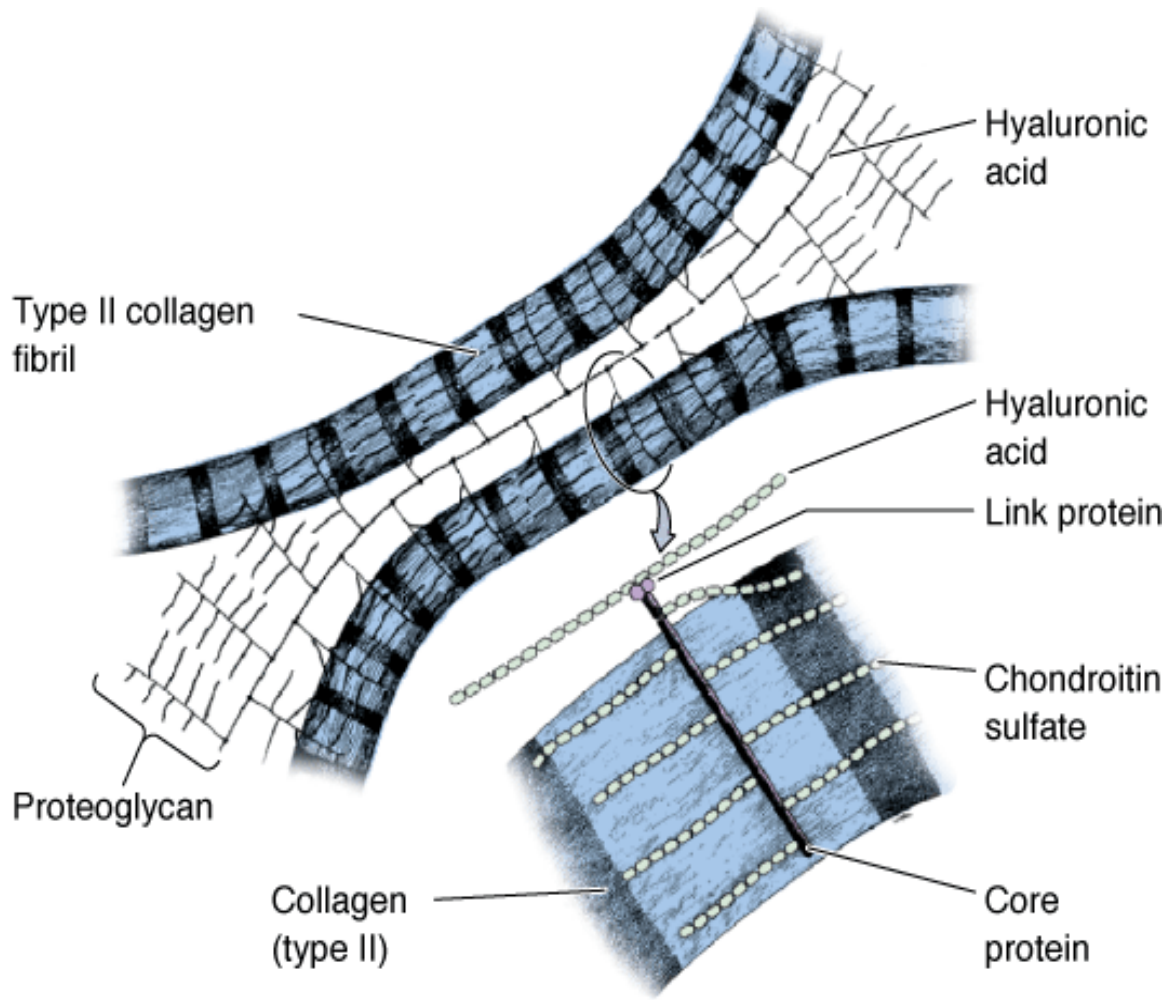
Figure 2.6 Components of cartilage extracellular matrix (ECM). Cartilage ECM is composed primarily of type II collagen and connected with large networks of proteoglycans that contain hyaluronic acid and chondroitin sulfate.
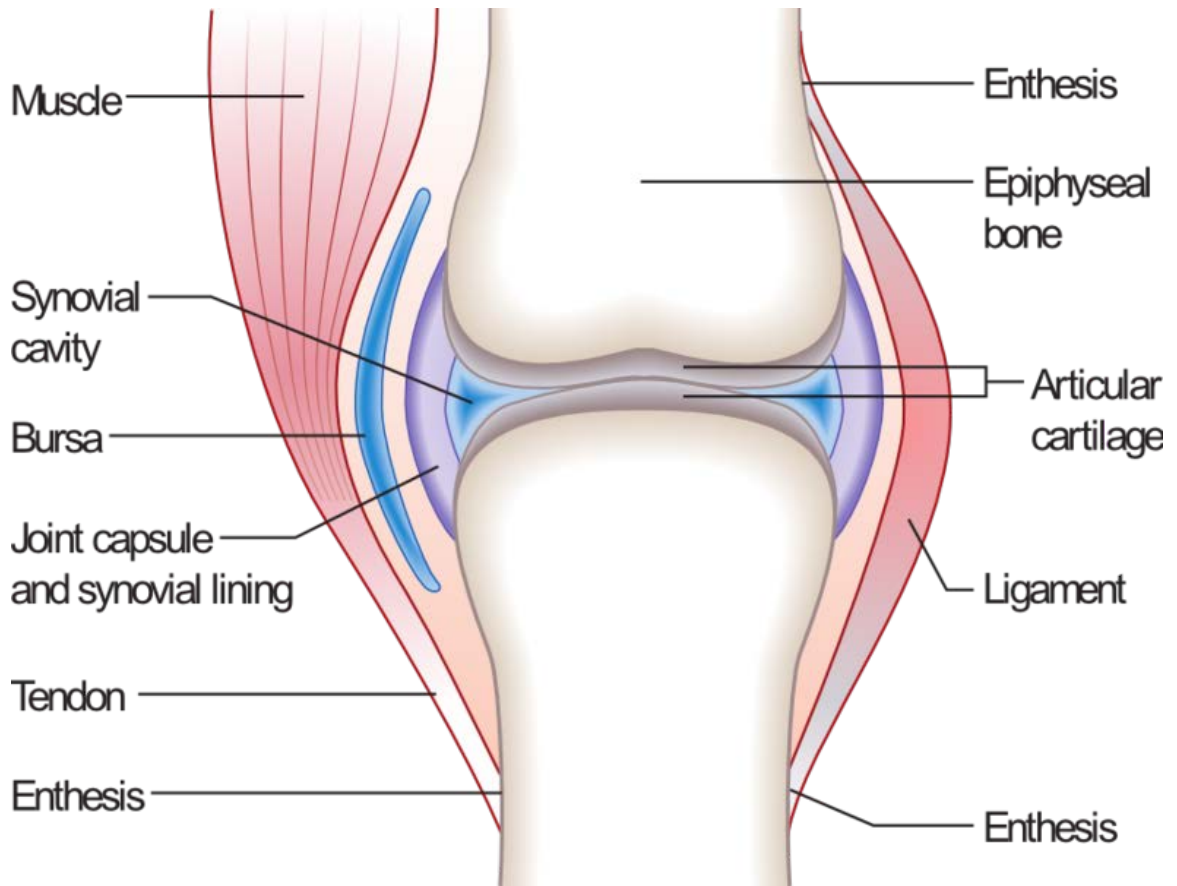
Figure 2.7 Illustration of a typical synovial joint. A fibrous joint capsule constitutes the outer boundary of a synovial cavity enclosing joined bones. The synovial cavity is filled with synovial fluid, which is sealed by an inner layer, the synovial membrane.
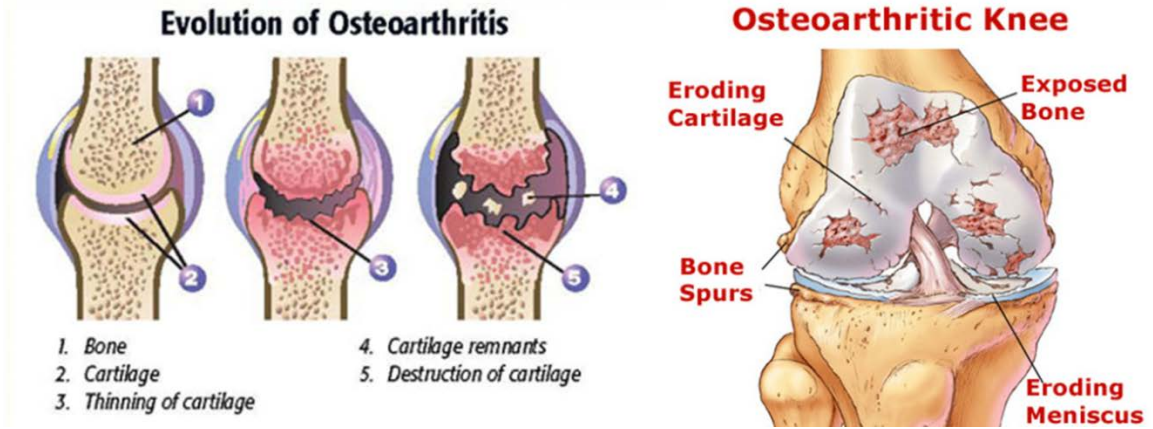
Figure 2.8 Progression of osteoarthritis (left) & illustration of osteoarthritic knee joint (right).
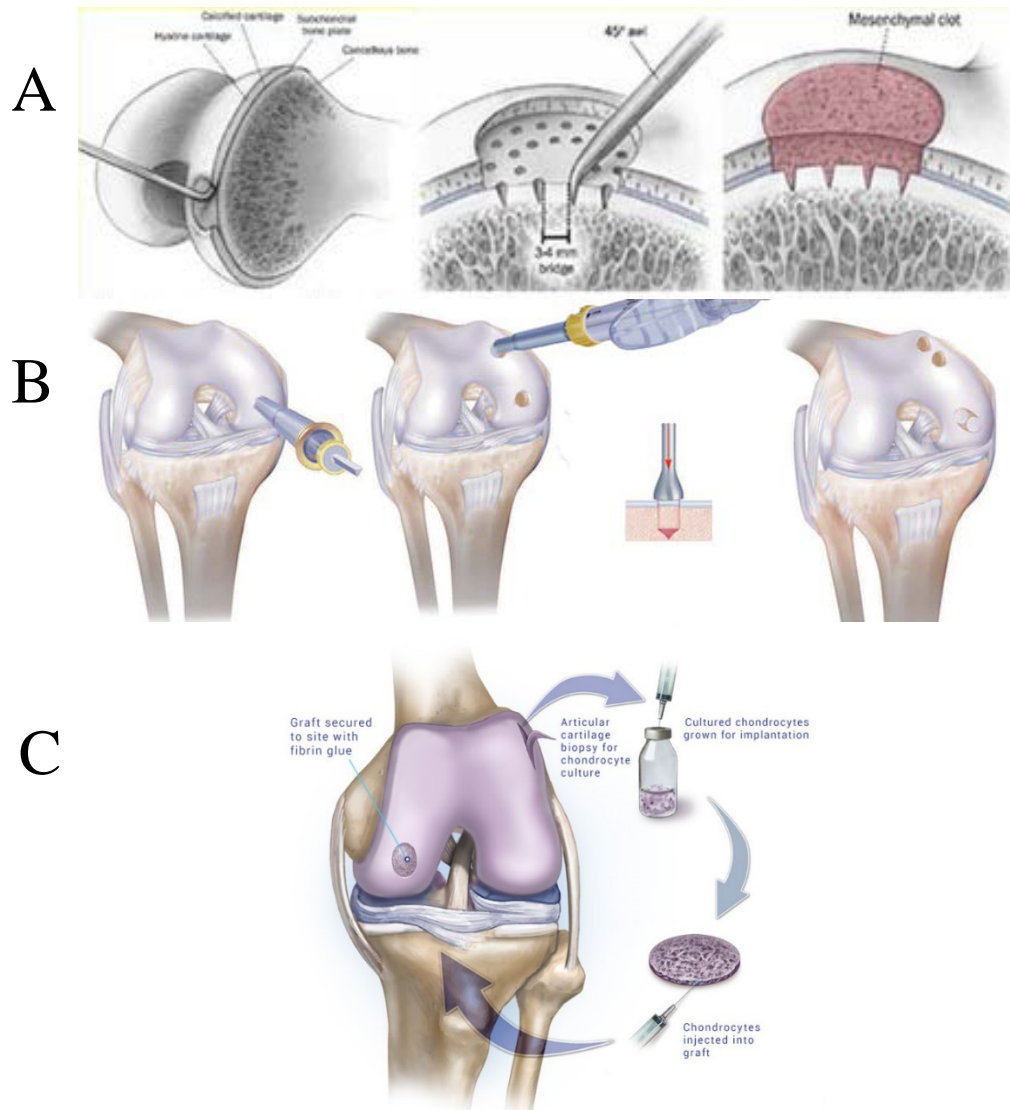
Figure 2.9 Cartilage repair techniques. A) Microfracture. B) Autograft transplantation (mosaicplasty graft). C) Autologous chondrocytes implantation (ACI).
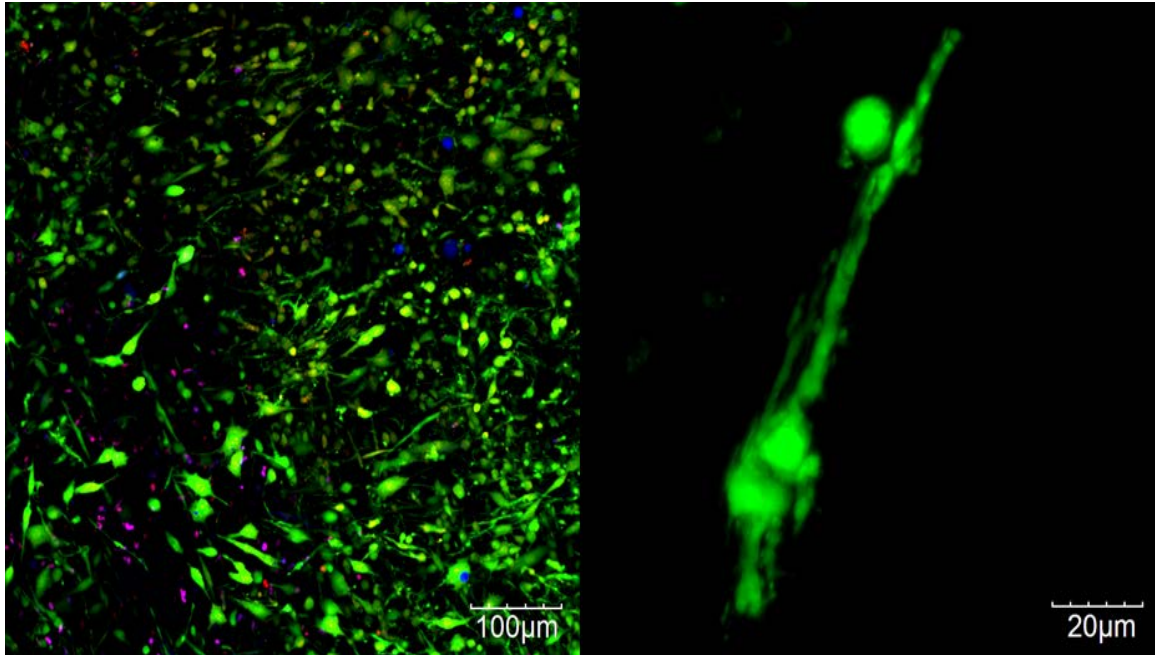
Figure 2.10 Morphology of chondrogenic progenitor cells (CPCs) and confocal images of CPCs (Calcein AM staining). CPCs (green) are gathered together after certain injury on cartilage (left). Higher magnification figure showing the morphology of a specific CPC (right).

1. RECOGNITION AND ATTACHMENT

Microbes bind to phagocyte receptors

Phagocytic receptor

2. ENGULFMENT

Phagocyte membrane zips up around microbe

Microbe ingested in phagosome

Phagosome with ingested microbe

Lysosome with enzymes

Fusion of phagosome with lysosome

iNOS

Arginine

NO

ROS

O₂

Phagocyte oxidase

Phagolysosome

Degradation of microbes by lysosomal enzymes in phagolysosome

Killing of microbes by ROS and NO

3. KILLING AND DEGRADATION

Figure 2.11 Illustration (upper) and process (lower) of phagocytosis.

CHONDROGENIC PROGENITOR CELLS (CPCS) ACTIVATION, MIGRATION AND FUNCTIONAL STUDIES

3.1 Background and significance

Stem/progenitor cells have been identified in injured and osteoarthritic cartilage during last decade, which was further named chondrogenic progenitor cells (CPCs). These cells are morphologically distinct with chondrocytes in cartilage and exhibit dramatic potencies toward to repair and regenerate neo-cartilage. However, very few studies have studied CPCs' function thoroughly.

In this chapter, we hypothesized that CPCs would be activated and emerged to injury sites upon cartilage injury. We used confocal microscopy to observe the morphology and emergence of CPCs on osteochondral explant surface. In addition, we isolated CPCs from cartilage surface and conducted a chondrogenesis differentiation assay to assess their chondrogenic potential compared to chondrocytes, and other knee joint cells (synoviocytes and synovial fluid cells). The results presented here suggested certain cartilage injury will cause substantial chondrocytes death along with the activation of CPCs, and CPCs possess a high-level migration capacity and chondrogenesis potential.

Stromal cell-derived factor 1 (SDF-1) is a well-investigated chemokine isolated from bone marrow stromal cells, directing the migration of hematopoietic cell as well as guiding angiogenesis by recruiting endothelial progenitor cells. The interaction of SDF-1 and its reception, CXCR4, not only plays an important role in catabolic process of OA cartilage through releasing MMPs and IL-6, also regulates the proliferative activity of OA chondrocytes. In addition, SDF-1 is also a stimuli for the production of vascular endothelial growth factor. Coincidently, our previous data showed that CPCs contain

28

highly elevated expression of SDF-1 compared to chondrocytes. To explore if the SDF-1 released by CPCs will have an effect on the VEGF expression of chondrocytes could lead us to better understand the vasculogenesis and angiogenesis events in cartilage post injury.

3.2 Hypotheses and specific aims

In this chapter, we hypothesized chondrogenic progenitor cells (CPCs) emerges and migrates to damaged sites upon injury in articular cartilage with following specific aims:

a) Identify the emergence and migration of CPCs on the cartilage surface post injury

b) Study the characterization and functions of CPCs towards cartilage regeneration

c) Investigate the vascular endothelial growth factor (VEGF) expression of chondrocytes stimulated by the chemokine released from CPCs.

3.3 Materials and methods

3.3.1 Osteochondral explants harvest and culture

Fresh osteochondral explants (2.5×2.5 cm^2) was harvested from bovine tibia plateaus of healthy stifle joints (Bud's Custom Meats, Riverside, IA). After gentle rinse in Hank's Balanced salt solution (HBSS) (Invitrogen Life technologies, Carlsbad, CA), the explants were cultured in Dulbecco's modified Eagle's medium (DMEM) and Ham's F12 with a 1:1 mixture, supplemented with 10% fetal bovine serum (FBS) (Invitrogen Life Technologies), 100 U/ml penicillin, 100 µg/ml streptomycin, and 2.5 µg/ml Amphotericin B at 37 ºC, 5% CO_2 and 5% O_2 for 2 days.

29

3.3.2 Chondrogenic progenitor cells (CPCs) and chondrocytes isolation

After 2-day equilibrium of culture media, a sterile needle (18 G) was dragged on the cartilage surface of the explant to aseptically create multiple matrix tears. The explants were then cultured for around 10 days with changing the culture media the every other day. The emergence and migration of CPCs on the injured cartilage surface was then confirmed. Briefly, explants were washed with Hanks' media and stained with 1 μM Calcein Green-AM (Invitrogen, Grand Island, NY) for 30 mins, followed by confocal microscopic detection at Alexa Fluor 488. For CPC isolation, the cartilage surface of each explant was treated with 0.25% Trypsin-EDTA (Gibco, Grand Island, NY) for 10 mins, culture media was added to end trypsinization, and cell suspension was then centrifuged at 300 G for 10 mins. Cells were resuspended and seeded as experiments' need. After isolation of CPCs, the underlying cartilage tissue was shaved off the subchondral bone, minced into smaller pieces, and digested in 0.03% collagenase/protease (dissolved in culture media) for 16 hrs. The digestion media was centrifuged (300 G for 10 mins) and resuspended, then seeded as experiments required. (Figure 3.1)

3.3.3 Chondrogenic differentiation assay

The chondrogenic differentiation potency of CPCs was examined by culturing them under chondrogenic conditions and also compared to some typical cells from knee joint, including chondrocytes, synoviocytes and synovial fluid cells (SFCs). 0.25×10^6 cells were seeded into each well of a 96-well, V-bottom, non-treated polystyrene

microplate (Costar, Corning, NY) and cultured with 200 µl chondrogenic differentiation media (DMEM supplemented with 10 ng/ml TGF-β1, 0.1 µM dexamethasone, 25 µg/ml pyruvate, 50 mg/ml ITS+ Premix and antibiotics). The microplates were then centrifuged for 5 mins at 500 G and placed in a low oxygen incubator to aggregate cell pellets. After two weeks culture with changing chondrogenic differentiation media every other day, the cell pellets were collected for sulfated glycosaminoglycan (sGAG) assay, briefly, the cell pellets were digested by 40 µl papain digest buffer (0.01 mM/mL L-Cysteine HCl, 0.2 mM/mL Na_2HPO_4, 0.01 mM/mL Papain type III) for four hours. The samples were then centrifuged at 12000 G for 10 mins to exclude insoluble materials. sGAG content of cell pellets was quantified using the dimethylmethylene blue (DMMB) assay. Absorbance was spectrophotometrically measured on a kinetic microplate reader (VMaz, Molecular Devices) with wavelength at 530 nm. sGAG content was then normalized to the DNA content of each cell pellet, where the measurement of the DNA content was performed by using Quant-iT TM PicoGreen® dsDNA Reagent and Kits (Invitrogen, Grand Island, NY) according to the manufacturer's manual. sGAG contents were reported as µg sGAG/µg DNA.

3.3.4 Vascular endothelial growth factor (VEGF) expression of chondrocytes stimulated by CPC-condition media

For VEGF protein expression, chondrocytes were plated on 6-well plates and treated with increasingly proportional CPCs conditioned media (0, 0.4 ml, 0.8 ml, 1.2 ml and 1.6 ml for 0, 20%, 40%, 60%, and 80%, respectively) for 24 hrs with or without the pretreatment of AMD3100 (200 ng/ml for 2 hrs), an SDF-1 receptor antagonist. All the

31

cultured cells were lysed for 20 mins with cold lysis buffer: 10 mM Tris-base, 150 mM NaCl, 0.1% sodium dodecyl sulfate (SDS), 1% Triton X-100, 0.1% sodium deoxycholate, 50 mM NaF, 1 mM ethyleneglycol bis tetraacetic acid (EGTA), 1 mM glycerol phosphate, 1 mM Na_3VO_4, 10 μg/ml aprotinin, 10 μg/ml leupeptin, 1 mM ethylenediaminetetraacetic acid (EDTA), 2.5 mM sodium pyrophosphate decahydrate with 1:100 fold dilution of protease inhibitor cocktail III. Equal volume and weight of the protein, determined by Pierce BCA Protein Assay Kit (Thermo Scientific), was applied per lane, and electrophoresis was then performed under denaturing conditions on a 10% SDS gel, and transferred to a nitrocellulose membrane. The blots were blocked with 5% BSA in TBST for 1 hr at room temperature and the probed with rabbit anti-bovine antibody against VEGF (1:200) at 4°C overnight and β-actin (1:2000) antibodies. After three TBST washes, the blots were subsequently incubated with a HRP-conjugated goat anti-rabbit IgG secondary antibody (1:2000) for 1 hr at room temperature. The blots were visualized by Super Signal Chemiluminescent Substrate kit.

3.3.4 Statistical analysis

Data are reported as means +/- standard deviations. The statistical differences of four cell types in sGAG assay were evaluated by one-way analysis of variance (ANOVA) with Tuckey's post hoc test using SPSS software (Version 21). A two-tailed P-value < 0.05 was considered statistically significant.

32

3.4 Results

3.4.1 Emergence and migration of CPCs on cartilage surface post injury

Confocal microscopy analysis showed CPCs' typical elongated, fibroblast-like morphology in the cartilage injured site. In addition, only typical round shape chondrocytes were detected on bovine osteochondral explant surface immediately after scratch injury, CPCs vigorously emerged and migrated to the scratch site on cartilage surface at day 11. (Figure 3.2)

3.4.2 Sulfated Glycosaminoglycan (sGAG) Assay

The sGAG/DNA (µg sGAG/µg DNA) level in chondrocytes is around 0.34 units, and 0.21 units in CPCs. A significant decrease (37.4%) was observed between CPCs and chondrocytes ($p<0.05$). The sGAG/DNA level in both SFCs and synoviocytes, 0.13 units and 0.16 units, respectively, were dramatically lower (63.2% and 53.0%, respectively) than chondrocytes ($p < 0.001$ in SFCs and $p < 0.01$ in synoviocytes). There is no significant difference both in the comparison of the sGAG/DNA between CPCs and SFCs and the comparison between CPCs and synoviocytes. This reveals that chondrocytes contain the highest glycosaminoglycan contents, while CPCs stay in the same level with SFCs and synoviocytes. (Figure 3.3)

3.4.3 Effects of CPCs conditioned media on chondrocytes' VEGF expression

The western blot analysis revealed that CPC-conditioned media had dose-dependent stimulatory effects on chondrocytes' VEGF expression, and that AMD3100

33

pretreatment completely suppressed this response. At higher doses of conditioned media (>40%), VEGF expression was driven to, even below, baseline. (Figure 3.4)

3.5 Discussion and conclusion

The results of these experiments revealed that the emergence of an elongated cell type upon cartilage injury surface in our bovine osteochondral explant model. The morphology, chondrogenic gene expression and potential are significantly consistent with our previous work and published descriptions of chondrogenic progenitor cells. Specifically extracted from our microarray data, CPCs over-expressed multiple stem/progenitor genes comparing to chondrocytes, including CD105 (1.5-fold), CD166 (8.99-fold), CD44 (13.18-fold), Notch1 (7.46-fold), ABCG2 (10.50-fold), etc. (Table 3.1) With the gene expression and *in vitro* culture experiments under chondrogenic condition, the data suggested that migratory CPCs were able to proliferate towards chondrogenic lineage, but inferior to chondrocytes. Although the chondrogenic potential of CPCs cannot reach chondrocytes' level due to chondrocytes' intrinsic properties, the elevated level still stands CPCs out compared to other typical knee joint cells (synoviocytes and synovial fluid cells). These results were fairly consistent with the gene expression data that chondrocytes possess the highest expression of ECM forming related genes described in Chapter 4.

Upon cartilage injury, multiple cell layer-thick of CPCs coating will cover around damaged cartilage, we previously identified these cells could be positively stained for lubricin by immunohistochemistry, which is a pivotal lubricant protein in knee joints reducing friction, as well as an important marker for superficial zone chondrocytes [67,

34

68]. Our microarray data suggested that, in regard of PRG4 (lubricin) gene expression, although CPCs are subtly down-regulated in lubricin comparing to chondrocytes (1.93-fold lower), they are in same level with synovial fluid cells (1.27-fold higher) and synoviocytes (1.07-fold lower). (Table 3.2) Taken these data together, we could infer that certain properties and characteristics of superficial zone chondrocytes are highly retained in CPCs.

It is well known that the presence of VEGF in osteoarthritic joints significantly accumulates the pathogenic process. The factors that CPCs themselves over-express SDF-1 and VEGF simultaneously, as well as CPCs conditioned media triggers dramatic VEGF expression in chondrocytes provides us another perspective of CPCs with caution. CPCs are responsive to SDF-1 stimulation with increased VEGF synthesis suggest us that these phenomenon might be involved with autocrine stimulation of SDF-1 pathway. To put all together, these findings uphold the probabilities that CPCs might be involved or contribute to boost the VEGF synthesis and expression in injured knee joint, which are commonly seen in osteoarthritic patients.

These series of experiments illustrate the existence of a novel cell type in knee articular cartilage. Certain functions of CPCs were characterized by gene expression, *in vitro* chondrogenic differentiation assay, and specific proteins expression. While these findings are intriguing and exciting, they are still far away from full understanding of CPCs. The origin of CPCs still remains unclear, certain stem/progenitor cell markers, as well as multiple combination of markers, are encouraged to identify and locate CPCs. However due to the running target properties of CPCs, they could differentiate to multiple cell lineages under varying circumstances, to accurately localize CPCs in normal cartilage

35

tissue would be troublesome and intractable. With the evidences from our isolated bovine explant model, another possibility would be that CPCs come from the cartilage matrix itself when provoked by cartilage injury, the location of CPCs are presumed in cartilage surface and superficial zone because of the factor that both CPCs and superficial zone cells are highly clonogenic when compared to bottom of the matrix.

How do thousands of CPCs accumulate around cartilage injury sites? Two unknowns need to be further explicated. 1) What attracts CPCs to injury sites and 2) how do CPCs migrate through extracellular matrix which are entangling and hindering to cell migration. For the first question, our previous publication suggests that the driven force of CPCs migration could be, or at least, debris from dead cell, which contains a number of homing factors drawing stem and immune cells to injured sites. For example, high-mobility group B1 (HMGB1) protein, mitochondrial DNA, they can act through toll-like receptors pathway [69]. In addition, the sustainable autocrine/paracrine circulation of SDF-1 in CPCs also suggests the induction of chemotaxis, which could possibly intensify CPCs recruitment to injury sites. For the second question, during the course of cell migration, CPCs could depopulate surrounding collagen matrices to provide themselves a relatively relaxing environment. Our microarray data indicated that CPCs possess relatively high expression in multiple proteases and matrix peptidases expression comparing to chondrocytes, including ADAMTS-1 (6.87-fold), ADAMTS-4 (8.37-fold), Cathepsin B (2.25-fold), MMP3 (6.43-fold) and MMP13 (9.21-fold). (Table 3.3) The enhanced proliferative rate of CPCs also contributes to the migration. During the *in vitro* culture of CPCs, we noticed that they proliferate twice to three times faster than chondrocytes, this is extremely vital during cell migration. Consistent cell proliferation,

36

cytokines and chemokines attraction together pave the way for CPCs to migrate to injury sites.

Due to the dual properties of CPCs, guidance to create a micro-environment for CPCs to appropriately function is urgently needed during cartilage injury restore process. To achieve this goal, more studies are needed to solve when and where to add proper chemokines to attract CPCs migration, as well as to study if these chemokines will provoke certain pathogenic events, which in turn would impede, or even negatively drive, the whole cartilage recover processes.
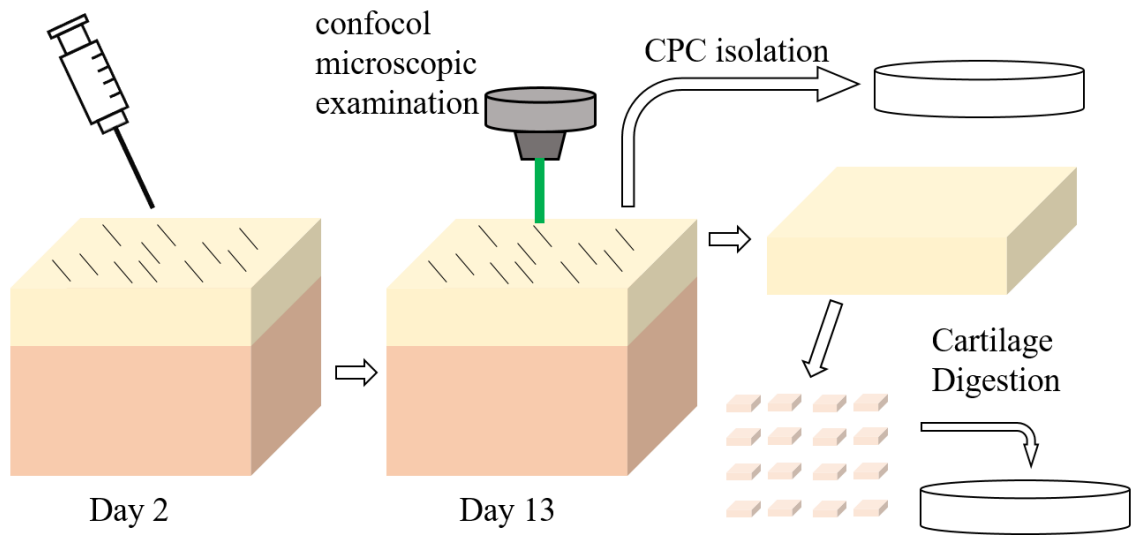
Figure 3.1 Cell isolation scheme. Schematic representation of the procedures for CPC and chondrocytes isolation.
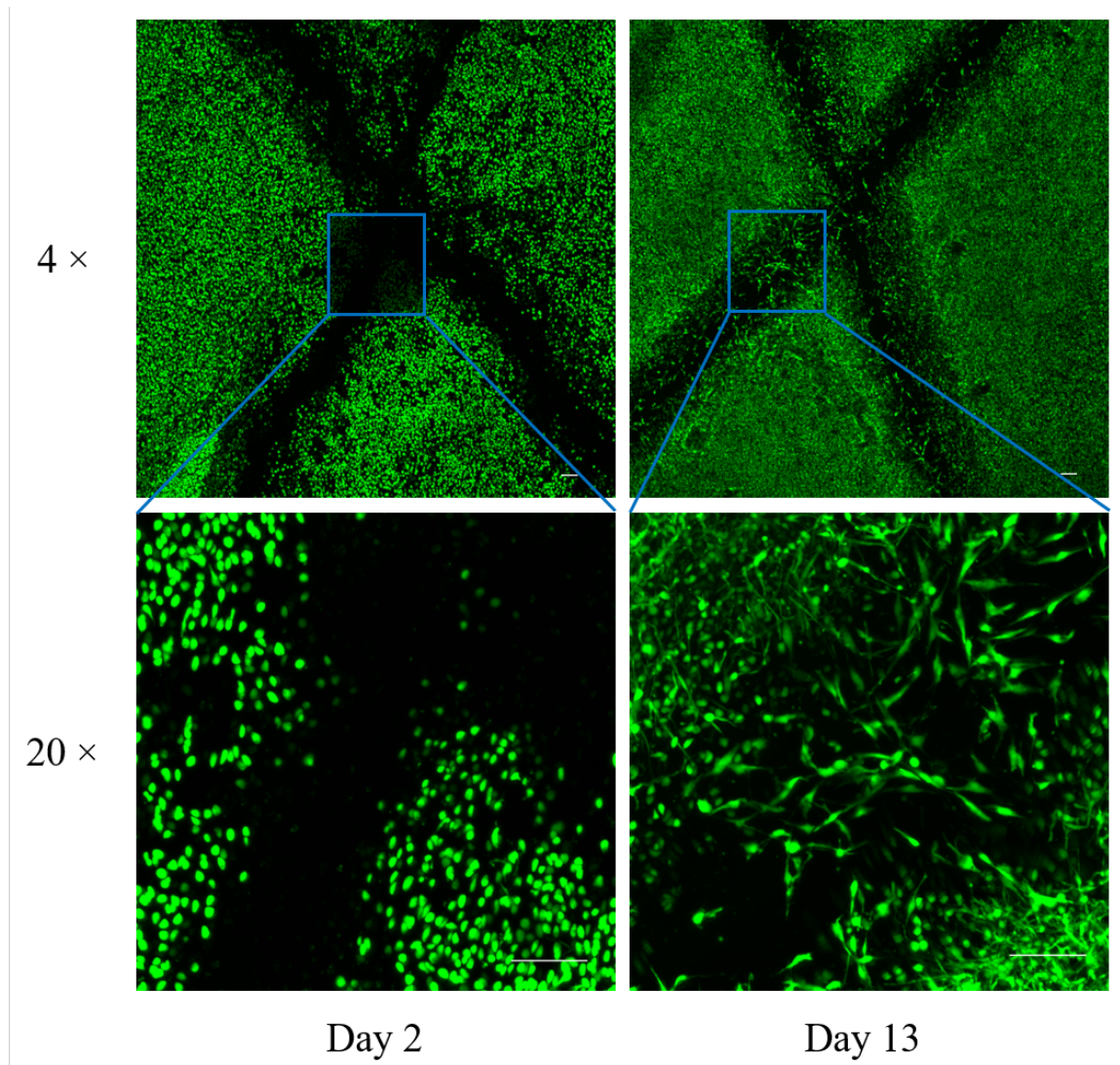
Figure 3.2 Emergence and migration of CPCs. Typical round shape chondrocytes were found at day 2 (day 0 after scratches) (left panel). Elongated fibroblast-like cells massively emerged at scratch sites at day 13 (right panel). Higher magnification images (lower panel) detail the cell morphology at day 2 (day 0 of cartilage scratches) and day 13. (bar = 100 µm)

sGAG amount in four cell types
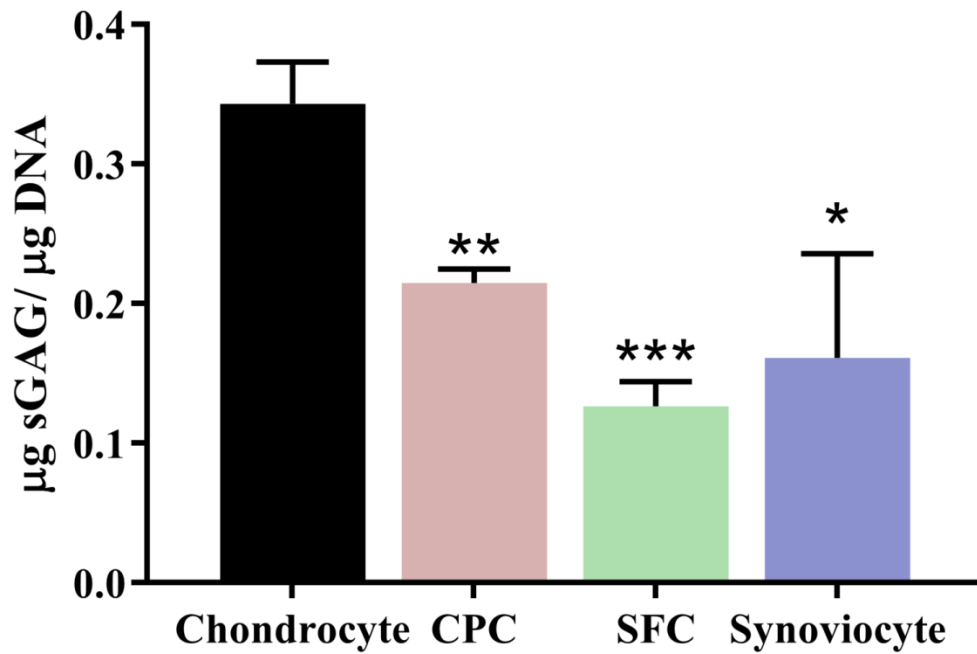
Figure 3.3 sGAG assay of chondrocytes, CPCs, SFCs and synoviocytes. sGAG assay legibly demonstrated the glycosaminoglycan contents in each cell type, revealing that chondrocytes contain the highest amount, and significant differences exist when comparing chondrocytes to the other cell types (n = 3 per group. *: $p<0.05$; **: $p<0.01$; ***: $p<0.001$)

	Baseline		-AMD3100 CPC-CM (%)					+AMD3100 CPC-CM (%)				
	Chondrocyte	CPC	0	20	40	60	80	0	20	40	60	80
VEGF												
β-act												
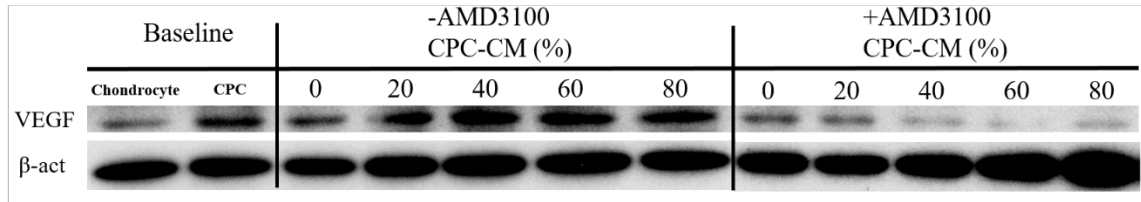
Figure 3.4 CPC-condition media stimulates chondrocyte VEGF expression. CPCs over-expressed VEGF compared to chondrocytes at basal level. In chondrocytes that were not treated with AMD3100 (Lanes 3-7), VEGF expression increased as the proportion of CPC-conditioned media increased from 0 to 20%. Expression peaked at 40% and declined slightly at the highest CPC-CM doses (60%, 80%). In contrast, CPC-CM had no effect on VEGF expression in chondrocytes treated with AMD3100 (Lanes 8-12). β-actin expression was used as an internal loading control. (CPC-CM: CPC-condition media)

Gene Symbol	Gene Title	Fold-Change	Description
CD105 (ENG)	endoglin	1.50	CPC up vs chondrocyte
CD166 (ALCAM)	activated leukocyte cell adhesion molecule	8.99	CPC up vs chondrocyte
NOTCH1	Notch homolog 1 Translocation-associated (Drosophila)	7.46	CPC up vs chondrocyte
CD44 (H-CAM)	CD44 molecule (Indian blood group)	13.18	CPC up vs chondrocyte
VCAM1	vascular cell adhesion molecule 1	9.93	CPC up vs chondrocyte
ABCG2	ATP-binding cassette, sub-family G (WHITE), member 2	10.51	CPC up vs chondrocyte
TFRC	transferrin receptor (p90, CD71)	3.25	CPC up vs chondrocyte
ITGB1	integrin, beta 1 (fibronectin receptor)	1.45	CPC up vs chondrocyte
KLF4	Kruppel-like factor 4 (gut)	2.38	CPC up vs chondrocyte

Table 3.1 Gene expression (stem/progenitor cell marker) comparison selected from microarray data.

Gene Symbol	Gene Title	Fold-Change	Description
PRG4 (lubricin)	proteoglycan 4	-1.93	CPC down vs chondrocyte
PRG4 (lubricin)	proteoglycan 4	1.27	CPC up vs synovial fluid cell
PRG4 (lubricin)	proteoglycan 4	-1.07	CPC down vs synoviocyte

Table 3.2 Gene expression comparison of interests selected from microarray data.

Gene Symbol	Gene Title	Fold-Change	Description
ADAMTS1	ADAM metallopeptidase with thrombospondin type 1 motif, 1	6.87	CPC up vs chondrocyte
ADAMTS4	ADAM metallopeptidase with thrombospondin type 1 motif, 4	8.37	CPC up vs chondrocyte
MMP3	matrix metallopeptidase 3 (stromelysin 1, progelatinase)	6.43	CPC up vs chondrocyte
MMP13	matrix metallopeptidase 13 (collagenase 3)	9.21	CPC up vs chondrocyte

Table 3.3. Gene expression (protease/matrix peptidase) comparison selected from microarray data.

CHAPTER 4

DISTINGUISH CHONDROGENIC PROGENITOR CELLS FROM CHONDROCYTES BY WHOLE GENE EXPRESSION

4.1 Background and significance

We have demonstrated the morphologically distinct CPCs could actively respond to injury associated alarmins (e.g. high-mobility group box 1 (HMGB1)) and migrate to cartilage damaged sites [60]. Contrasting the central dogma that chondrocytes are the only one cell type residing in cartilage, the identification of CPCs in cartilage proposes that CPCs also reside in cartilage and play pivotal roles in a variety of cartilage functionalities. Trauma-activated CPCs are more fibroblastic and dendritic in appearance, they are likely to be more proliferative and clonogenic than chondrocytes in cell culture system. CPCs also over-express many stem cell markers, such as CD105, CD44, Notch 1, and ABCG2 than chondrocytes.

As a capsule joint, synovium tissue encloses the whole knee joint and produces synovial fluid as nourishment source and major lubricant for articular cartilage [70]. Studies have shown that synoviocytes contribute to the progression of OA by secreting pro-inflammatory and chondrolytic cytokines into knee joints [71-73], even though synoviocytes support knee joint health under normal circumstance.

Taken these findings together, CPCs may be more akin to synoviocytes and synovial fluid cells (SFCs) phenotypically and functionally. In this chapter, we used microarray technique to profile global gene expression of CPCs and chondrocytes isolated from injured bovine osteochondral explants, synoviocytes from knee joint synovium tissue, and synovial fluid cells (SFCs) from joint knee fluid. Hierarchical analysis was perform to assess the general closeness among four cell types. Annotated gene expression heat maps

45

of four cell types were specially carried out based on their functionalities (inflammation, cytokine, collagen, extracellular matrix and metalloendopeptidase) for further specific inspection. Real-time PCR was performed to verify the expression difference of certain genes.

4.2 Hypotheses and specific aims

In this chapter, we hypothesized chondrogenic progenitor cells (CPCs) compose as a distinct cell type other than chondrocytes in cartilage of knee joints with following specific aims:

a) Examine the difference between CPCs and chondrocytes on whole gene expression level by microarray technique, including hierarchical cluster analysis, heat map comparison (global and annotated ones)

b) Compare CPCs with other knee joint synovial cells (synoviocytes and synovial fluid cells) in term of global gene expression pattern, matrix forming and inflammatory gene expression.

4.3 Materials and methods

4.3.1 Osteochondral explants harvest and culture

Fresh osteochondral explants (2.5×2.5 cm^2) was harvested from bovine tibia plateaus of healthy stifle joints (Bud's Custom Meats, Riverside, IA). After gentle rinse in Hank's Balanced salt solution (HBSS) (Invitrogen Life technologies, Carlsbad, CA), the explants were cultured in Dulbecco's modified Eagle's medium (DMEM) and Ham's F12 with a 1:1 mixture, supplemented with 10% fetal bovine serum (FBS) (Invitrogen Life

Technologies), 100 U/ml penicillin, 100 µg/ml streptomycin, and 2.5 µg/ml Amphotericin B at 37 ºC, 5% CO_2 and 5% O_2 for 2 days.

4.3.2 Chondrogenic progenitor cells (CPCs) and chondrocytes isolation

After 2-day equilibrium of culture media, a sterile needle (18 G) was dragged on the cartilage surface of the explant to aseptically create multiple matrix tears. The explants were then cultured for around 10 days with changing the culture media the every other day. For CPC isolation, the cartilage surface of each explant was treated with 0.25% Trypsin-EDTA (Gibco, Grand Island, NY) for 10 mins, culture media was added to end trypsinization, and cell suspension was then centrifuged at 300 G for 10 mins. Cells were resuspended and seeded as experiments' need. After isolation of CPCs, the underlying cartilage tissue was shaved off the subchondral bone, minced into smaller pieces, and digested in 0.03% collagenase/protease (dissolved in culture media) for 16 hrs. The digestion media was centrifuged (300 G for 10 mins) and resuspended, then seeded as experiments required. (Figure 3.1)

4.3.4 Synoviocytes and synovial fluid cells isolation and culture

Synovium tissues were collected from bovine knee joint and minced into smaller pieces (0.5 cm $\times$ 0.5 cm) to attach on culture dishes (Falcon, NJ). The culture media was added onto the synovium tissue drop by drop after 2-hour dry attachment (Figure 4.1). On the following day, more culture media was added using same culture media adding method to keep the tissue in a nutritious environment until the synovium tissue was no longer attached. The synovium tissue was then removed and the synoviocytes were remained and

47

cultured. For the synovial fluid cells (SFCs), synovial fluid was obtained from same bovine knee joints by sterile syringe, then mixed with culture media at 1:1 and cultured in incubator. Synoviocytes and SFCs were collected for further use when the cells reach 80 – 90% confluence.

4.3.5 RNA extraction

The RNA for gene expression analysis was isolated from passage two of four different kinds of cells (CPCs, chondrocytes, synoviocytes and SFCs) which were previously seeded into 6-well plates. The cells were homogenized in Trizol reagent (InvitrogenTM Life Technologies, CA, USA) and the total RNA was extracted by the RNeasy Mini Kit (Qiagen, CA, USA) according to the manufacturer's protocol.

After total mRNA was successfully extracted, the RNA concentration was measured according to the manufacturer's instruction through the use of a Nano-Drop spectrophotometer (Iowa Institute of Human Genetics Genomics Division, Iowa City, IA). The total RNA was further processed using microarray analysis, qPCR or stored at -80°C freezer for further use.

4.3.6 DNA microarray analysis

RNA was harvested from three independent batches of synoviocytes, SFCs, chondrocytes, two independent batches of CPCs. The RNA extraction procedure for each kind of cells was essentially identical as previously described (4.3.5). The RNA (50ng) was then reverse transcribed to single primer isothermal

48

amplification-amplified complementary DNA (cDNA) using an Ovation RNA Amplification System version 2 (NuGEN). Biotinylated cDNA was hybridized to Bovine Genome Arrays (Affymetrix). Arrays were scanned with an Affymetrix Model 3000, and the data was collected using GeneChip operating software (MAS 5.0). Statistical fold change expression was then applied via 1-way analysis of variance (ANOVA) model by using Method of Moments [74]. Fisher's Least Significant Difference (LSD) was employed as the contrast method. Heat maps and 5 annotated gene groups (metalloendopeptidase related, extracellular matrix related, collagen related, inflammatory related, cytokine related) were analyzed and created from the internal microarray database which discriminates a 5-fold change (either +5 or -5-fold change) between chondrocytes and CPCs. 3D Principle Component Analysis (PCA) plot and dendrogram were also generated using Partek Genomics Suite software.

4.3.7 Gene expression analysis

50 ng RNA of each cell samples was reverse transcribed to complimentary DNA by TaqMan reverse transcription reagents (Applied Biosystem, Grand Island, NY). qPCR reactions were then performed with SYBR Green reagent and custom specific Primers (Integrated DNA Technologies, Coralville, IA) (Table 4.1). All qPCR experiments were performed in triplicate for technical stability, and each gene expression level was normalized to β-actin. The fold change was calculated by the $2^{-\Delta\Delta Ct}$ method [75].

49

4.3.8 Statistical analysis

Data are reported as means +/- standard deviations. The statistical differences among four cell types in quantitative PCR analyses were evaluated by one-way analysis of variance (ANOVA) with Tuckey's post hoc test using SPSS software (Version 21). A two-tailed P-value < 0.05 was considered statistically significant.

4.4 Results

4.4.1 Gene expression profiling of chondrocytes, CPCs, SFCs, and synoviocytes

From the microarray assay, we detected and processed over 24,000 genes by the chip, which is specifically designed for the bovine species. These results showed that chondrocytes significantly over-expressed cartilage matrix markers such as Collagen II (COL2A1), Aggrecan (ACAN), Cartilage Oligomeric Matrix Protein (COMP) and Hyaluronan and Proteoglycan Link Protein (HAPLN) (20.5-fold, 5.9-fold, 76.9-fold and 1.8-fold, respectively) when comparing to CPCs. The same gene expression patterns were observed in chondrocytes versus SFCs (15.4-fold, 29.1-fold, 180-fold and 221-fold, respectively) and chondrocytes versus synoviocytes (16.1-fold, 39.1-fold, 145-fold and 433-fold, respectively). (Table 4.2)

Genes related to inflammation, Interleukin 6 (IL6), IL 8, Chemokine (C-C motif) ligand 2 (CCL2), Chemokine (C-X-C motif) Ligand 12 (CXCL12), were all up-regulated in CPCs compared to chondrocytes (225-fold, 9.7-fold, 32.3-fold and 12.1 fold, respectively). Similar fold changes compared with chondrocytes were observed for both SFCs (84.6-fold, 17.2 fold, 50-fold and 4.8-fold, respectively)

50

and synoviocytes (33-fold, 15-fold, 51.6-fold and 10.8-fold, respectively). (Table 4.2)

4.4.2 Heat maps and hierarchical clustering (dendrogram) analysis

A global gene expression heat map including all four cell types were generated based on genes expressed at levels that were five-fold higher or lower in CPCs than chondrocytes. Considering the overall gene expression pattern of chondrocytes, CPCs, SFCs and synoviocytes, the global 5-fold based heat map clearly showed that the CPCs were remarkably different when compared to chondrocytes and similar when compared to SFCs and synoviocytes. (Figure 4.2)

Five annotated heat maps (collagen, cytokine, extracellular, inflammatory and metalloendopeptidase) were generated based on the functionalities of genes that are filtered by the annotations of database. Despite some exceptions for specific genes, almost all the five heat maps showed that CPCs, SFCs, and synoviocytes were distinct from chondrocytes. (Figure 4.3)

4.4.3 3D principal component analysis (PCA) plot

In the context of the genes detected by the bovine genome chip, a 3D PCA plot was created to visually reveal the closeness of four cell types. (Figure 4.4) SFCs and synoviocytes are tightly distributed to each other demonstrating highest relatedness, while CPCs are much closer to SFCs and synoviocytes rather than normal chondrocytes (NCs). Since the inevitably existing batch variation, the three NCs are fairly distant to each other.

51

4.4.4 Quantitative real-time PCR validation of microarray results

Gene expression analysis revealed substantially lower expression of matrix forming marker genes in CPCs, synoviocytes, and SFCs when compared to chondrocytes. Collagen II expression in chondrocytes was 26-fold higher than synoviocytes, 34-fold higher than SFCs and 20-fold higher than CPCs. Aggrecan expression in chondrocytes was 368-fold higher than synoviocytes, 129-fold higher than SFCs and 3-fold higher than CPCs. Link Protein expression in chondrocytes was more than 10000-fold higher than synoviocytes, 215-fold higher than SFCs and 14-fold higher than CPCs. COMP expression in chondrocyte was 12-fold higher than synoviocytes, 25-fold higher than SFCs and 138-fold higher than CPCs. (Figure 4.5)

In addition, qPCR results showed the inflammatory gene expression in chondrocytes was down-regulated compared to CPCs, SFCs and synoviocytes. These results were fairly consistent with microarray data, except for the expression of IL6. IL6 expression in chondrocytes was 6.36-fold over synoviocytes, 2.05-fold over SFCs and 2.86-fold over CPCs. IL8 expression in chondrocytes was dramatically down-regulated, 0.0085-fold of synoviocytes, 0.0005-fold of SFCs and 0.122-fold of CPCs. CCL2 expression in chondrocytes was 0.012-fold of synoviocytes, 0.003-fold of SFCs and 0.402-fold of CPCs. CXCL12 expression in chondrocytes was 0.21-fold of synoviocytes, 0.835-fold of SFCs and 0.69-fold of CPCs. Meanwhile, IL6 expression in CPCs was 2.23-fold over synoviocytes and 0.72-fold of SFCs. IL8 expression in CPCs was 0.07-fold of

synoviocytes, 0.005-fold of SFCs. CCL2 expression in CPCs was 0.03-fold of synoviocytes and 0.008-fold of SFCs. CXCL12 expression in CPCs was 0.3-fold of synoviocytes and 1.21-fold over SFCs. (Figure 4.6)

For the transcriptional marker genes, SOX9 expression showed similar gene expression trend when compared to the matrix forming marker genes. Chondrocytes were 7-fold higher than synoviocytes, 2.6-fold higher than SFCs, and there was no significant difference between chondrocytes and CPCs. Chondrocytes were down-regulated compared to CPCs, SFCs and synoviocytes in term of RUNX2, a key transcription factor associated with osteoblast differentiation. (Figure 4.7)

4.5 Discussion and conclusion

Microarray technology confirmed that CPCs compose a distinct cell type that more resembles synoviocytes and SFCs than chondrocytes in cartilage. This finding is a critical challenge to the universal opinion that all cells residing in cartilage are chondrocytes. The global heat map and 3D PCA plot offered us the notion that CPCs are far away from chondrocytes in the regard of huge scale of genes and share substantial similarities with SFCs and synoviocytes. The hierarchical clustering analysis divided all four cell types into chondrocytes and non-chondrocyte group straightforwardly, conveying the idea of distinguishing between CPCs and chondrocytes. Additionally, the 5 annotated heat maps of selected functional categories of genes that are relevant to OA drew essentially the same conclusion as the global heat map.

53

qPCR analyses validated microarray results for the most part in term of ECM-forming and inflammation related genes. Significantly higher expression was observed in chondrocytes other than the other three cell types, and opposite trend appeared for pro-inflammatory genes. The gene expression differences of ECM-forming and inflammation paralleled differences in SOX9 expression, a crucial chondrogenic transcriptional factor that was expressed at high, moderate, and low levels by chondrocytes, CPCs, and synoviocytes/SFCs, respectively. However, IL-6 expression in qPCR and microarray are quite different, which may reflect deficiencies in the probes used in the microarrays to detect IL-6 mRNA splice variants expressed by chondrocytes [76].

Our previous work have shown that migrating CPCs could synthesize, produce and deposit lubricin on damaged cartilage surface [60], which is a key function of superficial zone chondrocytes. Moreover, consistent with superficial zone cartilage when compared with chondrocytes isolated from deeper zones cartilage [77], CPC pellets culture also showed relatively weak proteoglycan deposition. Taken these findings together, CPCs share more similarities with superficial zone chondrocytes rather than with deep zone chondrocytes [78], which also reflects many published researches documenting the recruitment and enrichment of CPCs in the superficial zone/surface of normal cartilage [1, 59]. Thus we speculated that CPCs, which originally reside in the superficial zone and remain in quiescent state, migrate onto the cartilage damaged surface and populate upon activation by injury.

To sum up, although the inferiority of CPCs in term of ECM forming function relative to chondrocytes suggested that CPCs might not be an optimal cell resource for cartilage matrix regeneration, CPCs still possess superior chondrogenic potency to synovial cells. More detailed comparisons to other candidate cell sources (such as MSCs, iPSCs, etc) for cartilage regeneration is highly needed. Instead, our findings provide an insight that CPCs are more inclined to be involved in alarmins initiated pro-inflammatory cascade in acute trauma of joints [79]. Particularly, the significantly higher expression of certain chemokines by CPCs indicates that they possess capacity to migrate toward specific chemoattractants (i.e. HMGB1) and amplify pro-inflammatory signals arising from cartilage injuries.
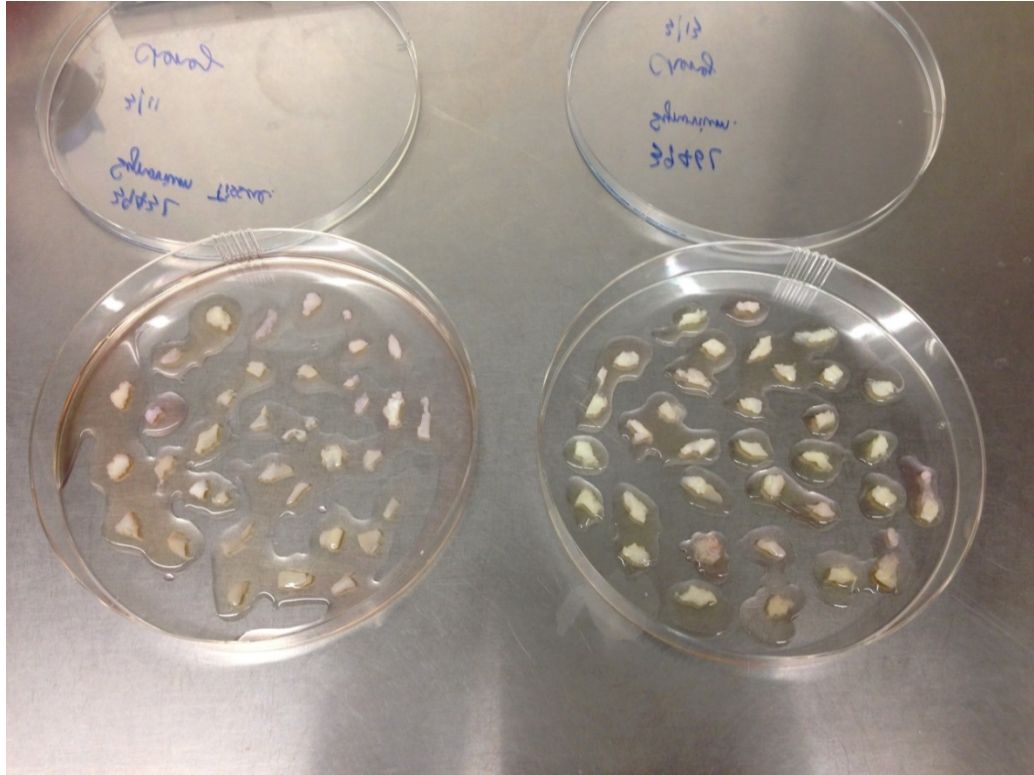
Figure 4.1 Synovium tissue attachment and culture technique. Dissect and stretch the synovium tissue to its maximal extension. After 2 hours of dry attachment, the tissue was replenished with small amount of culture media for the following days to keep the synovium nutritious.
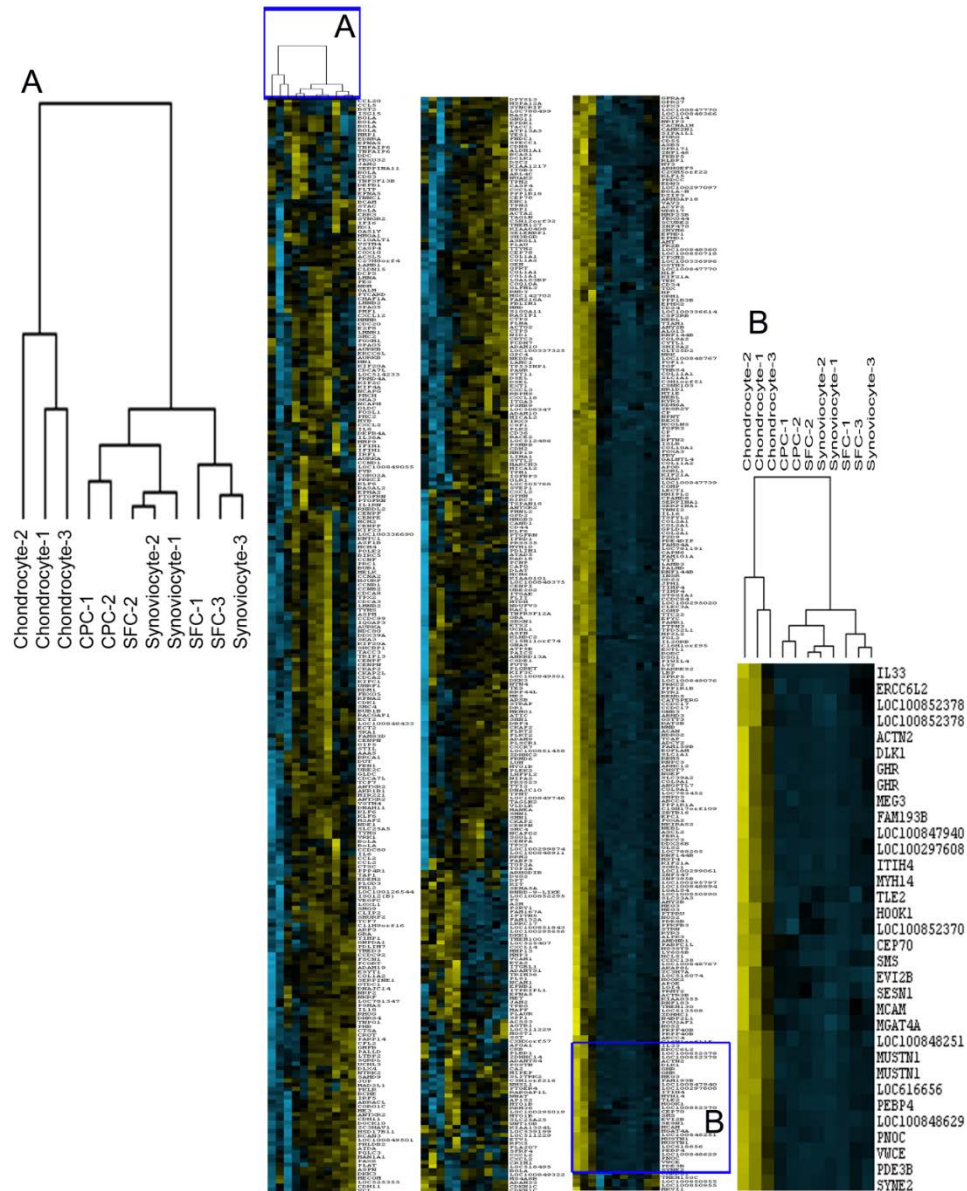
Figure 4.2 Global heat map and hierarchical cluster analysis of chondrocytes, CPCs, synoviocytes and SFCs. The 5-fold change based global heat map revealed the enormous difference between chondrocytes and CPCs as well as to show the similarities among CPCs, synoviocytes and SFCs (specific region was enlarged in B). The hierarchical cluster analysis showed the similarities among four cell types and directly divided all cell types into two major categories (chondrocytes and the other combined cell types) (dendrogram was enlarged in A).

57

Figure 4.3 Annotated heat maps based on various gene functions. Five gene function based annotated heat maps (A. metalloendopeptidase, B. collagen, C. cytokine, D. inflammatory, E. extracellular) exhibited the differences among four cell types.
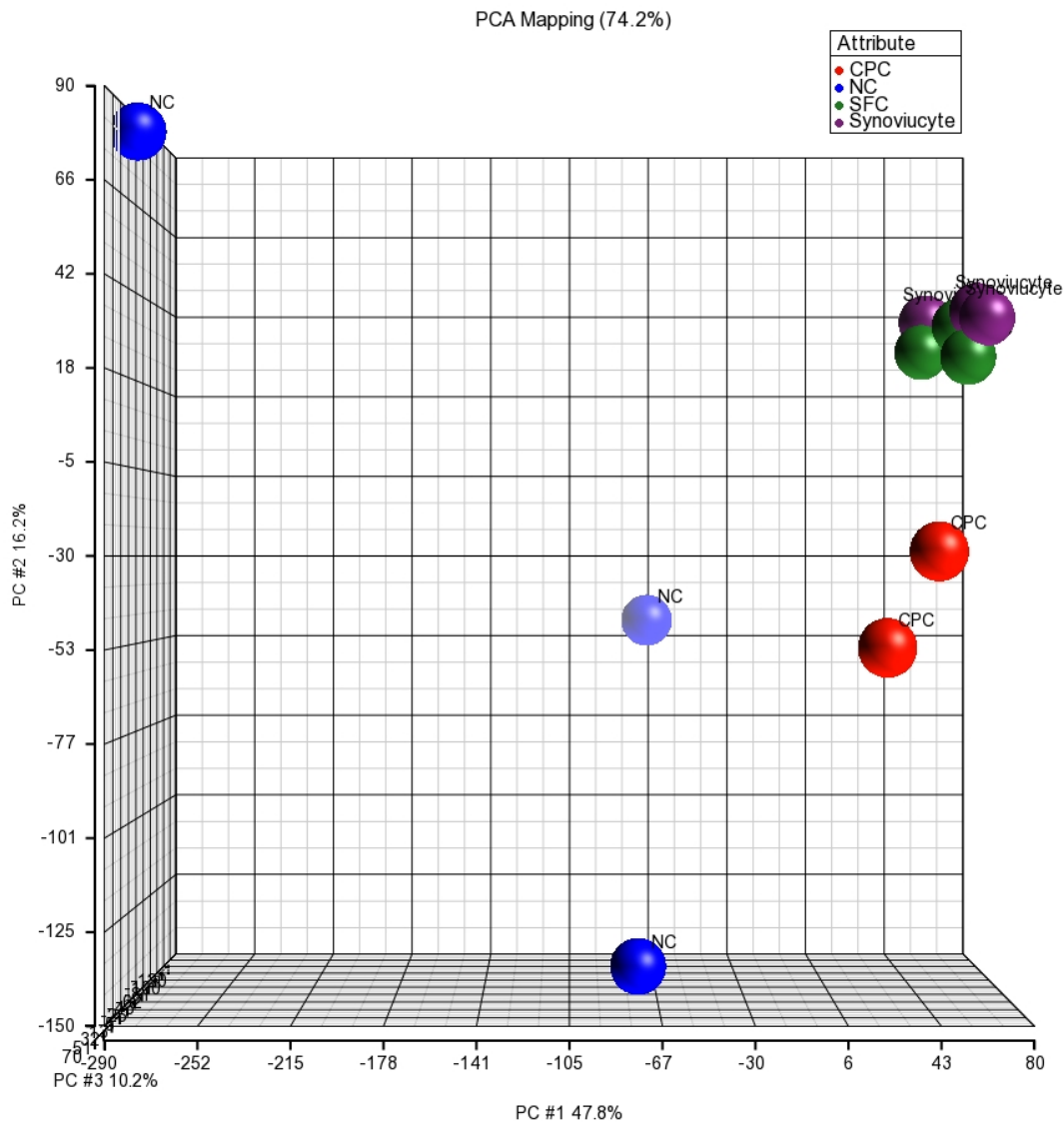
Figure 4.4 3D PCA plot demonstration. The 3D PCA plot visually revealed the closeness of four cell types. SFCs and synoviocytes are extremely close to each other, while CPCs are much closer to SFCs and synociocytes than to NCs. Noisy effect exists among normal chondrocytes (NCs) samples. (n = 3 for synoviocytes, SFCs and NCs, n = 2 for CPCs)

59

Matrix Forming Gene Expression
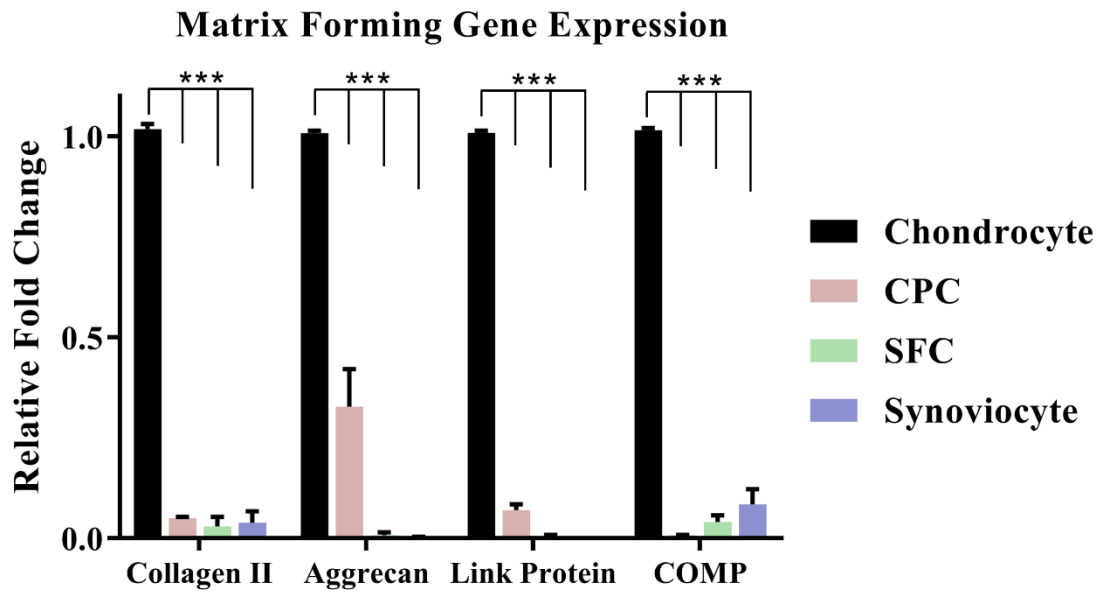
Figure 4.5 Matrix forming gene expression analysis. qPCR showed substantially higher expression of all matrix forming genes (Collagen II, Aggrecan, Link protein and COMP) in chondrocytes than in other three cell types. (n = 3 per group. ***: p<0.001)
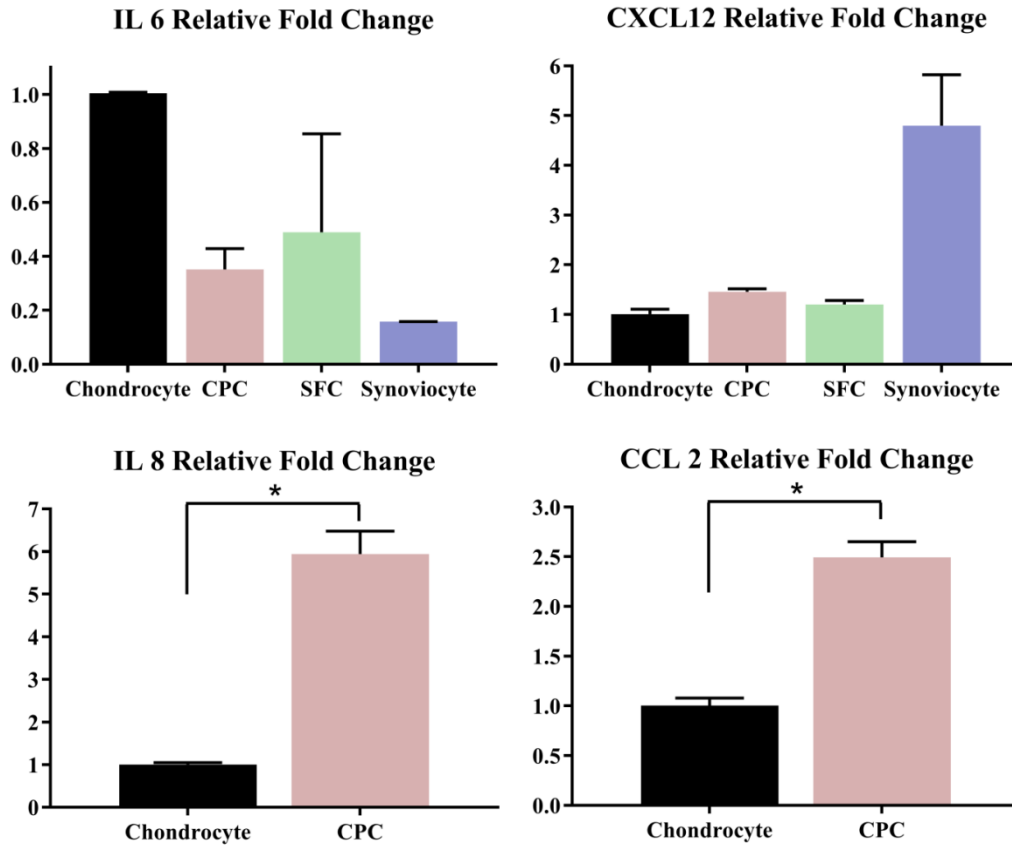
Figure 4.6 Inflammatory gene expression analysis. qPCR exhibited dramatically lower expression of most inflammatory related genes (IL8, CCL2 and CXCL12) in chondrocytes than in the other three cell types. Chondrocytes showed significantly up-regulated expression over synoviocytes and SFCs and significantly down-regulated expression of synoviocytes and SFCs in the context of SOX9 and RUNX2, respectively. (n = 3 per group. *: $p < 0.05$)

Transcriptional Gene Expression Relative Fold Change
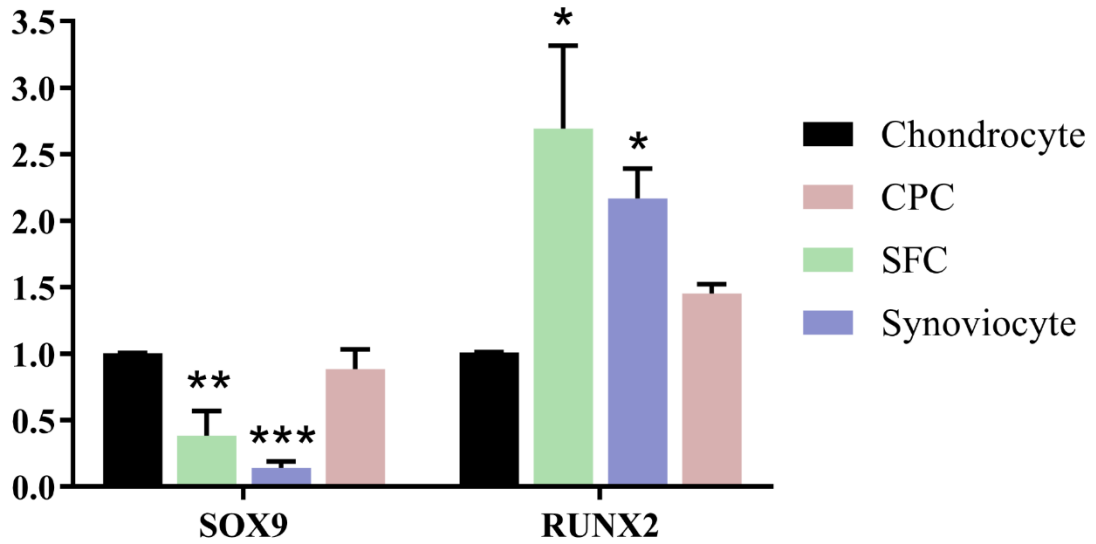
Figure 4.7 Transcriptional gene expression analysis Chondrocytes showed significantly up-regulated expression over synoviocytes and SFCs and significantly down-regulated expression of synoviocytes and SFCs in the context of SOX9 and RUNX2, respectively. (n = 3 per group. *: $p<0.05$; **: $p<0.01$; ***: $p<0.001$)

Gene	Forward primer 5' – 3'	Reverse primer 5' – 3'
β-actin	TCGACACCGCAACCAGTTCGC	CATGCCGGAGCCGTTGTCGA
Collagen Type II	AAGACGCAGAGCGCTGCTGG	GGGTCTCTACCGCGCCCTCA
Aggrecan	CAGCCAGGCCACCCTAGAG	GGGTGTAGCGCGTGGAGAT
Link Protein	ACTTCTTCTGGTGCTGATT	CTGTAGGGTCTCGGTAAA
COMP	TTCGGAACGCACTGTGG	TGCAGGAACCAGCGGTA
IL6	GGCTGCTCCTGGTGATGACT	CTCCTTGCTGCTTTCACACTCA
IL8	CCACACCTTTCCACCCCAAA	CCTTGGGGTTTAGGCAGACC
CXCL12	GCTCCACGTAGAACTGCCAT	AGGGAGAGGCTGGGAATGAT
CCL2	TCGCTGCAACATGAAGGTCT	TATAGCAGCAGGCGACTTGG
SOX9	ACGCCGAGCTCAGCAAGA	CACGAACGGCCGCCTCT
RUNX2	CGCACCGACAGCCCCAACTT	CTTGAAGGCCACGGGCAGGG

Table 4.1 Primer information for quantitative real-time PCR.

Gene Symbol	Gene Title	Fold-Change (CPC vs. chondrocyte)	Fold-Change (CPC vs. SFC)	Fold-Change (CPC vs. Synoviocyte)	Fold-Change (chondrocyte vs. SFC)	Fold-Change (chondrocyte vs. synoviocyte)
COL2A1	collagen, type II, alpha 1	-20.54	-1.33	-1.27	15.42	16.13
ACAN	Aggrecan	-5.94	4.89	6.58	29.06	39.06
COMP	cartilage oligomeric matrix protein	-76.92	2.35	1.89	180.39	145.06
HAPLN1	hyaluronan and proteoglycan link protein 1	-1.84	120.11	235.43	220.97	433.11
IL6	interleukin 6 (interferon, beta 2)	225.32	2.66	6.82	-84.63	-33.05
IL8	interleukin 8	9.75	-1.77	-1.54	-17.21	-14.98
CXCL12	chemokine (C-C motif(ligand 2	12.11	2.52	1.12	-4.81	-10.77
CCL2	chemokine (C-X-C motif) ligand 12	32.26	-1.49	-1.60	-47.98	-51.64
COL1A1	collagen, type I, alpha 1	44.48	-1.04	-1.06	-46.14	-47.10

Table 4.2 Gene expression (matrix forming/inflammatory) comparison selected from microarray data.

CHAPTER 5

ENHANCED PHAGOCYTOSIS CAPACITY IN CHONDROGENIC PROGENITOR CELLS

5.1 Background and significance

We have identified the emergence of CPCs upon cartilage injury and illuminated some fundamental functions of CPCs. We also distinguish CPCs from chondrocytes on gene expression level, setting them as a separate cell type in cartilage, they behave more akin to synoviocytes and synovial fluid cells morphologically and functionally.

Phagocytosis is referred to the engulfment and degradation of extracellular substances by certain cells. Engagement of surface receptors with ligands leads to internalization via phagosomes and endosomes, and followed by degradation in lysosome. Clearing pro-inflammatory debris from necrotic tissue and cells is a crucial event in immune system responding tissue damage and maintaining local homeostasis. Many cell types are capable of chemotaxis and phagocytosis, including macrophages, monocytes, and neutrophils. Synovial cells from synovium are well known as specialized macrophages. Derived from blood-borne mononuclear cells, they are non-fixed cells that can phagocytose actively cell debris and wastes in the joint cavity, and possess an antigen-presenting ability [80]. Phagocytosis occurs regularly in vascularized tissue where macrophages can easily relocate and scavenge debris. It is unlikely and unfavorable that distant macrophages and synoviocytes from vascularized synovium migrate to damaged cartilage in large number. This important phenomena led us to consider the phagocytosis function of CPCs after cartilage injury, since major chondrocytes in cartilage were entrapped by surrounding extracellular matrix. Limited migration results in chondrocytes' unresponsiveness to chemokines with weak debris scavenging ability [60].

65

In this chapter, we used confocal microscopy and flow cytometry analyses to compare CPCs and chondrocyte in term of the internalization of fluorescently labelled debris from cells and ECM as initial tests. Secifically, DiO (3-octadecyl-2-[3-(3-octadecyl-2(3H)-benzoxazolylidene)-1-propenyl]-, perchlorate) and FITC (fluorescein isothiocyanate) were used to fluorescently label cell debris and fibronectin fragments (Fn-fs), respectively. Despite the fact that fibronectin is a minor cartilage matrix component, they drive chondrolysis in injured cartilage, which makes them a high-priority target for scavenged [81]. Macrophages, synoviocyte and chondrocytes from superficial zone were also included for the quantitative comparison. Furthermore, lysosomal activities, represented by cathepsin B activity, was evaluated to see the degradation of engulfed cell debris. The relative expression of phagocytosis related markers in CPCs and chondrocytes were also assessed by qPCR and western blot.

5.2 Hypotheses and specific aims

In this chapter, we hypothesized CPCs could phagocytose cartilage debris either from cell or extracellular matrix (ECM) more effectively than chondrocytes with following specific aims:

a) Evaluate CPCs and chondrocytes phagocytic capacity of cell debris and ECM protein fragments.

b) Quantify the phagocytosis positive cell percentage in each cell type, including macrophages as positive control, and other related cells from knee joint.

c) Determine the gene & protein expression of phagocytosis related markers of CPCs and chondrocytes.

d) Assess the lysosome activity & indicator of CPCs and chondrocytes.

e) Evaluate debris degradation in CPCs and chondrocytes post engulfment.

5.3 Materials and methods

5.3.1 Osteochondral explants harvest and culture

Fresh osteochondral explants (2.5×2.5 cm^2) was harvested from bovine tibia plateaus of healthy stifle joints (Bud's Custom Meats, Riverside, IA). After gentle rinse in Hank's Balanced salt solution (HBSS) (Invitrogen Life technologies, Carlsbad, CA), the explants were cultured in Dulbecco's modified Eagle's medium (DMEM) and Ham's F12 with a 1:1 mixture, supplemented with 10% fetal bovine serum (FBS) (Invitrogen Life Technologies), 100 U/ml penicillin, 100 µg/ml streptomycin, and 2.5 µg/ml Amphotericin B at 37 ℃, 5% CO2 and 5% O2 for 2 days.

5.3.2 Chondrogenic progenitor cells (CPCs) and chondrocytes (whole thickness) isolation

After 2-day equilibrium of culture media, a sterile needle (18 G) was dragged on the cartilage surface of the explant to aseptically create multiple matrix tears. The explants were then cultured for around 10 days with changing the culture media the every other day. For CPC isolation, the cartilage surface of each explant was treated with 0.25% Trypsin-EDTA (Gibco, Grand Island, NY) for 10 mins, culture media was added to end trypsinization, and cell suspension was then centrifuged at 300 G for 10 mins. Cells were resuspended and seeded as experiments' need. After isolation of CPCs, the underlying

67

cartilage tissue (whole thickness) was shaved off the subchondral bone, minced into smaller pieces, and digested in 0.03% collagenase/protease (dissolved in culture media) for 16 hrs. The digestion media was centrifuged (300 G for 10 mins) and resuspended, then seeded as experiments required. (Figure 3.1)

5.3.3 Isolation and culture of other related cells (synoviocytes, superficial zone chondrocytes, macrophages)

Synovium tissues were collected from bovine knee joint and minced into smaller pieces (0.5 cm × 0.5 cm) to attach on culture dishes (Falcon, NJ). The culture media was added onto the synovium tissue drop by drop after 2-hour dry attachment. On the following day, more culture media was added using same culture media adding method to keep the tissue in a nutritious environment until the synovium tissue was no longer attached. The synovium tissue was then removed and the synoviocytes were remained and further cultured.

Chondrocytes from the upper 1/3 cartilage were also prepared by separating from the bottom 2/3 prior to cell isolation using a customized fixture [82]. (Figure 5.1) All cells were allowed to adapt to culture conditions for two days in culture media.

The mouse macrophages cell line (RAW 264.7) was a generous gift obtained from Dr. Wendy Maury (The University of Iowa). Macrophages were cultured in macrophage-specific culture media (DMEM supplemented with 10% fetal bovine serum, 100 U/ml penicillin, 100 μg/ml streptomycin, and 2.5 μg/ml fungizone)

68

5.3.4 Generation of DiO-labeled cell debris

The lipophilic fluorescent tracer DiO (3-octadecyl-2-[3-(3-octadecyl-2(3H)-benzoxazolylidene)-1-propenyl]-perchlorate) was used to label isolated chondrocytes in suspension. DiO solution (Molecular Probes, Eugene, OR) was added at concentration of 5 µl/ml to 10^6 cells/ml cell suspension for 20 mins at 37 ºC. The mixture was then centrifuged (1500 rpm for 5 mins) and resuspended in 2 ml culture media (around 1×10^7 cells), 10 freeze-thaw cycles (liquid nitrogen and 37 ºC water bath for 20 mins, alternatively) were applied to generate the DiO-labeled cell debris.

5.3.5 Generation of FITC-labeled fibronectin fragments (Fn-fs)

Human fibronectin fragments (Fn-fs) mixture, containing Fn-fs of 29 kDa, 40-60 kDa and 120-160 kDa (generated by Dr. Gene Homandberg) was dialyzed against 0.1 M $NaHCO_3$ for 6 hrs, then incubated with FITC stock solution (3 mg/ml) at the ratio of 1:170 (Fn-fs : FITC) for 2 hrs at room temperature. FITC conjugated Fn-fs solution was then dialyzed against $1\times$ PBS exhaustively to remove excess materials.

5.3.6 Detection and quantification of debris (from cell or ECM) ingested cells

After 1 – 2 days culture of CPCs and chondrocytes, DiO-labeled cell debris (100 µl) or FITC-labeled Fn-fs (optimal loading amount determined by does-dependent assay) was added to each dish (35 mm), the cells were then cultured for multiple time periods (3 hrs, 6 hrs, 12 hrs, and 24 hrs). For confocal microscopy

69

analysis, cells were washed with Hanks' solution and stained with 1 µM Calcein Red-Orange (Invitrogen, Grand Island, NY) for 30 mins. As for flow cytometry analysis, cells were trypsinized after washing in Hanks' solution, and then suspended in 1 ml culture media in 5 ml Falcon Polystyrene Tubes (BD Bioscience, San Jose, CA). Hoechst 33258 (BD Bioscience, San Jose, CA) at concentration of 4 µg/ml was added to each sample to label dead cells. To find the optimal loading amount of FITC-labeled Fn-fs for flow cytometry analysis, does-dependent assay (0.1 µg, 0.5 µg, 1 µg and 5 µg) was performed to evaluate the comparable difference between CPCs and chondrocytes.

5.3.7 Detection and quantification of lysosomal activity

After 1 – 2 days culture, CPCs and chondrocytes were subjected to DiO-labeled cell debris (100 µl) for 12 hrs, then stained with cathepsin B substrate and Hoechst 33342 provided in VIVAprobeTM Lysosome Assay Kit (VIVA Bioscience, UK) according the manufacturer's instruction for microscopy analysis. Similar as described above in 5.3.5, cell suspension was also prepared and quantified by flow cytometry.

5.3.8 Pulse-chase experiment of cell debris degrading time evaluation

CPCs and chondrocytes, incubated with DiO-labeled cell debris (100 µl), were also treated with or without 4 µM Z-Phe-Gly-NHO-Bz-pMe, a cathepsin B inhibitor (Calbiochem, Billerica, MA) for 12 hrs. The cells were then washed with Hanks solution three times and were cultured for an additional 12 hrs or 24 hrs with or without

70

cathepsin B inhibitor. The cells were then isolated and processed for flow cytometry analysis.

5.3.9 RNA extraction & gene expression analysis for phagocytosis related markers

The RNA for gene expression analysis was isolated from primary cells (CPCs and chondrocytes) which were previously seeded into 6-well plates. The cells were homogenized in Trizol reagent (InvitrogenTM Life Technologies, Carlsbad, CA) and the total RNA was extracted by the RNeasy Mini Kit (Qiagen, Valencia, CA) according to the manufacturer's protocol.

After total mRNA was successfully extracted, the RNA concentration was measured according to the manufacturer's instruction through the use of a Nano-Drop spectrophotometer (Iowa Institute of Human Genetics Genomics Division, Iowa City, IA). 50 ng RNA of each cell samples was reverse transcribed to complimentary DNA by TaqMan reverse transcription reagents (Applied Biosystem, Grand Island, NY). qPCR reactions were then performed with SYBR Green reagent and custom specific Primers (Integrated DNA Technologies, Coralville, IA) (Table 5.1). All qPCR experiments were performed in triplicate for technique stability, and each gene expression level was normalized to β-actin. The fold change was calculated by the $2^{-\Delta\Delta Ct}$ method [75].

5.3.10 Western blot analysis for phagocytosis related markers

Lysosomal – associated membrane protein 1 (LAMP1), CD 68, CD 14, and GULP1 were analyzed by western blot, primary CPCs and chondrocytes with or

71

without cell debris (100 µl), were seeded in 6-well plates. Cells were lysed in cold lysis buffer when cells were confluent and total protein concentration was determined with the BCA Protein Assay Kit (Thermo Fisher Scientific, Rockford, IL). Proteins were denatured with $2\times$ sample buffer, 5 µg protein of each cell lysate sample was resolved in 12.5% SDS gels and blotted onto nitrocellulose membranes, after blocking with 5% non-fat milk for 1 hr, the blots were incubated at 4ºC overnight with LAMP1, CD 68, CD 14, GULP1, and β-actin antibody respectively. The blots were incubated with horseradish peroxidase-conjugated anti-mouse IgG for LAMP1, CD 68, CD 14, and anti-rabbit IgG for GULP1 and β-actin in 5% BSA in TBST for 1 hr at room temperature, followed by reaction with Super Signal West Dura Chemiluminescent Substrate (Thermo Fisher Scientific, Rockford, IL). Chemiluminescence signals were detected with Kodak Biomax Xar film (Sigma Aldrich, Rochester, NY)

5.3.11 Immunocytochemistry staining for phagocytosis related markers

Fresh isolated CPCs and chondrocytes were seeded at 8-well chamber slides (1×10^5 cells/chamber) and cultured for 2 days to reach confluency. Cells were washed with ice cold $1\times$ PBS (three times 5 mins each), 4% paraformaldehyde was used to fix cells for 10 mins at room temperature. 0.1% Triton X-100 was then applied to each chamber for cell permeabilization followed with PBS washing for three times. Cells were further blocked for 40 mins at room temperature (25 ml blocking solution: 2.5 ml goat serum + 0.25 g BSA + 25 µl Tween 20 + 22.5 ml PBS) and wash cells with PBS for three times. Cells were incubated with primary

antibodies (CD 14, CD 68, GULP1 and LAMP1) for overnight at 4 ℃ (antibodies diluted as 1:100, 1:100, 1:100 and 1:250, respectively). After three times of PBS wash, cells were further blocked for 40 mins and followed with Alexa 488 conjugated secondary antibody (Central Microscopy Research Facility, University of Iowa) incubation (1:250 dilution) for 30 mins at room temperature in dark. After three times of PBS wash, chambers were removed and slides were mounted as well as counterstained with DAPI (VECTASHIELD Antifade Mounting Medium with DAPI). Slides were then examined under confocal microscopy.

5.3.12 Immunohistochemistry staining for LAMP1

Fresh cartilage was either surface scratched or non-scratched and continued to be cultured for 10 days. Full thickness cartilage was removed from underlying subchondral bone. Cartilage tissue was frozen sectioned vertically. Sectioned samples were further stained for LAMP1 expression. Briefly, 4% paraformaldehyde was used to fix cartilage tissue for 10 mins at room temperature. Samples were further blocked for 40 mins at room temperature (blocking solution: 2.5 ml goat serum + 0.25 g BSA + 25 µl Tween 20 + 22.5 ml PBS) and washed with PBS for three times. Tissue samples were incubated with LAMP1 primary antibody (1:250 dilution) for overnight at 4 ℃. After three times of PBS wash, Slides were further blocked for 40 mins and followed with secondary antibody (Central Microscopy Research Facility, University of Iowa) treatment (1:250 dilution) for 30 mins at room temperature in dark. After three times of PBS wash, Tissue samples were counterstained with DAPI (VECTASHIELD Antifade

73

Mounting Medium with DAPI) and mounted with coverslip. Slides were then examined under confocal microscopy.

5.3.13 Statistical analysis

Data were presented as means +/- standard deviations. Statistical analyses were performed with IBM SPSS (Version 23) and charts were generated by GraphPad Prism 7. All data were assumed to be independent. For phagocytosis+ cell quantification, CPCs and chondrocytes (whole thickness) were isolated from three independent bovine explants, synovium tissue and chondrocytes (superficial zone) were isolated from another three independent bovine explants, and macrophages were from three batches of the Raw 264.7 cell line. Two-sided two-sample t-test was applied to assess the difference between CPC and chondrocytes (from whole thickness and superficial zone, respectively) at each time point (3 hrs, 6 hrs, 12 hrs, and 24 hrs). For lysosome activity assessment and pulse-chase experiments, CPCs and chondrocytes of each group were isolated from three independent bovine explants and two-sided two-sample t-test was performed to evaluate difference between CPCs and chondrocytes, as well as two groups of CPCs (12 hrs versus 12 hrs with cathepsin B inhibitor and 24 hrs versus 24 hrs with cathepsin B inhibitor). For gene expression analysis, CPCs and chondrocytes were isolated from three independent bovine explants and each data point was the mean of three technical repeats. Two-sided two-sample t-test was used to evaluate gene expression difference between CPCs and chondrocytes. A two-tailed P-value < 0.05 was considered statistically significant.

74

5.4 Results

5.4.1 Phagocytosis activity comparison between CPCs and chondrocytes

For cells added with cell debris, it showed that both CPCs and chondrocytes were labelled with DiO florescence (green); however, most of the label in CPCs was intracellular, whereas most chondrocyte labeling was on the cell surface. (Figure 5.2) For cells treated with FITC labeled Fn-fs, similar phenomenon was observed. Florescent signal were detected inside CPCs, but not in chondrocytes. (Figure 5.3)

5.4.2 Quantitative analysis of phagocytosis activity comparison among CPCs, chondrocytes, synoviocytes and macrophages

For cell debris treated samples, flow cytometry analysis quantitatively confirmed that the percentage DiO+ CPCs was significantly higher than chondrocytes at each time point (3 hrs, 6 hrs, 12 hrs, and 24 hrs). (Figure 5.4.A) In addition, DiO+ CPCs increased dramatically (12.6% for 3 hrs, 28.6% for 6 hrs) and peaked at 12 hrs (68.1%). Notably, CPCs were in the same level with macrophages at first two time points (DiO+ macrophages were 11.5%, 26.4% for 3 hrs, 6 hrs, respectively), and surpassed macrophages (54.4%) at 12 hrs, macrophages (66.0%) reversed over CPCs (46.8%) at 24 hrs, while DiO+ chondrocytes (from whole thickness) augmented gradually (4.2%, 6.7%, 8.1%, and 11.6% for each time point, respectively), superficial zone chondrocytes were slightly higher than chondrocytes from whole thickness (4.9%, 7.6%, 11.3% and 18.8% for each time point, respectively), but no significant zone-related

75

differences were observed. DiO+ synoviocytes showed similar increasing pattern with macrophages throughout the whole time course. (Figure 5.4.B)

For Fn-fs treated samples, 4 different loading amounts (0.1 µg, 0.5 µg, 1 µg and 5 µg) were applied to each well (35mm), noticeable and comparable difference was detected in samples of 1 µg loading amount. (Figure 5.5) Thus, 1 µg loading amount was applied for following quantitative experiments. Flow cytometry analyses confirmed that the percentage Fn-fs+ CPCs was significantly higher than chondrocytes at all 4 time points. (Figure 5.6.A) Moreover, similar with cell debris scenario, Fn-fs CPCs increased dramatically (9.7% for 3 hrs and 37.45% for 6 hrs) and peaked at 12 hrs (56.1%), while Fn-fs+ chondrocytes elevated steadily (5.65%, 11.39%, 18.65% and 26.3% for each time point, respectively). (Figure 5.6.B)

5.4.3 Lysosomal activity comparison between CPCs and chondrocytes

The activities of cathepsin B, a major lysosomal protease degrading polypeptides and proteins, of CPCs and chondrocytes were stained to be assessed. Confocal microscopy imaging indicated that almost all the cytoplasm of CPCs was red-fluorescent, while significantly dimmer red-fluorescent signal was detected in chondrocytes. Moreover, DiO-labeled cell debris (green florescence) were also detected in the cytoplasm of CPCs, while not detectable inside chondrocytes. (Figure 5.7.A) This revealed greater per cell lysosome activity in CPCs. This impression was further confirmed by flow cytometry analysis, which exhibited an

76

average of 3.1-fold higher signal intensity in CPCs over chondrocytes. (Figure 5.7.B)

The pulse-chase experiment revealed that the percentage of CPCs with internalized debris decreased after removing the debris from 39.2% at 12 hrs post-removal to 28.7% at 24 hrs post-removal, while chondrocytes maintained essentially the same level at the two time points (12.9% at 12 hrs and 13.5% at 24 hrs). The percentage of positive CPCs was significantly higher at both time points when treated with cathepsin B inhibitor (53.4% at 12 hrs at 33.0% 24 hrs). In contrast, cathepsin inhibition had minimal effects on chondrocyte debris ingestion, and the percentage of positive chondrocytes remained at similar (11.2% positive at 12 hrs and 16.2% positive at 24 hrs). (Figure 5.8)

5.4.5 Quantitative real-time PCR analysis and microarray data of phagocytosis related markers

Gene expression analysis revealed significantly higher expression of all phagocytosis related markers in CPCs versus chondrocytes (4.9 fold, 4.5 fold, 3.8 fold and 3.5 fold for CD 68, CD 14, GULP1 and LAMP1, respectively). (Figure 5.9)

5.4.6 Western blot analysis of phagocytosis related markers

Lysate samples from CPCs possessed significantly enhanced band signals compared to samples from chondrocytes, indicating increased CD 14, CD 68, and LAMP1 expression. Moreover, significantly higher expression of these three

phagocytosis related markers were observed when samples were induced by cell debris in chondrocytes, but no obvious change found in chondrocytes. It should be noted that no significant difference was found between CPCs and chondrocytes in the context of GULP1 expression. (Figure 5.10)

5.4.7 Immunocytochemistry/immunohistochemistry staining of phagocytosis related markers

For the immunocytochemistry staining, higher fluorescence signals were detected in CPCs for all phagocytosis markers (CD 14, CD 68, GULP1 and LAMP1), indicating significantly greater expression of these markers in CPCs rather than chondrocytes. (Figure 5.11)

For the LAMP1 immunohistochemistry staining, noticeable LAMP1 expression was observed along the whole thickness cartilage tissue in the scratched sample, enhanced fluorescence signal were detected in cartilage surface/superficial zone. Although non-scratched sample also indicate mild expression in surface layer, the overall fluorescent signal were substantially dimmer when comparing with surface-scratched sample. (Figure 5.12)

5.5 Discussion and conclusion

With these series of extensive experiments, CPCs were able to be characterized in a more detailed fashion with emphasis on the phagocytosis function. Cartilage debris, either from cells (apoptotic or necrotic) or ECM, were internalized by CPCs more avidly than chondrocytes. The percentage of CPCs

78

with intracellular cell debris was upregulated by almost 6-fold, from 12% at 3 hours, to 68% at 12 hours. Comparable increase were found in synoviocytes and macrophages in term of the uptake of cell debris. Nevertheless, chondrocytes isolated from the top 1/3 of the cartilage did not show any significant difference comparing to the whole thickness chondrocytes. Relative to chondrocytes, phagocytosis related markers were also significantly over-expressed in CPCs at both mRNA and protein level, validated by real-time PCR and western blot, respectively. These results were consistent with relative boost of lysosomal mass and cathepsin activity in CPCs. Our microarray data also indicate that majority of cathepsin family and phagocytosis related genes were substantially over-expressed in CPCs rather than chondrocytes. (Table 5.2) Moreover, immunostaining of cells and cartilage tissue revealed that phagocytosis related markers were highly over-expressed in CPCs and surface-scratched cartilage tissue, coinciding with the above experiment results. More importantly, the enhanced LAMP1 expression in superficial zone of both normal and surface-scratched cartilage tissue might provide some hints that CPCs, remaining quiescent, reside in cartilage superficial zone before injury and become highly active provoked by injury.

Fn-fs, a form of ECM debris which induces the chondrolytic events of chondrocytes with possibilities that competes interleukin-1 β [83], internalization in CPCs also provides a spectacular insight to our hypothesis, indicating CPCs' consistently superior uptake of debris from both cells and cartilage matrix. A majority of fibronectins locate in pericellular matrices, where proteolytic fragments are seemed to easily affect matrix synthesis via integrin and toll-like

79

receptors [84]. Our previous work showed that Fn-fs were highly elevated in cartilage which provoked activation and chemotaxis of CPCs [81]. The clearance of Fn-fs by CPCs might be significantly crucial in order to biologically stabilize cartilage matrix synthesis/degradation balance, as a major threat that Fn-fs possessed to proteolyze cartilage matrix.

The phagocytosis related protein markers chosen for this set of analyses have been applied to identify a variety of cells associated with phagocytosis events, including cells isolated from the monocyte-macrophage lineage [85-88]. However, their expression have not been illustrated in stem/progenitor cells. Although most phagocytosis-related markers (CD14, CD68, LAMP1) were significantly over-expressed in CPCs over chondrocytes, confirmed by both western blots and immunocytochemistry staining methods. GULP1 expression seemed to be an exception in the context of western blot, contrasting immunocytochemistry staining. The reason remains unclear to us, but might be explained that the GULP1 antibody we used for western blot is application-specific [89].

It is well known that inflammatory related cells originated from hematopoiesis are attracted by alarmins from necrotic and apoptotic cells in vascular system. After binding with immune receptors, chemotaxis and phagocytosis of certain immunocytes are greatly enhanced to injured tissue with ensuring inflammatory reactions toward clearing and debriding injuries [90]. Since cartilage is free of vascular system, how this procedures unfold in injured cartilage is still unclear. Our findings to data suggest that CPCs could provide

80

similar debris clearing capacities as macrophages and other professional phagocytes. Consistently with our previous data, which showed that alarmin-activated CPCs over-expressed pro-inflammatory chemokines and cytokines including IL8 and CXCL12 [61], this indicates the potential for a CPC-initiated pro-inflammatory cascade similar to that initiated by immunocytes in wounded sites. Notably, since CPCs also possess phagocytic capabilities that ultimately quench the alarmin signaling driving inflammation, like macrophages they may be empowered to complete the inflammatory cycle and make way for tissue regeneration. However, additional experiments are needed to characterize the fate of the debris internalized by CPCs before we can conclude that they are fully capable of debris clearance in this setting.

In addition to CPCs, other cells, including synoviocytes, mesenchymal stem cells and dendritic cells, originating from knee joint also showed debris scavenging capacities and are likely to respond to heal some injured joint tissue [91-97]. Nonetheless, the favor goes entirely to CPCs in cartilage scenario since those cells must migrate relatively long distance to reach cartilage injured sites, in which might be also impeded by the anti-adhesive lubricin existing on cartilage surfaces. This problematic issue is obviously alleviated by CPCs, which are activated and attracted from local cartilage near injured sites where lubricin coating is typically extinct. The advantages of CPCs' scavenging function would appear to be important for repairing cartilage injuries, as CPCs residing near cartilage defects easily migrate into and populate scaffolds, where they can be induced to regenerate hyaline cartilage *in situ*[98]. Even if these processes never

81

occur spontaneously *in vivo*, there is clearly some intrinsic repairing potential available to exploit therapeutically.

Although, significant findings have been revealed in CPCs' scavenging capacity towards cartilage wound healing, the results of our analyses should be interpreted with some caution. First, the debris that was not labeled by the lipophilic DiO (e.g. non-membrane proteins, mitochondrial DNA) might be internalized by CPCs and chondrocytes at different rates. This may cause divergence in term of phagocytosis performance exhibited in our results. Second, the freeze-thaw cycles we used to generate cell debris might not generate same mixture of cell debris from necrosis and apoptosis. Since it is well established that apoptotic bodies engulfed by macrophages are likely to moderate the inflammatory responses (chemotaxis and phagocytosis), thus, if the engulfment of apoptotic bodies in CPCs is assumed to be in the similar level of macrophages, weaker phagocytosis events might be expected *in vivo* than indicated in our experimental setting, which based on cell debris purely from necrosis. Last but not least, we cannot rule out the possibility that ECM synthesized and produced by chondrocytes could hinder debris from binding and interacting phagocytosis associated receptors.
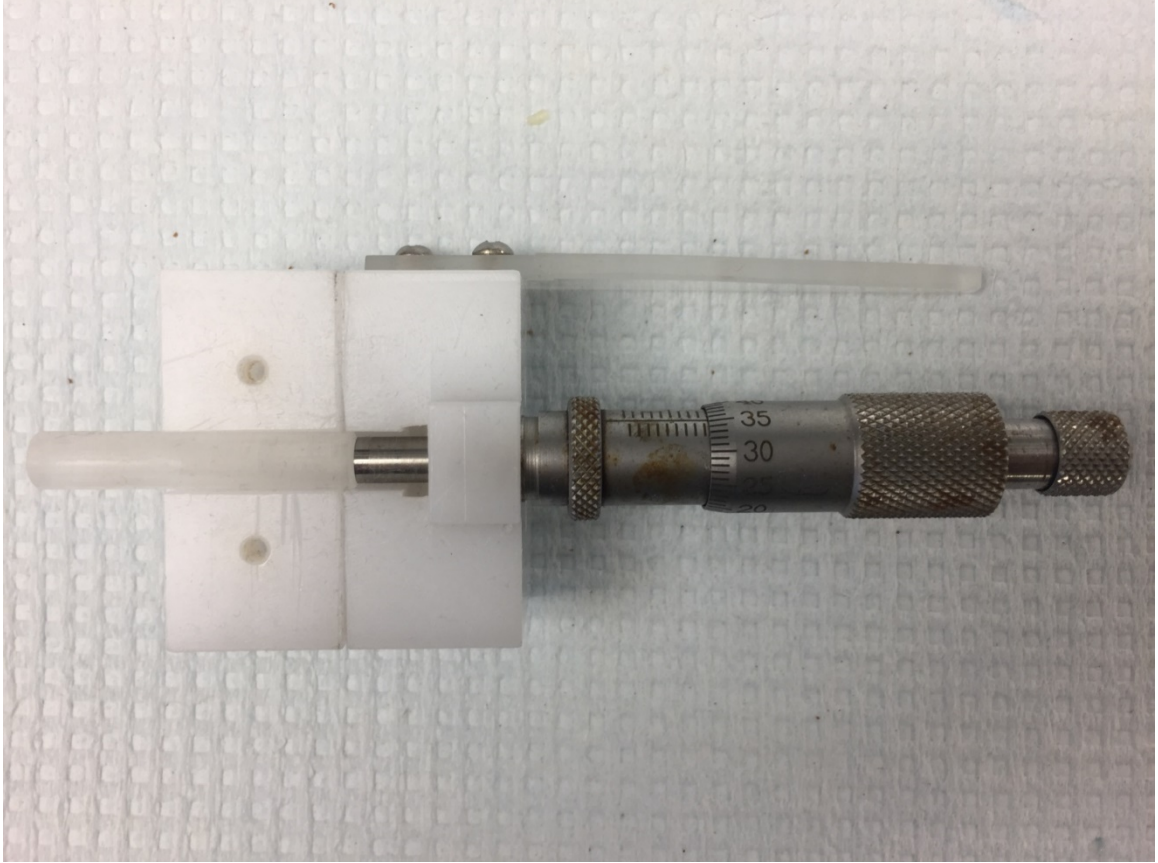
Figure 5.1 Customized cartilage thickness measurement fixture. This fixture was applied to separate the top 1/3 from the bottom 2/3 of the cartilage and allowed attachment of a micrometer with precision of 2 µm and a blade.
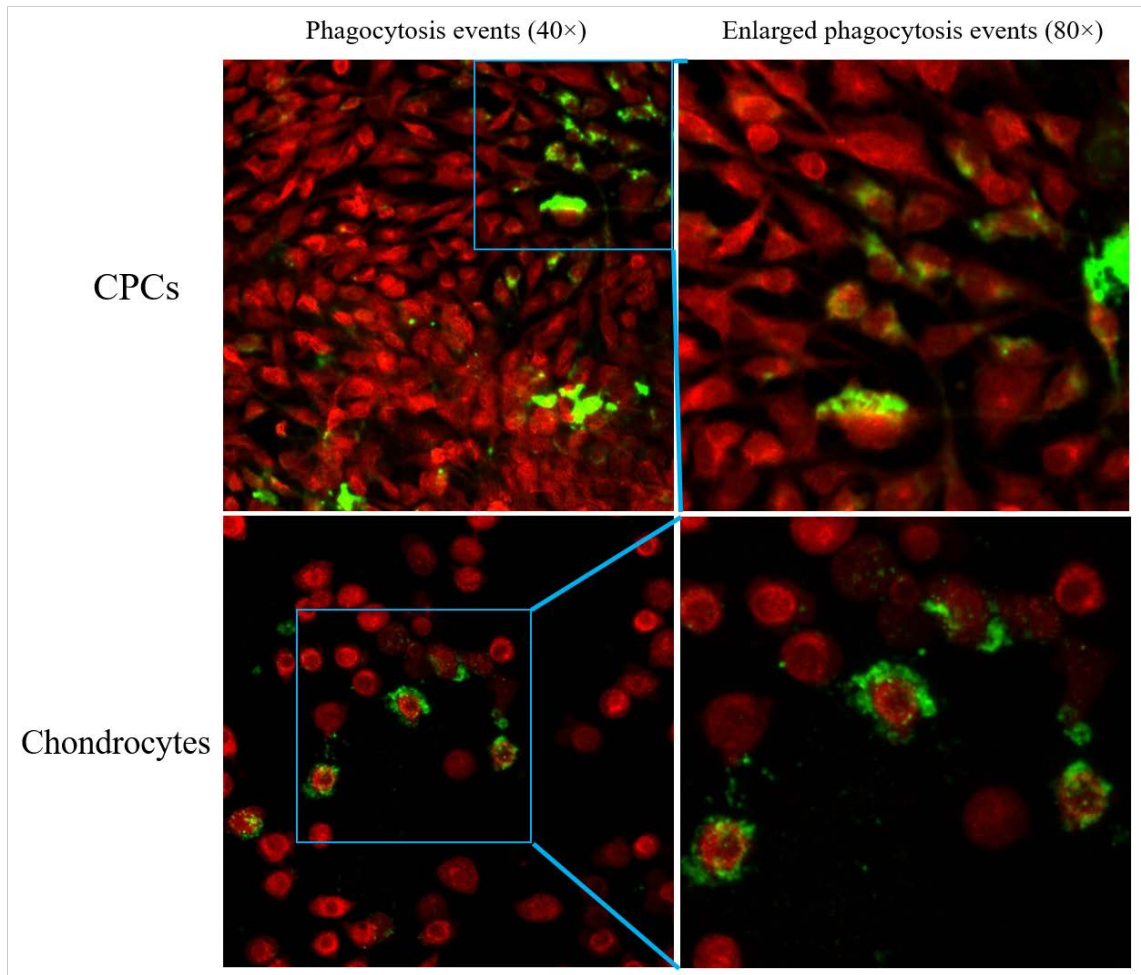
Figure 5.2 Cell debris engulfment in CPCs and chondrocytes. Confocal images show green labeled cell debris with cells counter-stained with Calcein Red-Orange. The majority of the green-labeled debris in the CPC culture was internalized (upper panels), whereas in chondrocytes the label was surface-bound (lower panels).
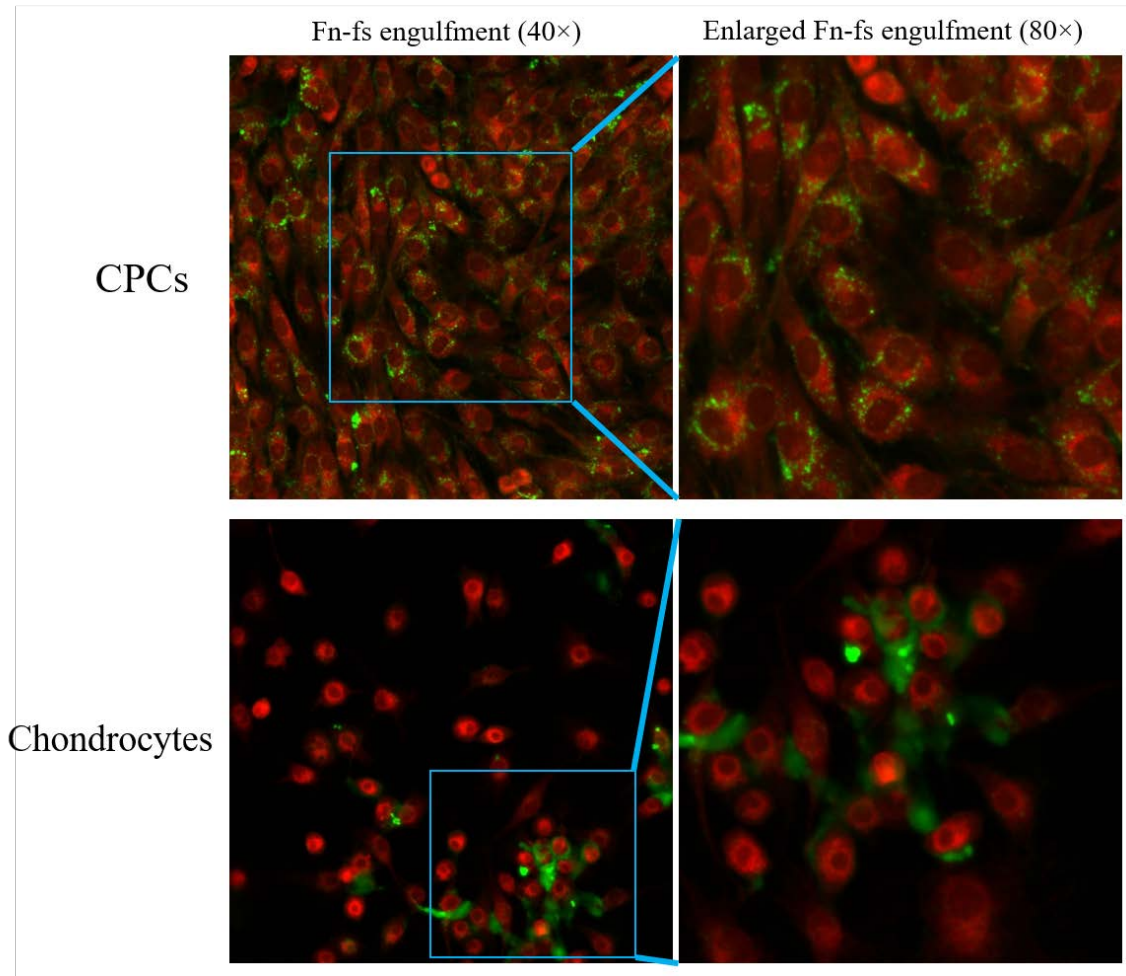
Figure 5.3 Fn-fs engulfment in CPCs and chondrocytes. Confocal imaging revealed that FITC-labeled Fn-fs (green) were engulfed by CPCs (upper panel), to a much greater extent than chondrocytes (lower panel).
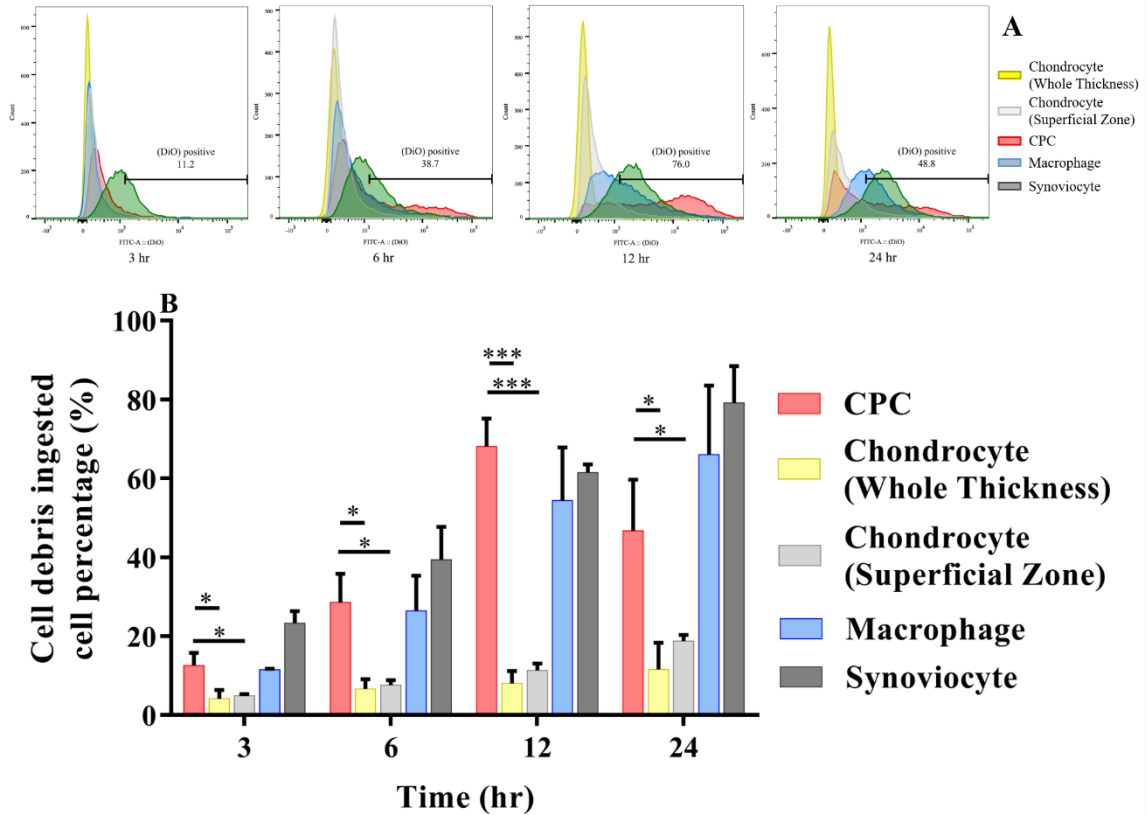
Figure 5.4 Quantification of cell debris ingested cell percentages. A) Representative comparisons among CPCs, chondrocytes (Whole thickness), chondrocytes (Superficial/transitional zones), synoviocytes and macrophages. CPCs were comparable to macrophages and synoviocytes, which showed a significantly higher percentage of DiO+ than chondrocytes at every time point. The number in each figure represents DiO+ CPC percentage. (DiO+ cell percentage of other 4 cell types not shown). B) DiO+ cell percentages increased over time for all cell types and were higher in CPCs, synoviocytes, and macrophage populations than in chondrocyte populations isolated from full-thickness cartilage or from the upper zones (n = 3 per group per time point). The differences between CPCs and chondrocytes were significant at all time points. (*: $p<0.05$; ***: $p<0.001$)

86
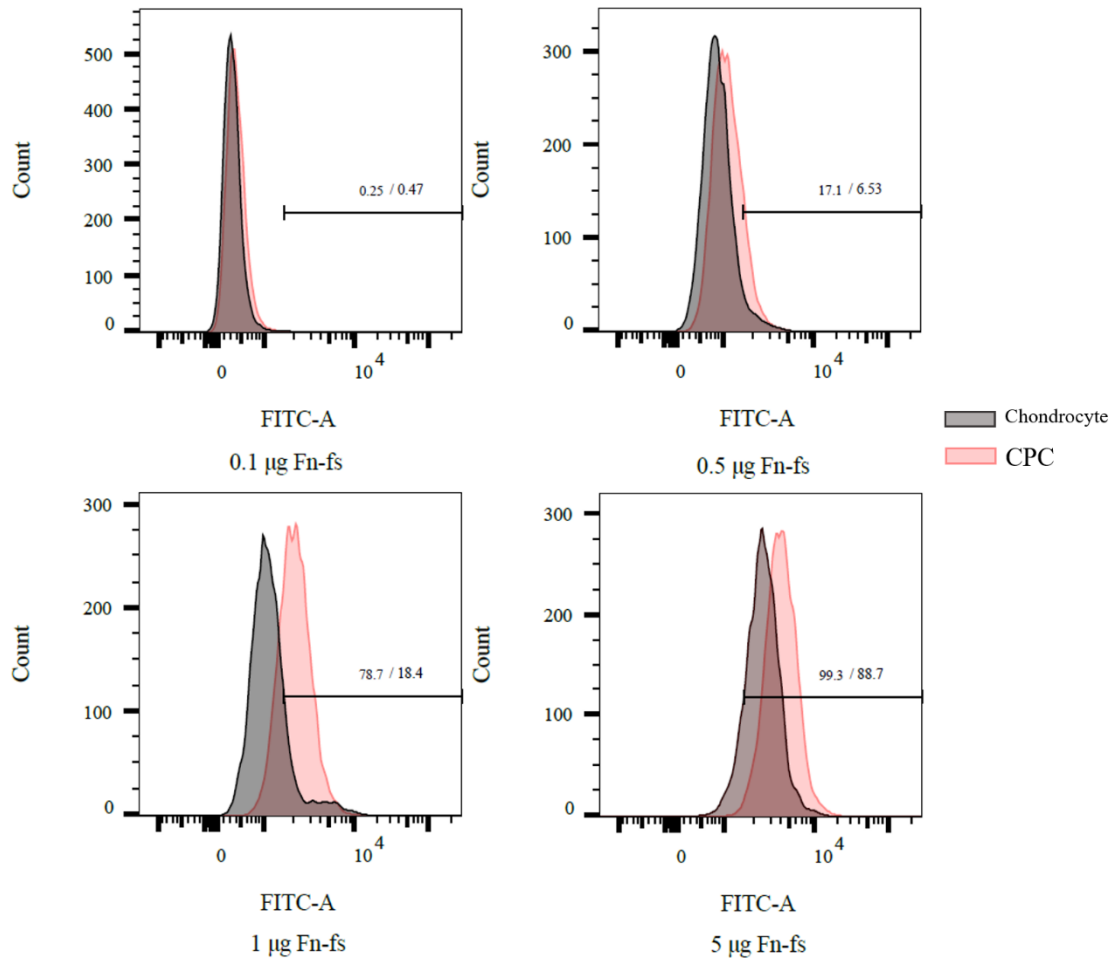
Figure 5.5 Optimal Fn-fs loading amount determination. Four loading amounts (0.1 µg, 0.5 µg, 1 µg, and 5 µg per well) were added to assess the difference between CPC and chondrocytes during flow cytometry analysis. For the samples loaded with 1 µg Fn-fs, the Fn-fs+ cell percentage is comparable in cell debris scenario, while differences were not obvious in other three loading amounts. The numbers in each figure represent Fn-fs+ CPC percentage/Fn-fs+ chondrocyte percentage.
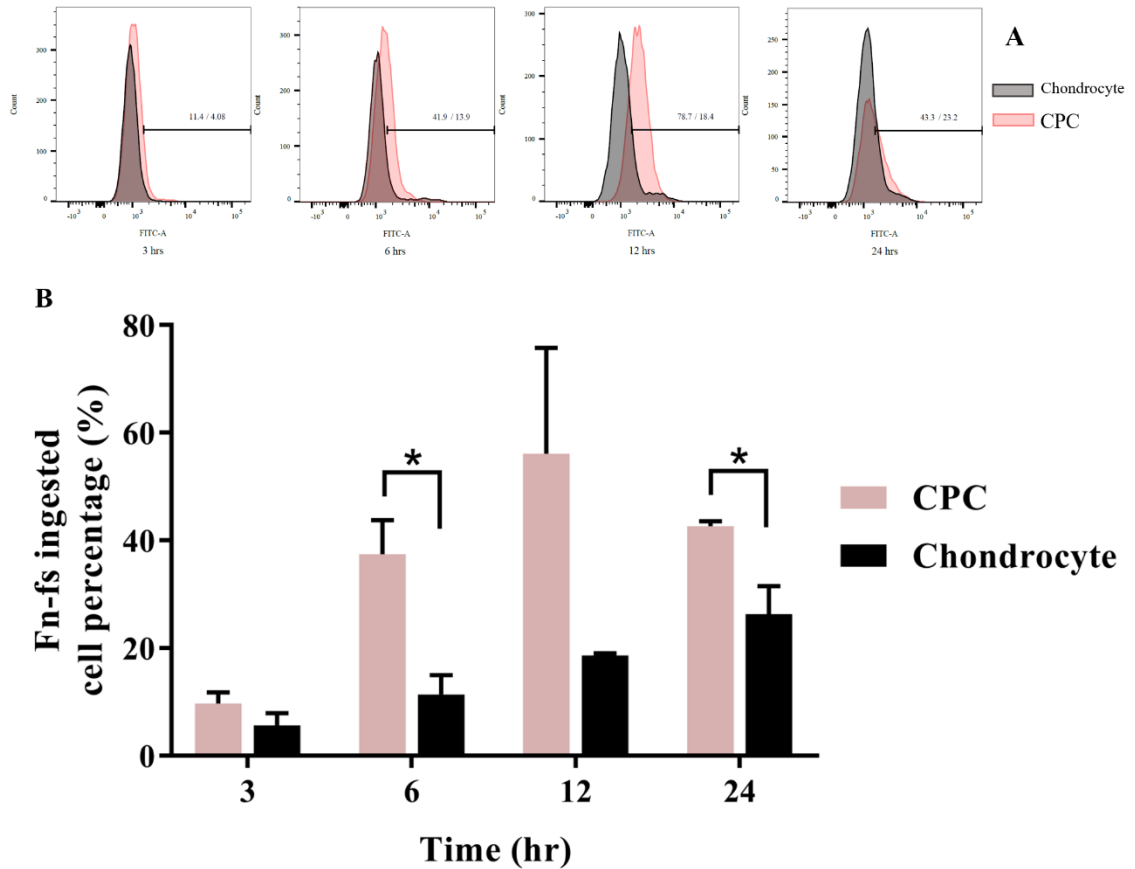
Figure 5.6 Quantification of Fn-fs ingested cell percentages. A) Representative comparisons between CPCs and chondrocytes. CPCs showed a significantly higher percentage of Fn-fs+ than chondrocytes at every time point. The numbers in each figure represent Fn-fs+ CPC percentage/Fn-fs+ chondrocyte percentage. B) Fn-fs+ cell percentages increased and peaked at 12 hrs for CPCs while gradually augmented over time for chondrocytes and CPC populations were higher than chondrocyte populations at each time point. (n = 3 per group per time point. *: $p < 0.05$)
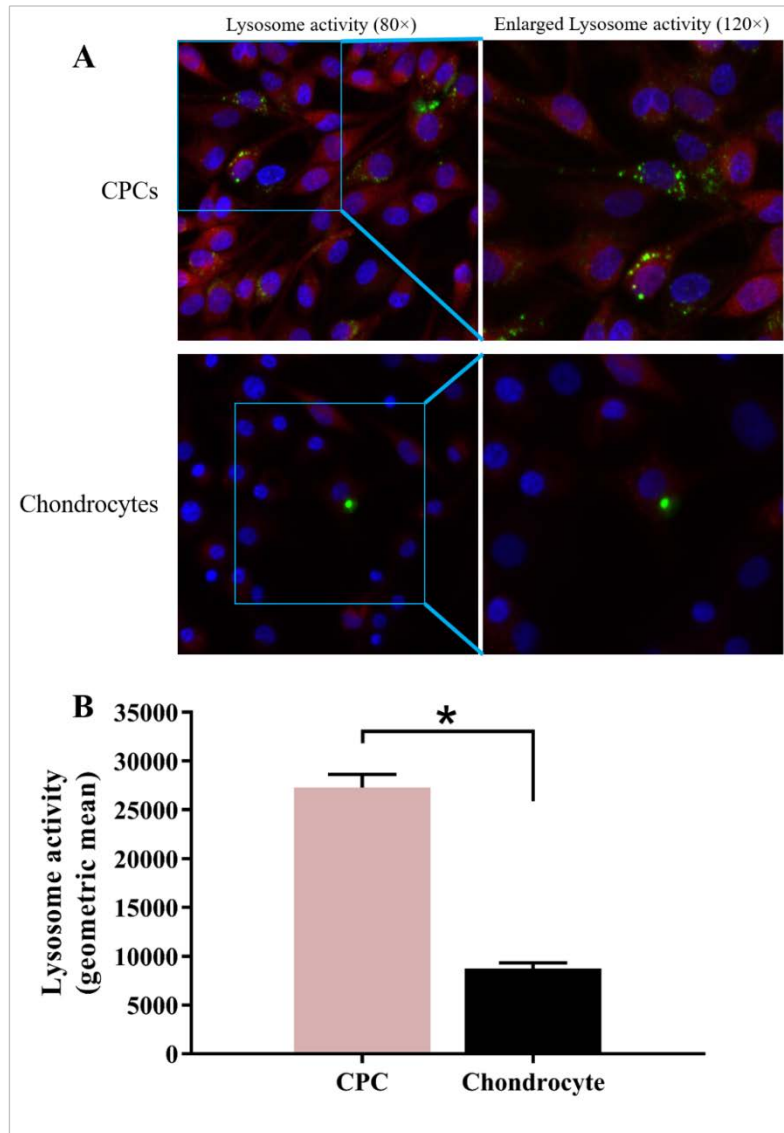
Figure 5.7 Lysosome activity in CPCs and chondrocytes. A) Confocal images show lysosome activity in CPCs and chondrocytes incubated with labeled cell debris. In the panels on the right, the fluorescent lysosome activity probe (red) and cell debris (green) was imaged in cells that were counter stained with a nuclear probe (blue). Both the green and red probes stained CPCs much more intensely than chondrocytes. B) Flow cytometric analysis showed lysosome activities in CPCs were significantly higher than chondrocytes. (n = 3 per group. *: p<0.05)
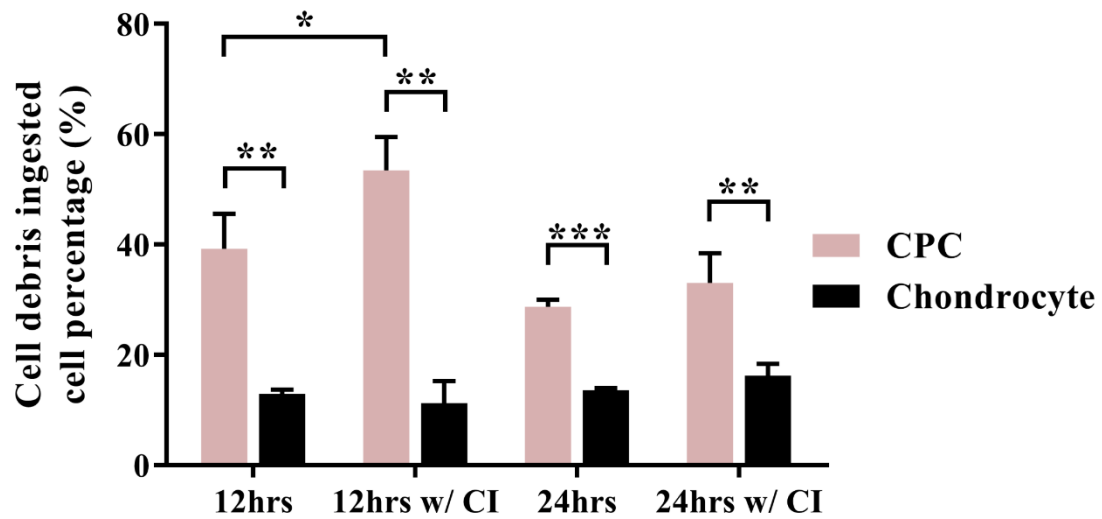
Figure 5.8 Lysosomal degradation of cell debris post engulfment. DiO+ CPC percentages are significantly higher than chondrocytes at 12 hrs and 24 hrs with or without cathepsin B inhibitor, DiO+ CPC percentage was significantly elevated with cathepsin B inhibitor at 12 hrs, and was slightly elevated at 24 hrs. No change was observed in chondrocytes in any situation. (n = 3 per group. CI: cathepsin B inhibitor. *: $p<0.05$; **: $p<0.01$; ***: $p<0.001$)
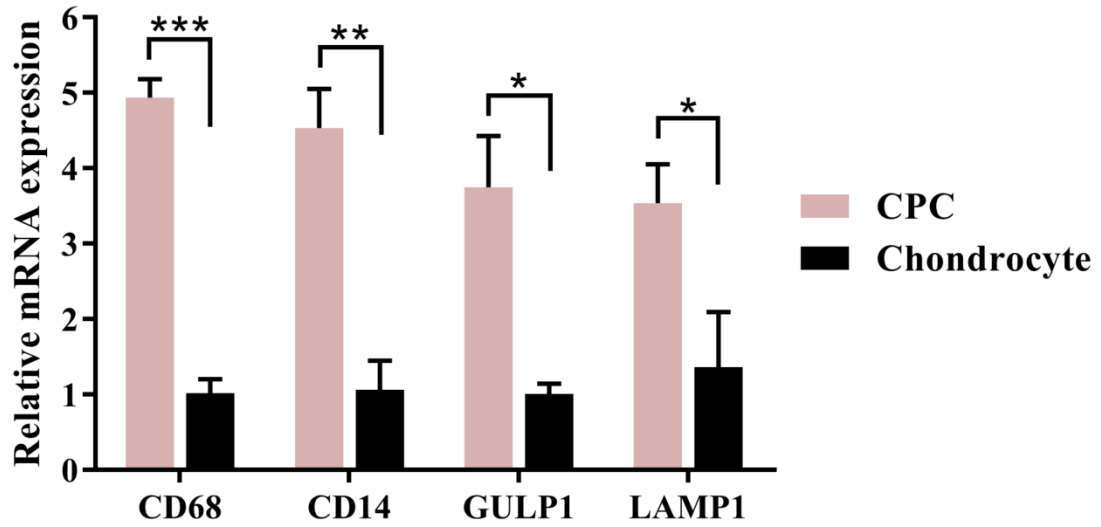
Figure 5.9 Gene expression of phagocytosis markers in CPC and chondrocyte. real-time PCR showed that CPCs significantly over-expressed in all four phagocytosis markers relative to chondrocytes. (n = 3 per group. *: $p<0.05$; **: $p<0.01$; ***: $p<0.001$)
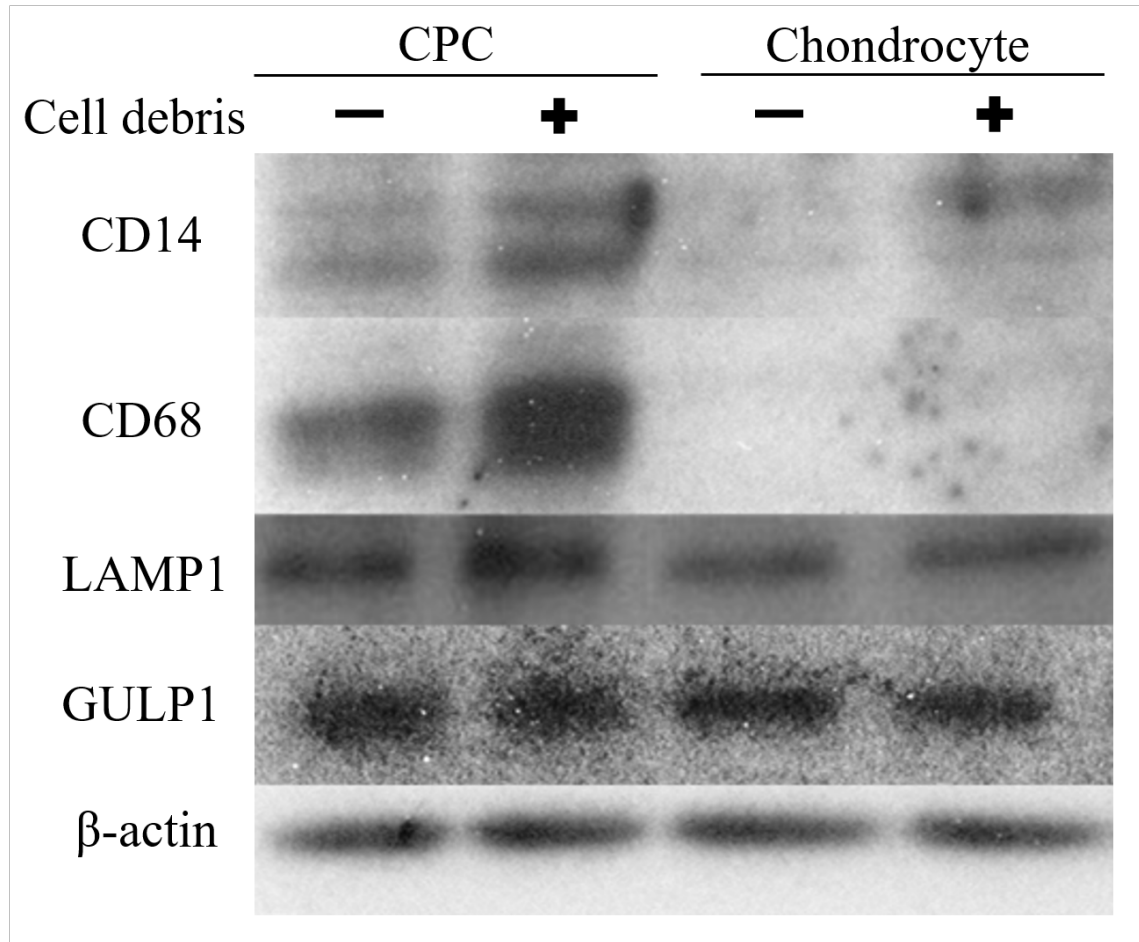
Figure 5.10 Protein expression of phagocytosis markers in CPC and chondrocyte. Western blots showed higher CD14, CD68, and LAMP1 protein expression in CPCs than in chondrocytes. Incubation with cell debris induced expression in CPCs, but not in chondrocytes. GULP1 was expressed at similar levels in CPCs and chondrocytes. β-actin expression was served as loading control.
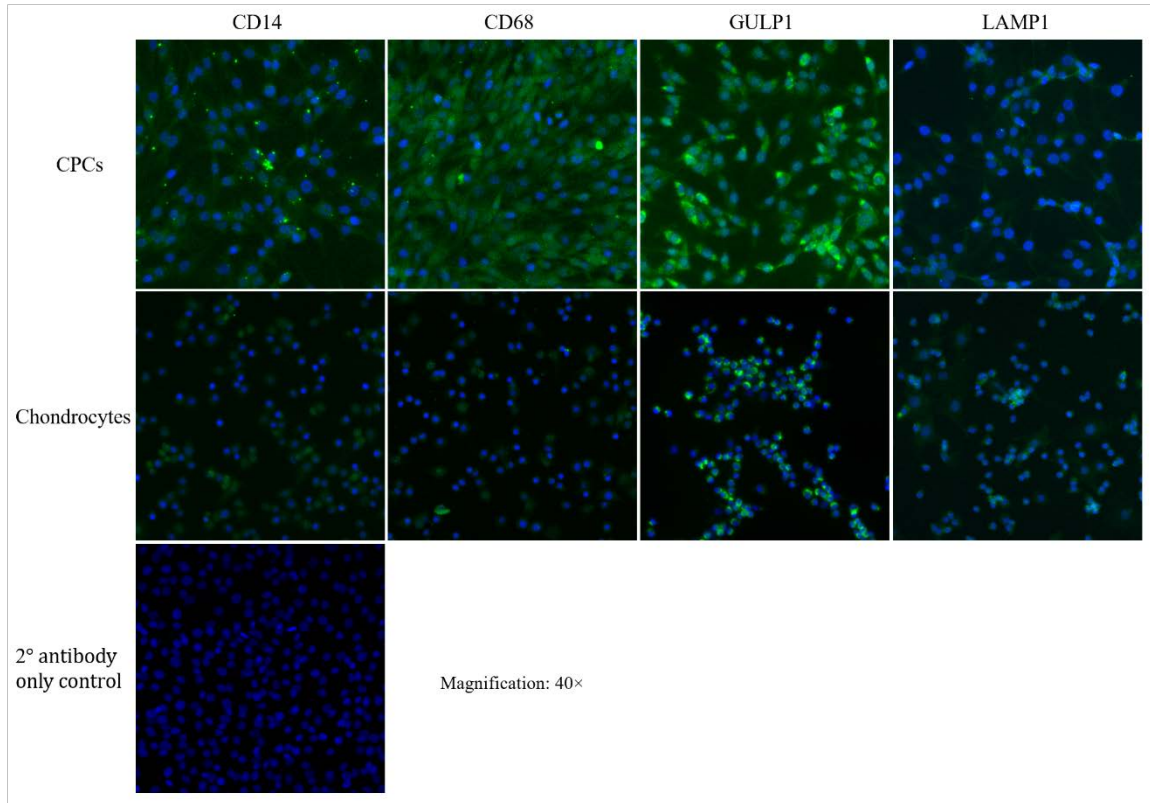
Figure 5.11 Immunocytochemistry staining of phagocytosis related markers. CPCs showed dramatically higher expression than chondrocytes in term of CD14, CD68, GULP1, and mild higher expression in LAMP1. (Secondary antibody only control was used to not obscure specific staining or resemble the specific staining pattern. Magnification: 40×)
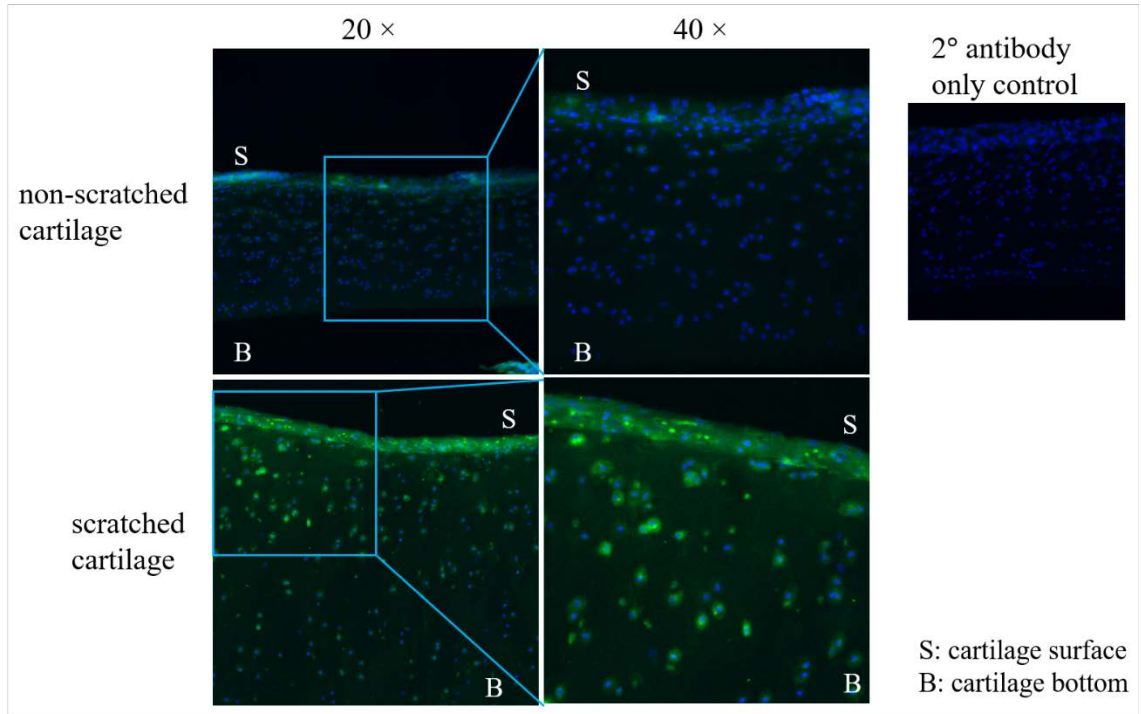
Figure 5.12 Immunohistochemistry staining of LAMP1 in cartilage tissue (scratched and non-scratched). Scratched cartilage tissue section displayed substantially more enhanced expression than non-scratched cartilage tissue throughout the depth. Elevated expression was detected in surface/superficial zone for both scratched and non-scratched cartilage tissue. (Secondary antibody only control was used to not obscure specific staining or resemble the specific staining pattern. S: cartilage surface B: cartilage bottom)

Gene	Forward primer 5' – 3'	Reverse primer 5' – 3'
β-actin	TCGACACCGCAACCAGTTCGC	CATGCCGGAGCCGTTGTCGA
CD68	GGAGTAATGGTTCCCAGCCC	CTGCAGTGGATCCTGCTTGA
CD14	ACCACCCTCAGTCTCCGTAA	GCCGAGACTGGGATTGTCAG
GULP1	TGGATGCATACTCCCGAAGC	AGCTGGCAATTGTGTTGAACT
LAMP1	GTGAAGAATGGCAACGGGAC	TTATTCTGGGGCCCACTCCT

Table 5.1 Primer (phagocytosis related) information for quantitative real-time PCR.

Gene Symbol	Gene Title	Fold-Change	Description
LAMP1	lysosomal-associated membrane protein 1	2.01	CPC up vs chondrocyte
CD68	CD68 molecule	3.79	CPC up vs chondrocyte
CTSS	cathepsin S	2.86	CPC up vs chondrocyte
CTSK	cathepsin K	3.14	CPC up vs chondrocyte
CTSL1	cathepsin L1	7.84	CPC up vs chondrocyte
CTSC	cathepsin C	35.12	CPC up vs chondrocyte
CTSA	cathepsin A	7.22	CPC up vs chondrocyte
CTSB	cathepsin B	2.25	CPC up vs chondrocyte
CTSL2	cathepsin L2	4.19	CPC up vs chondrocyte
CTSB	cathepsin B	2.33	CPC up vs chondrocyte
CTSZ	cathepsin Z	2.17	CPC up vs chondrocyte
CTSH	cathepsin H	3.98	CPC up vs chondrocyte
CTSF	cathepsin F	-1.79	CPC down vs chondrocyte
CTSW	cathepsin W	-1.39	CPC down vs chondrocyte
CTSD	cathepsin D	1.83	CPC up vs chondrocyte
CTSG	cathepsin G /// cathepsin G-like	-1.72	CPC down vs chondrocyte
CTSW	cathepsin W	-1.61	CPC down vs chondrocyte
CTSO	cathepsin O	1.92	CPC up vs chondrocyte

Table 5.2. Gene expression (phagocytosis related/cathepsin family) comparison selected from microarray data.

CHAPTER 6

CONCLUSIONS

With previous researches from our laboratory and other groups' work, we identified a distinct cell population, other than chondrocytes, residing in cartilage. CPCs are speculated to stay quiescent in cartilage surface/superficial zone under normal circumstance, and become highly active – migratory, proliferative, differentiative – provoked by focal cartilage injury and repopulate damaged sites. Although inferior to chondrocytes, CPCs possess stronger chondrogenic potential to other common cell candidates for cartilage regeneration. PTOA is thought to be initiated by focal cartilage matrix lesion along with massive death of superficial zone chondrocytes, as well as adhesive lubricant coating on cartilage surface. We previously confirmed that, in our bovine osteochondral model, with the help of CPCs, cartilage can be regenerated with considerate mechanical strength and biological functionalities [60, 98]. However, this phenomenon does not occur spontaneously in osteoarthritic patients or animals indicate the *in vivo* situation is far more complicated and might be detrimental to CPCs. Early stage inflammation related cytokines, reactive oxygen species, and mechanical loading stress may all plausibly impede CPC-mediated regeneration. New interventions need to be developed to create a befitting environment for CPCs' maximal functionalities and potentially for future clinical and therapeutic applications.

In this thesis, we also discovered the scavenger role of CPCs in clearing cartilage injury related debris (from cells and matrix). This is a significant finding since debris can be implausibly removed by intrinsic phagocytes in avascular cartilage. CPCs exhibited tremendously enhanced phagocytic capacity compared to resident chondrocytes, their

97

debris engulfment capacities, as well as highly elevated lysosomal activities/proteases, pave the avenue to complementarily understand the role of CPCs in cartilage regeneration and post-traumatic osteoarthritis (PTOA). In addition, lysosome related biomarkers might be a useful tool to target CPCs in normal and diseased cartilage.

In summary, as a unique and distinct cell type, CPCs are more akin to synovial cells on gene expression level. More importantly, CPCs' scavenger role is as important as their cartilage regenerating function. Two-step usage of CPCs (debris clearing and then cartilage regeneration) might be a feasible direction in the near future.

REFERENCES

1. Dowthwaite GP, Bishop JC, Redman SN, Khan IM, Rooney P, Evans DJ, et al. The surface of articular cartilage contains a progenitor cell population. J Cell Sci 2004; 117: 889-897.
2. Alsalameh S, Amin R, Gemba T, Lotz M. Identification of mesenchymal progenitor cells in normal and osteoarthritic human articular cartilage. Arthritis Rheum 2004; 50: 1522-1532.
3. Pelletier JP, Martel-Pelletier J, Abramson SB. Osteoarthritis, an inflammatory disease: potential implication for the selection of new therapeutic targets. Arthritis Rheum 2001; 44: 1237-1247.
4. Gibilisco PA, Schumacher HR, Jr., Hollander JL, Soper KA. Synovial fluid crystals in osteoarthritis. Arthritis Rheum 1985; 28: 511-515.
5. Dieppe P, Swan A. Identification of crystals in synovial fluid. Ann Rheum Dis 1999; 58: 261-263.
6. Buckwalter JA, Mankin HJ, Grodzinsky AJ. Articular cartilage and osteoarthritis. Instr Course Lect 2005; 54: 465-480.
7. Sophia Fox AJ, Bedi A, Rodeo SA. The basic science of articular cartilage: structure, composition, and function. Sports Health 2009; 1: 461-468.
8. Wong M, Wuethrich P, Eggli P, Hunziker E. Zone-specific cell biosynthetic activity in mature bovine articular cartilage: a new method using confocal microscopic stereology and quantitative autoradiography. J Orthop Res 1996; 14: 424-432.
9. Schumacher BL, Hughes CE, Kuettner KE, Caterson B, Aydelotte MB. Immunodetection and partial cDNA sequence of the proteoglycan, superficial zone protein, synthesized by cells lining synovial joints. J Orthop Res 1999; 17: 110-120.
10. Buckwalter JA, Mankin HJ. Articular cartilage: tissue design and chondrocyte-matrix interactions. Instr Course Lect 1998; 47: 477-486.
11. Bhosale AM, Richardson JB. Articular cartilage: structure, injuries and review of management. Br Med Bull 2008; 87: 77-95.
12. Broom ND, Poole CA. A functional-morphological study of the tidemark region of articular cartilage maintained in a non-viable physiological condition. J Anat 1982; 135: 65-82.
13. C. Ross Ethier CAS. Introductory Biomechanics: From Cells to Organisms, Cambridge University Press 2007.
14. Aydelotte MB, Greenhill RR, Kuettner KE. Differences between sub-populations of cultured bovine articular chondrocytes. II. Proteoglycan metabolism. Connect Tissue Res 1988; 18: 223-234.
15. Aydelotte MB, Kuettner KE. Differences between sub-populations of cultured bovine articular chondrocytes. I. Morphology and cartilage matrix production. Connect Tissue Res 1988; 18: 205-222.
16. Muir H. The chondrocyte, architect of cartilage. Biomechanics, structure, function and molecular biology of cartilage matrix macromolecules. Bioessays 1995; 17: 1039-1048.

99

17. Brighton CT, Heppenstall RB. Oxygen tension in zones of the epiphyseal plate, the metaphysis and diaphysis. An in vitro and in vivo study in rats and rabbits. J Bone Joint Surg Am 1971; 53: 719-728.

18. Setton LA, Elliott DM, Mow VC. Altered mechanics of cartilage with osteoarthritis: human osteoarthritis and an experimental model of joint degeneration. Osteoarthritis Cartilage 1999; 7: 2-14.

19. Pearle AD, Warren RF, Rodeo SA. Basic science of articular cartilage and osteoarthritis. Clin Sports Med 2005; 24: 1-12.

20. Dasuri K, Antonovici M, Chen K, Wong K, Standing K, Ens W, et al. The synovial proteome: analysis of fibroblast-like synoviocytes. Arthritis Res Ther 2004; 6: R161-168.

21. Henderson B, Edwards JC. The Synovial Lining in Health and Disease. London, England, Lippincott Williams & Wilkins Publishers 1987.

22. Edwards JC. The nature and origins of synovium: experimental approaches to the study of synoviocyte differentiation. J Anat 1994; 184 (Pt 3): 493-501.

23. Smith MD, Triantafillou S, Parker A, Youssef PP, Coleman M. Synovial membrane inflammation and cytokine production in patients with early osteoarthritis. J Rheumatol 1997; 24: 365-371.

24. Fan J, Myant C, Underwood R, Cann P. Synovial fluid lubrication of artificial joints: protein film formation and composition. Faraday Discuss 2012; 156: 69-85; discussion 87-103.

25. Jay GD. Lubricin and surfacing of articular joints. Current Opinion in Orthopaedics 2004; 15: 355-359.

26. Schmidt TA, Gastelum NS, Nguyen QT, Schumacher BL, Sah RL. Boundary lubrication of articular cartilage: role of synovial fluid constituents. Arthritis Rheum 2007; 56: 882-891.

27. Staikos C, Ververidis A, Drosos G, Manolopoulos VG, Verettas DA, Tavridou A. The association of adipokine levels in plasma and synovial fluid with the severity of knee osteoarthritis. Rheumatology (Oxford) 2013; 52: 1077-1083.

28. Kurz B, Lemke AK, Fay J, Pufe T, Grodzinsky AJ, Schunke M. Pathomechanisms of cartilage destruction by mechanical injury. Ann Anat 2005; 187: 473-485.

29. Burrage PS, Mix KS, Brinckerhoff CE. Matrix metalloproteinases: role in arthritis. Front Biosci 2006; 11: 529-543.

30. Nesic D, Whiteside R, Brittberg M, Wendt D, Martin I, Mainil-Varlet P. Cartilage tissue engineering for degenerative joint disease. Adv Drug Deliv Rev 2006; 58: 300-322.

31. Ding L, Heying E, Nicholson N, Stroud NJ, Homandberg GA, Buckwalter JA, et al. Mechanical impact induces cartilage degradation via mitogen activated protein kinases. Osteoarthritis Cartilage 2010; 18: 1509-1517.

32. Buckwalter JA, Martin JA. Osteoarthritis. Adv Drug Deliv Rev 2006; 58: 150-167.

33. Martin JA, Buckwalter JA. The role of chondrocyte senescence in the pathogenesis of osteoarthritis and in limiting cartilage repair. J Bone Joint Surg Am 2003; 85-A Suppl 2: 106-110.

34. Martin JA, Buckwalter JA. Roles of articular cartilage aging and chondrocyte senescence in the pathogenesis of osteoarthritis. Iowa Orthop J 2001; 21: 1-7.
35. Martin JA, Buckwalter JA. Aging, articular cartilage chondrocyte senescence and osteoarthritis. Biogerontology 2002; 3: 257-264.
36. Martin JA, Buckwalter JA. Post-traumatic osteoarthritis: the role of stress induced chondrocyte damage. Biorheology 2006; 43: 517-521.
37. Lawrence RC, Helmick CG, Arnett FC, Deyo RA, Felson DT, Giannini EH, et al. Estimates of the prevalence of arthritis and selected musculoskeletal disorders in the United States. Arthritis Rheum 1998; 41: 778-799.
38. Helmick CG, Felson DT, Lawrence RC, Gabriel S, Hirsch R, Kwoh CK, et al. Estimates of the prevalence of arthritis and other rheumatic conditions in the United States. Part I. Arthritis Rheum 2008; 58: 15-25.
39. Gabriel SE, Crowson CS, Campion ME, O'Fallon WM. Direct medical costs unique to people with arthritis. J Rheumatol 1997; 24: 719-725.
40. Buckwalter JA, Brown TD. Joint injury, repair, and remodeling: roles in post-traumatic osteoarthritis. Clin Orthop Relat Res 2004: 7-16.
41. Martin JA, McCabe D, Walter M, Buckwalter JA, McKinley TO. N-acetylcysteine inhibits post-impact chondrocyte death in osteochondral explants. J Bone Joint Surg Am 2009; 91: 1890-1897.
42. Saklatvala J. Tumour necrosis factor alpha stimulates resorption and inhibits synthesis of proteoglycan in cartilage. Nature 1986; 322: 547-549.
43. Goodwin W, McCabe D, Sauter E, Reese E, Walter M, Buckwalter JA, et al. Rotenone prevents impact-induced chondrocyte death. J Orthop Res 2010; 28: 1057-1063.
44. Mithoefer K, Williams RJ, 3rd, Warren RF, Potter HG, Spock CR, Jones EC, et al. Chondral resurfacing of articular cartilage defects in the knee with the microfracture technique. Surgical technique. J Bone Joint Surg Am 2006; 88 Suppl 1 Pt 2: 294-304.
45. Mithoefer K, Williams RJ, 3rd, Warren RF, Potter HG, Spock CR, Jones EC, et al. The microfracture technique for the treatment of articular cartilage lesions in the knee. A prospective cohort study. J Bone Joint Surg Am 2005; 87: 1911-1920.
46. Steadman JR, Briggs KK, Rodrigo JJ, Kocher MS, Gill TJ, Rodkey WG. Outcomes of microfracture for traumatic chondral defects of the knee: average 11-year follow-up. Arthroscopy 2003; 19: 477-484.
47. Centeno CJ, Busse D, Kisiday J, Keohan C, Freeman M, Karli D. Increased knee cartilage volume in degenerative joint disease using percutaneously implanted, autologous mesenchymal stem cells. Pain Physician 2008; 11: 343-353.
48. Robert H. Chondral repair of the knee joint using mosaicplasty. Orthop Traumatol Surg Res 2011; 97: 418-429.
49. Smith GD, Richardson JB, Brittberg M, Erggelet C, Verdonk R, Knutsen G, et al. Autologous chondrocyte implantation and osteochondral cylinder transplantation in cartilage repair of the knee joint. J Bone Joint Surg Am 2003; 85-A: 2487-2488; author reply 2488.
50. Brittberg M, Lindahl A, Nilsson A, Ohlsson C, Isaksson O, Peterson L. Treatment of deep cartilage defects in the knee with autologous chondrocyte transplantation. N Engl J Med 1994; 331: 889-895.

51. Brittberg M. Autologous chondrocyte transplantation. Clin Orthop Relat Res 1999: S147-155.
52. Pittenger MF, Mackay AM, Beck SC, Jaiswal RK, Douglas R, Mosca JD, et al. Multilineage potential of adult human mesenchymal stem cells. Science 1999; 284: 143-147.
53. Richter W. Cell-based cartilage repair: illusion or solution for osteoarthritis. Curr Opin Rheumatol 2007; 19: 451-456.
54. Bianco P, Robey PG, Simmons PJ. Mesenchymal stem cells: revisiting history, concepts, and assays. Cell Stem Cell 2008; 2: 313-319.
55. Quesenberry PJ, Colvin G, Dooner G, Dooner M, Aliotta JM, Johnson K. The stem cell continuum: cell cycle, injury, and phenotype lability. Ann N Y Acad Sci 2007; 1106: 20-29.
56. Spees JL, Whitney MJ, Sullivan DE, Lasky JA, Laboy M, Ylostalo J, et al. Bone marrow progenitor cells contribute to repair and remodeling of the lung and heart in a rat model of progressive pulmonary hypertension. FASEB J 2008; 22: 1226-1236.
57. Williams RJ, 3rd, Harnly HW. Microfracture: indications, technique, and results. Instr Course Lect 2007; 56: 419-428.
58. Koelling S, Kruegel J, Irmer M, Path JR, Sadowski B, Miro X, et al. Migratory chondrogenic progenitor cells from repair tissue during the later stages of human osteoarthritis. Cell Stem Cell 2009; 4: 324-335.
59. Hattori S, Oxford C, Reddi AH. Identification of superficial zone articular chondrocyte stem/progenitor cells. Biochem Biophys Res Commun 2007; 358: 99-103.
60. Seol D, McCabe DJ, Choe H, Zheng H, Yu Y, Jang K, et al. Chondrogenic progenitor cells respond to cartilage injury. Arthritis Rheum 2012; 64: 3626-3637.
61. Zhou C, Zheng H, Seol D, Yu Y, Martin JA. Gene expression profiles reveal that chondrogenic progenitor cells and synovial cells are closely related. J Orthop Res 2014; 32: 981-988.
62. Aderem A, Underhill DM. Mechanisms of phagocytosis in macrophages. Annu Rev Immunol 1999; 17: 593-623.
63. Underhill DM, Ozinsky A. Phagocytosis of microbes: complexity in action. Annu Rev Immunol 2002; 20: 825-852.
64. Greenberg S, Grinstein S. Phagocytosis and innate immunity. Curr Opin Immunol 2002; 14: 136-145.
65. Aderem A. Phagocytosis and the inflammatory response. J Infect Dis 2003; 187 Suppl 2: S340-345.
66. Jiao K, Zhang J, Zhang M, Wei Y, Wu Y, Qiu ZY, et al. The identification of CD163 expressing phagocytic chondrocytes in joint cartilage and its novel scavenger role in cartilage degradation. PLoS One 2013; 8: e53312.
67. Schumacher BL, Block JA, Schmid TM, Aydelotte MB, Kuettner KE. A novel proteoglycan synthesized and secreted by chondrocytes of the superficial zone of articular cartilage. Arch Biochem Biophys 1994; 311: 144-152.
68. Darling EM, Hu JC, Athanasiou KA. Zonal and topographical differences in articular cartilage gene expression. J Orthop Res 2004; 22: 1182-1187.

69. Garcia-Arnandis I, Guillen MI, Gomar F, Pelletier JP, Martel-Pelletier J, Alcaraz MJ. High mobility group box 1 potentiates the pro-inflammatory effects of interleukin-1beta in osteoarthritic synoviocytes. Arthritis Res Ther 2010; 12: R165.

70. Wolf J. Blood supply and nutrition of articular cartilage. Folia Morphol (Praha) 1975; 23: 197-209.

71. Villiger PM, Terkeltaub R, Lotz M. Production of monocyte chemoattractant protein-1 by inflamed synovial tissue and cultured synoviocytes. J Immunol 1992; 149: 722-727.

72. Winchester R, Su F, Ritchlin C. Alteration of synoviocytes by inflammation--the source of a persistent non-immunologic drive in synovitis: analysis of levels of mRNA expression by a simple multi-gene assay. Clin Exp Rheumatol 1993; 11 Suppl 8: S87-90.

73. Haslauer CM, Elsaid KA, Fleming BC, Proffen BL, Johnson VM, Murray MM. Loss of extracellular matrix from articular cartilage is mediated by the synovium and ligament after anterior cruciate ligament injury. Osteoarthritis Cartilage 2013.

74. Eisenhart C. The assumptions underlying the analysis of variance. Biometrics 1947; 3: 1-21.

75. Livak KJ, Schmittgen TD. Analysis of relative gene expression data using real-time quantitative PCR and the 2(-Delta Delta C(T)) Method. Methods 2001; 25: 402-408.

76. Denessiouk KA, Denesyuk AI, Johnson MS. Negative modulation of signal transduction via interleukin splice variation. Proteins 2008; 71: 751-770.

77. Schuurman W, Gawlitta D, Klein TJ, ten Hoope W, van Rijen MH, Dhert WJ, et al. Zonal chondrocyte subpopulations reacquire zone-specific characteristics during in vitro redifferentiation. Am J Sports Med 2009; 37 Suppl 1: 97S-104S.

78. Grogan SP, Duffy SF, Pauli C, Koziol JA, Su AI, D'Lima DD, et al. Zone-specific gene expression patterns in articular cartilage. Arthritis Rheum 2013; 65: 418-428.

79. Sokolove J, Lepus CM. Role of inflammation in the pathogenesis of osteoarthritis: latest findings and interpretations. Ther Adv Musculoskelet Dis 2013; 5: 77-94.

80. Iwanaga T, Shikichi M, Kitamura H, Yanase H, Nozawa-Inoue K. Morphology and functional roles of synoviocytes in the joint. Arch Histol Cytol 2000; 63: 17-31.

81. Ding L, Guo D, Homandberg GA, Buckwalter JA, Martin JA. A single blunt impact on cartilage promotes fibronectin fragmentation and upregulates cartilage degrading stromelysin-1/matrix metalloproteinase-3 in a bovine ex vivo model. J Orthop Res 2014; 32: 811-818.

82. Yu Y, Zheng H, Buckwalter JA, Martin JA. Single cell sorting identifies progenitor cell population from full thickness bovine articular cartilage. Osteoarthritis Cartilage 2014; 22: 1318-1326.

83. Homandberg GA, Ummadi V, Kang H. High molecular weight hyaluronan promotes repair of IL-1 beta-damaged cartilage explants from both young and old bovines. Osteoarthritis Cartilage 2003; 11: 177-186.

103

84. Hwang HS, Park SJ, Cheon EJ, Lee MH, Kim HA. Fibronectin fragment-induced expression of matrix metalloproteinases is mediated by MyD88-dependent TLR-2 signaling pathway in human chondrocytes. Arthritis Res Ther 2015; 17: 320.

85. Devitt A, Moffatt OD, Raykundalia C, Capra JD, Simmons DL, Gregory CD. Human CD14 mediates recognition and phagocytosis of apoptotic cells. Nature 1998; 392: 505-509.

86. Travaglione S, Falzano L, Fabbri A, Stringaro A, Fais S, Fiorentini C. Epithelial cells and expression of the phagocytic marker CD68: scavenging of apoptotic bodies following Rho activation. Toxicol In Vitro 2002; 16: 405-411.

87. Huynh KK, Eskelinen EL, Scott CC, Malevanets A, Saftig P, Grinstein S. LAMP proteins are required for fusion of lysosomes with phagosomes. EMBO J 2007; 26: 313-324.

88. Sullivan CS, Scheib JL, Ma Z, Dang RP, Schafer JM, Hickman FE, et al. The adaptor protein GULP promotes Jedi-1-mediated phagocytosis through a clathrin-dependent mechanism. Mol Biol Cell 2014; 25: 1925-1936.

89. Algenas C, Agaton C, Fagerberg L, Asplund A, Bjorling L, Bjorling E, et al. Antibody performance in western blot applications is context-dependent. Biotechnol J 2014; 9: 435-445.

90. Kraus S, Arber N. Inflammation and colorectal cancer. Curr Opin Pharmacol 2009; 9: 405-410.

91. Tso GH, Law HK, Tu W, Chan GC, Lau YL. Phagocytosis of apoptotic cells modulates mesenchymal stem cells osteogenic differentiation to enhance IL-17 and RANKL expression on CD4+ T cells. Stem Cells 2010; 28: 939-954.

92. Hinds KA, Hill JM, Shapiro EM, Laukkanen MO, Silva AC, Combs CA, et al. Highly efficient endosomal labeling of progenitor and stem cells with large magnetic particles allows magnetic resonance imaging of single cells. Blood 2003; 102: 867-872.

93. Schwachula A, Riemann D, Kehlen A, Langner J. Characterization of the immunophenotype and functional properties of fibroblast-like synoviocytes in comparison to skin fibroblasts and umbilical vein endothelial cells. Immunobiology 1994; 190: 67-92.

94. Bartok B, Firestein GS. Fibroblast-like synoviocytes: key effector cells in rheumatoid arthritis. Immunol Rev 2010; 233: 233-255.

95. Savina A, Amigorena S. Phagocytosis and antigen presentation in dendritic cells. Immunol Rev 2007; 219: 143-156.

96. Nagl M, Kacani L, Mullauer B, Lemberger EM, Stoiber H, Sprinzl GM, et al. Phagocytosis and killing of bacteria by professional phagocytes and dendritic cells. Clin Diagn Lab Immunol 2002; 9: 1165-1168.

97. Albert ML, Pearce SF, Francisco LM, Sauter B, Roy P, Silverstein RL, et al. Immature dendritic cells phagocytose apoptotic cells via alphavbeta5 and CD36, and cross-present antigens to cytotoxic T lymphocytes. J Exp Med 1998; 188: 1359-1368.

98. Yu Y, Brouillette MJ, Seol D, Zheng H, Buckwalter JA, Martin JA. Use of recombinant human stromal cell-derived factor 1alpha-loaded fibrin/hyaluronic acid hydrogel networks to achieve functional repair of full-thickness bovine

articular cartilage via homing of chondrogenic progenitor cells. Arthritis Rheumatol 2015; 67: 1274-1285.